ENT000214
Submitted: March 29, 2012

EPRI

Materials Reliability Program (MRP) Evaluation of Fatigue Data Including Reactor Water Environmental Effects (MRP-49)

This report describes research sponsored by EPRI and the U.S. Department of Energy under the Nuclear Energy Plant Optimization (NEPO) Program.

Technical Report

Materials Reliability Program (MRP) Evaluation of Fatigue Data Including Reactor Water Environmental Effects (MRP-49)

1003079

Final Report, December 2001

EPRI Project Manager
S. Rosinski

EPRI • 3412 Hillview Avenue, Palo Alto, California 94304 • PO Box 10412, Palo Alto, California 94303 • USA
800.313.3774 • 650.855.2121 • askepri@epri.com • www.epri.com

DISCLAIMER OF WARRANTIES AND LIMITATION OF LIABILITIES

ORGANIZATION(S) THAT PREPARED THIS DOCUMENT

Applied Science and Technology

ORDERING INFORMATION

Requests for copies of this report should be directed to EPRI Customer Fulfillment, 1355 Willow Way, Suite 278, Concord, CA 94520, (800) 313-3774, press 2.

CITATIONS

This report was prepared by

Applied Science and Technology
16630 Sagewood Lane
Poway, CA 92064

Principal Investigator
Dr. R. E. Nickell

Consultants:
Dr. William A. Van Der Sluys
1488 Glenking Lane
Alliance, OH 44601

Dr. Sumio Yukawa
4925 Valkyrie Drive
Boulder, CO 80301

This report describes research sponsored by EPRI and the U.S. Department of Energy under the Nuclear Energy Plant Optimization (NEPO) Program.

This report is a corporate document that should be cited in the literature in the following manner:

Materials Reliability Program (MRP) Evaluation of Fatigue Data Including Reactor Water Environmental Effects (MRP-49), EPRI, Palo Alto, CA, and the U.S. Department of Energy, Washington, D.C.: 2001. 1003079.

REPORT SUMMARY

Laboratory data have been assembled in the past decade indicating a significant reduction in component fatigue life when reactor water environmental effects are experimentally simulated. However, these laboratory data have not been supported by nuclear power plant component operating experience. The laboratory data are being used to support arguments for revising the design-basis fatigue curves in the ASME Code Section III, Division 1, for Class 1 components. A thorough review of their applicability to actual component operating conditions has been performed. This report provides the results of that data review and recommends additional laboratory testing intended to improve the applicability of laboratory test results under simulated reactor water environmental conditions.

Background

License renewal applicants have been asked by staff of the U. S. Nuclear Regulatory Commission (NRC) to evaluate the potential significance of reduced cyclic fatigue life caused by the exposure of carbon, low-alloy, and austenitic stainless steels to both BWR and PWR reactor water environments. The industry has collectively responded to these requests with generic studies that apply reactor water environment penalty factors to 40-year design-basis fatigue calculations. In some cases, the penalty factors are sufficient to generate environmentally adjusted fatigue lives that approach or possibly exceed the limiting cumulative usage factor (CUF) of 1.0. These calculations show that the most affected component locations (for example, surge line locations in PWR plants) should already be exhibiting observable manifestations of fatigue cracking. This cracking has not been detected during periodic inservice examinations carried out in accordance with the ASME Code Section XI. Individual license renewal applicants have used these generic studies as guidance for plant-specific evaluations showing that relatively few component locations are affected, with the potential fatigue damage at those few locations being managed during the extended operating period by continuing or augmenting existing inservice inspections. The applicability of the laboratory fatigue data with simulated reactor water environmental effects bears directly on these license renewal commitments.

Objectives

- To assemble, review, and assess existing laboratory fatigue data, including reactor water environmental effects
- To determine the range of applicability of the data to nuclear power plant components operating under actual plant conditions

Approach

This study divided the assembly, review, and assessment of existing laboratory fatigue data and its applicability to plant operating conditions into four principal tasks: (1) review of available laboratory data relative to thresholds for environmental parameters such as temperature, reactor water oxidation potential, strain rate, strain amplitude, reactor water flow rate, and component

metal sulfur content; (2) determination of the relevance of the laboratory data to actual plant operating conditions; (3) review of laboratory S-N data curve-fitting models; and (4) assessment of existing ASME Code Section III Class 1 margins.

Results

Fatigue data from laboratory testing that simulates reactor water environmental effects have been collected and analyzed, building upon an S-N data evaluation performed by the Pressure Vessel Research Council's Steering Committee on Cyclic Life and Environmental Effects for the ASME Board on Nuclear Codes and Standards in the early 1990s. The data analyses found that reactor water environmental effects for carbon and low-alloy steels are fully accommodated by a moderate environmental effects factor, Z, of 3, representing a fraction of the margin of 20 in the low-cycle portion of the ASME Code fatigue design curves. The Z factor is independent of, and adds to, other fatigue design conservatism from cycle transient definitions, stress indices, and plastic strain concentration factors. BWR data for carbon steel subjected to very high strain amplitudes at 8 ppm dissolved oxygen, well above the nominal operating condition levels of 0.2 ppm, are an exception.

The evaluations also found that a large portion of the reactor water environmental effects for austenitic stainless steel can be accommodated by a Z factor of 1.5. Data obtained at very low strain rates under simulated conditions of low dissolved oxygen and low temperature are the exception to this finding. The entire simulated reactor water environmental effects data set was evaluated relative to its applicability to actual operating conditions and was found to be deficient in three important ways. First, the simulated coolant flow rates were about three orders of magnitude lower than nominal coolant flow rates. Second, questions about strain control conditions for the austenitic stainless steel data set persist. Component cyclic plastic straining is clearly under strain control, and strain-controlled laboratory testing is the basis for ASME Code fatigue design. Finally, component cyclic plastic straining is very localized, as opposed to the uniform plastic straining in the laboratory tests. Laboratory and full-scale testing of carbon steel specimens and components have demonstrated the importance of coolant flow rate. Nominal flow rates have been found to essentially eliminate the effects of low strain rates and, thereby, eliminate all but the most severe reactor water environmental effects. A test program is proposed to extend these findings to low-alloy steel and austenitic stainless steel. Full-scale testing of carbon, low-alloy, and austenitic stainless steel components with at least one surface exposed to an oxygenated water environment confirm the conservatism of the fatigue design procedures and the moderate environmental effects factor.

EPRI Perspective

The apparent reduction in component fatigue life due to laboratory-simulated reactor water environment, and the management of this phenomenon, has become a significant issue for those utilities seeking license renewal. These laboratory data have not been supported by nuclear power plant component operating experience. Results of the comprehensive review performed on available laboratory and component/structural fatigue test data provide a strong technical justification for reconciliation of laboratory data with actual plant operating conditions. It is anticipated that the results of this review will be an integral step toward the resolution of this issue for license renewal.

Keywords

Fatigue
License renewal
Life cycle management

CONTENTS

LIST OF FIGURES

LIST OF TABLES

1
INTRODUCTION

Laboratory and component-scale fatigue crack initiation data under simulated water reactor environmental conditions have been obtained over the past two decades and indicate a significant reduction in cyclic life when compared to fatigue crack initiation data obtained in air environments. An early report on these effects was published by the General Electric Company in 1982 [1], based on carbon steel piping component tests in high-temperature (550°F [288°C]), high dissolved oxygen (8 ppm), and nominal BWR (0.2 ppm dissolved oxygen) environments. The greatest effects were observed at high-amplitude, low-cyclic frequency (that is, low strain rate) loading at temperature, in particular at loads causing stresses in the plastic range. It was found that an environmental correction factor, K_{en}, was needed to restore ASME Code fatigue design margins under the worst-case conditions. This factor was not needed when the water temperature was less than 400°F (204°C), nor was the factor needed when the cyclic frequency was relatively rapid, greater than or equal to 0.1 Hz. K_{en} was found to depend on strain amplitude and dissolved oxygen, with a value of 1.0 for small plastic strains. For large plastic strains, K_{en} was found to have a maximum of about 3.4 for 8 ppm dissolved oxygen and about 2.4 for 0.2 ppm dissolved oxygen (see Figure 1-1, which is Figure 21 from Appendix C of EPRI report NP-2406 [1]).

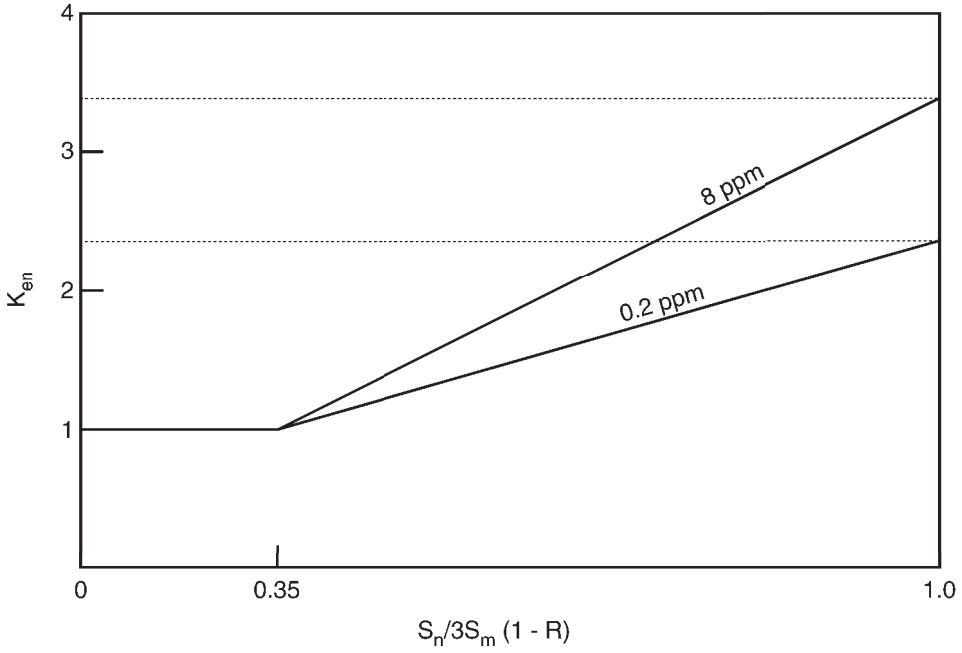

Figure 1-1
K_{en} as a Function of ASME Code Plastic Strain Adjustment Factor [$S_n/3S_m$ (I-R)] for Dissolved Oxygen Content of 0.2 and 8 ppm [1]

Approximately a decade later, Japanese investigators published a set of fatigue crack initiation data for carbon, low-alloy, and austenitic stainless steels [2]. These data were then presented to ASME Code bodies and to staff of the U. S. Nuclear Regulatory Commission (NRC), leading to concerns about the structural integrity of both existing light-water reactor (LWR) components and potential new construction. The data set included the carbon steel data obtained previously by the General Electric Company, but also included data for low-alloy and austenitic stainless steels showing somewhat lesser but still significant reductions in fatigue life. During the subsequent discussions between the industry and the NRC, in particular within the context of nuclear plant license renewal, the industry argued that:

- The carbon steel data were well known.
- A procedure for addressing severe BWR reactor water environmental effects was available in the form of the K_{en} stress concentration factor; K_{en} is a maximum of 2.4 for nominal BWR conditions and even less for nominal PWR conditions, well within the moderate environmental effects range.
- Therefore, K_{en} needed to be applied only under high-strain-amplitude conditions at temperature, with saturated dissolved oxygen, under slow, cyclic loading conditions, a combination of conditions that is rarely encountered in actual operation.
- The reduction in fatigue life for low-alloy and austenitic stainless steels could be accommodated by the assignment of a fraction of the factor of 20 at the low-cycle end of the ASME Code fatigue design curve to account for some of the environmental effects.

This latter argument was based on the statement in the ASME Code Background Document [3] regarding the factor of 20 at the high-strain-amplitude, low-cycle end of the ASME Code fatigue design curve that:

> "These factors were intended to cover such effects as environment, size effect, and scatter of data, and thus it is not to be expected that a vessel will actually operate safely for twenty times its specified life."

Furthermore, the industry argued that the new laboratory data were not supported by nuclear power plant component operating experience.

In spite of these arguments, a new Generic Safety Issue (GSI) 166 [4] was identified by the NRC staff because of concerns about the effects of reactor water environments on component fatigue life during both the current term and any license renewal term. The GSI was closed for current operating plants with the issuance of SECY-95-245 [5], but remained open as a license renewal issue, renumbered as GSI 190 [6]. GSI 190 was closed in December 1999, based on an internal NRC memorandum [7].

In spite of the issue closure, license renewal applicants continue to be required to address reactor water environmental effects on fatigue life in their license renewal applications.

These additional license renewal requirements are based, in part, on more recent laboratory fatigue data under simulated BWR and PWR reactor water coolant conditions. A considerable amount of new data has been generated during the period from 1993 to 1999 [8,9,10,11,12]. The combined set of laboratory data is being used to support arguments for revising the design-basis

fatigue curves in the ASME Code Section III, Division 1, for new construction of Class 1 components. Also, these same data are being used to support revisions of non-mandatory Appendix L of the ASME Code Section XI, Division 1, for fatigue evaluation of operating components. Therefore, the U. S. nuclear power industry, through the EPRI Materials Reliability Program (MRP), performed a thorough review of the applicability of these data to actual component operating conditions. This report provides the results of that data review. This report also contains recommendations for additional laboratory testing intended to improve the applicability of laboratory test results under simulated reactor water environmental conditions.

This report is based on four work tasks:

- Review of available laboratory data relative to thresholds for environmental parameters, such as temperature, reactor water oxidation potential, strain rate, strain amplitude, reactor water flow rate, and component metal sulfur content
- Determination of the relevance of the laboratory data to actual plant operating conditions
- Review of laboratory S-N data curve-fitting models
- Assessment of current ASME Code Section III Class 1 margins

In addition, the project involved two reporting tasks—preparation of the final report and project coordination with EPRI and the industry.

This report is divided into seven sections. Section 1 is this Introduction. Section 2 contains the primary results of the data review—the analysis of the existing fatigue crack initiation data sets for carbon, low-alloy, and austenitic stainless steels. Section 3 contains the results of an evaluation of the relevance of the existing fatigue crack initiation data sets to component operation under actual plant operating conditions. Section 4 describes the models used to characterize fatigue crack initiation in both air and reactor water environments, and their capability to model the shifts from one environmental condition to another. Section 5 discusses the margins in the fatigue design curves and the appropriate allocation of those margins to such factors as moderate environmental effects, size effects, and surface roughness. Finally, Section 6 describes a proposed test program intended to provide data that is currently not available or to provide further confirmation of expected environmental effects. Conclusions are provided in Section 7.

1.1 References

1. *BWR Environmental Cracking Margins for Carbon Steel Piping.* EPRI, Palo Alto, CA and General Electric Company, San Jose, California: May 1982. NP-2406.

2. "JNUFAD Data Base," Prepared by the Japanese EFD Committee, Thermal and Nuclear Power Engineering Society, Tokyo, Japan, 1991.

3. *Criteria of the ASME Boiler and Pressure Vessel Code for Design by Analysis in Sections III and VIII, Division 2.* The American Society of Mechanical Engineers, New York, 1969.

4. U.S. Nuclear Regulatory Commission. *Adequacy of Fatigue Life of Metal Components*. Generic Safety Issue 166.

5. U.S. Nuclear Regulatory Commission, James M. Taylor, Executive Director for Operations. *Completion of the Fatigue Action Plan*. SECY-95-245, September 25, 1995.

6. U.S. Nuclear Regulatory Commission. *Fatigue Evaluation of Metal Components for 60-Year Plant Life*. Generic Safety Issue 190.

7. Memorandum, Ashok C. Thadani, Director, Office of Nuclear Regulatory Research, to William D. Travers, Executive Director for Operations, U.S. Nuclear Regulatory Commission, Washington, DC dated December 26, 1999. Closeout of Generic Safety Issue 190, *Fatigue Evaluation of Metal Components for 60-Year Plant Life.*

8. Majumdar, S., Chopra, O. K., and Shack, W. J., *Interim Fatigue Design Curves for Carbon, Low-Alloy, and Austenitic Stainless Steels in LWR Environments.* NUREG/CR-5999 (ANL-93/3), Argonne National Laboratory, Argonne, IL, April 1993.

9. Keisler, J., Chopra, O. K., and Shack, W. J., *Statistical Analysis of Fatigue Strain-Life Data for Carbon and Low-Alloy Steels.* NUREG/CR-6237 (ANL-94/21), Argonne National Laboratory, Argonne, IL, August 1994.

10. Keisler, J., Chopra, O. K., and Shack, W. J., *Fatigue Strain-Life Behavior of Carbon and Low-Alloy Steels, Austenitic Stainless Steels, and Alloy 600 in LWR Environments.* NUREG/CR-6335 (ANL-95/xx), Argonne National Laboratory, Argonne, IL, August 1995.

11. O. K. Chopra and W. J. Shack, *Effects of LWR Coolant Environments on Fatigue Design Curves of Carbon and Low-Alloy Steels.* NUREG/CR-6583 (ANL-97/18), Argonne National Laboratory, Argonne, IL, March 1998.

12. O. K. Chopra and W. J. Shack, *Effects of LWR Coolant Environments on Fatigue Design Curves of Austenitic Stainless Steels.* NUREG/CR-5704 (ANL-98/31), Argonne National Laboratory, Argonne, IL, April 1999.

2
REVIEW OF AVAILABLE LABORATORY DATA

2.1 PVRC Committee on Cyclic Life and Environmental Effects

In the early 1990s, the effects of reactor water environments on fatigue crack initiation emerged as a major issue affecting both operating nuclear plants in both the current and the license renewal term. Efforts to address the issue included a request by the ASME Board on Nuclear Codes and Standards (BNCS) to the Pressure Vessel Research Council (PVRC) to evaluate the available data. The June 1991 request stated that:

> **"**BNCS looks to PVRC to obtain, characterize and report in sufficient detail to ASME such data as may be useful to ASME in its evaluation of the Fatigue curves of Section III and Section XI."

In response, the PVRC formed a steering group, called the Cyclic Life and Environmental Effects (CLEE) Steering Committee. The CLEE Steering Committee, in turn, formed three Working Groups—the Working Group on S-N Data Analysis, the Working Group on da/dN Data Analysis, and the Working Group on Evaluation Methods. The effort of the Working Group on S-N Data Analysis represents an important precursor to this report.

A preliminary report on the PVRC CLEE fatigue crack initiation data review was provided by Van Der Sluys and Yukawa in 1995 [1]. One of the key findings reported by the PVRC CLEE at that time was that a combination of independent environmental parameters is required before reactor water environmental effects become significant. To quote from Van Der Sluys and Yukawa [1],

> "It has been observed that in order to have a large effect of the environment on the S-N fatigue life, a critical combination of conditions is necessary. If any one of the conditions is missing, the effect of the environment on the fatigue life will be moderate."

The six independent environmental parameters are applied strain amplitude, applied strain rate, dissolved oxygen concentration in the reactor water coolant, component metal temperature, component metal sulfur content, and reactor water flow rate. The critical threshold values for carbon and low-alloy steels are:

Strain Amplitude	$\leq 0.1\%$
Strain Rate	$\geq 0.1\%$/sec
Dissolved Oxygen	≤ 0.1 ppm
Temperature	$\leq 150^{\circ}$C (300°F)
Steel Sulfur Content	$\leq 0.003\%$
Water Flow Velocity	> 3 m/sec (120 in/sec)

More recently, the PVRC CLEE has updated the critical thresholds, as given below [2]:

- The **strain amplitude threshold** for carbon and low-alloy steels is 0.07%. F_{en} (ratio of fatigue life in a reactor water environment to fatigue life in air) values shall be used at strain amplitudes equal to or exceeding 0.08%. A linear interpolation can be used to calculate F_{en} values for strain amplitudes between 0.07% and 0.08%. The **strain amplitude threshold** for wrought and cast stainless steels is 0.10%. F_{en} values shall be used at strain amplitudes equal to or exceeding 0.11%. A linear interpolation can be used to calculate F_{en} values for strain amplitudes between 0.10% and 0.11%.
- The **strain rate threshold** is 1.0%/second for carbon and low-alloy steels, and 0.4%/second for wrought and cast stainless steels. If the strain rate associated with the tensile stress load set for any other load set pair exceeds the threshold value, F_{en} is 1.0 for that load set pair.
- The **temperature threshold** for carbon and low-alloy steels is 150°C (302°F). The temperature threshold for wrought and cast stainless steels is 180°C (356°F).
- The **effective dissolved oxygen (DO) content threshold** is applicable only to carbon and low-alloy steels. If the DO is less than or equal to 0.05 ppm, the threshold criterion is satisfied and F_{en} is 1.0.

No threshold criteria are provided in the Van Der Sluys and Yukawa report, "S-N Fatigue Properties of Pressure Boundary Materials in LWR Coolant Environments," [2] for either the component metal sulfur content or the reactor water flow rate. The component metal sulfur content threshold is thought to be too low to provide any relief for typical vessel (< 0.015%) and piping (< 0.025%) materials. It was thought that insufficient information on water flow rate effects was available. Reactor water coolant flow rate has, however, been shown to have an extremely pronounced effect on fatigue life, as discussed in a subsequent section of this report.

The environmental factor F_{en}, cited in the PVRC CLEE threshold parameter discussion, was developed jointly by EPRI and the General Electric Company in 1995 [3]. This factor is defined as the ratio of fatigue life in a reactor water environment to fatigue life in air. The temperature to be used to determine this ratio is a subject of some dispute. The logical choice would be to determine the ratio of fatigue life in reactor water **at temperature** to fatigue life in air **at temperature**. However, the NRC staff requires that F_{en} be defined as the ratio of fatigue life in reactor water **at temperature** to fatigue life in air at **room temperature**. This difference is discussed further in subsequent sections of the report.

The current recommendations of the PVRC CLEE for the F_{en} expressions are provided below, as provided in EPRI report TR-105759 [3]:

For carbon steels the expression is:

$$F_{en} = \exp(0.585 - 0.00124T - 0.101S^*T^*O^*\eta^*). \qquad \textbf{Eq. 2-1}$$

For low-alloy steels the expression is:

$$F_{en} = \exp (0.929 - 0.00124T - 0.101S^*T^*O^*\eta^*). \quad \textbf{Eq. 2-2}$$

In these expressions,

$O^* = 0$ (DO<0.05 ppm)
$O^* = \ln(DO/0.04)$ (0.05 ppm $\leq$ DO $\leq$ 0.5 ppm)
$O^* = \ln(12.5)$ (DO > 0.5 ppm)

For stainless steels, except 316NG, the analytical expression for F_{en} is:

$$F_{en} = \exp [0.935 + \eta_1^*(T_1^* - T_2^*O^*)]. \quad \textbf{Eq. 2-3}$$

In this case, T_1^* and η_1^* are transformed temperature and strain rate, respectively, defined as follows:

$T_1^* = 0$ [T < 250°C (482°F)]
$T_1^* = [(T-250)/525]^{0.84}$ [250 $\leq$ T < 400°C (752°F)]

$\eta_1^* = 0$ (η_1 > 0.4%/sec)
$\eta_1^* = \ln(\eta_1/0.4)$ (0.0004 $\leq \eta_1 \leq$ 0.4%/sec)
$\eta_1^* = \ln(0.0004/0.4)$ (η_1 < 0.0004%/sec)

The parameters T_2^* and O^* are transformed temperature and dissolved oxygen (DO), respectively, defined as follows:

$T_2^* = 0$ [T < 200°C (392°F)]
$T_2^* = 1.0$ [T $\geq$ 200°C (392°F)]

$O^* = 0.260$ (DO < 0.05 ppm)
$O^* = 0.172$ (DO $\geq$ 0.05 ppm)

Van Der Sluys and Yukawa [1] also provided the PVRC CLEE technical position on moderate environmental effects for carbon and low-alloy steels. Their analysis of the collected data in air showed a factor of about 4 to account for temperature effects and for data scatter, leaving a factor of 4 on the ASME mean air data as a reasonable working definition of moderate environmental effects. The PVRC CLEE also observed that the appropriate portion for austenitic stainless steels is about a factor of 2, out of the ASME Code factor of 20 at the low-cycle end of the fatigue design curve. This same sub-factor of around 4 was observed as the actual safety margins in the PVRC fatigue tests on large-scale vessels reported in *Criteria of the ASME Boiler and Pressure Vessel Code for Design by Analysis in Sections III and VIII, Division 2* [4].

Moderate environmental effects are accounted for by adjusting F_{en} by what is referred to as a Z factor. The Z factor is considered to be the available margin that can be used in the determination

of the acceptability of fatigue evaluations that are calculated using environmentally-adjusted fatigue curves appropriate for the material and strain rate of actual plant components.

Part of the justification for the Z factor is based on the characteristics of equations used to fit the laboratory-simulated environmental fatigue data. These equations do not revert to the equations used to fit laboratory air data; instead, even for testing conditions such that simulated reactor water environmental effects are minimal, the equations contain an *environmental shift* much greater than 1. For example, the equation that fits reactor water environmental fatigue data for austenitic stainless steels predicts an asymptotic environmental shift of 2.55, even for temperatures below the environmental threshold.

The above reasoning supports a moderate environmental effects factor of at least 3 for carbon and low-alloy steels, and a factor of at least 1.5 for austenitic stainless steels. It should be pointed out that, in their most recent publications, the PVRC (see "S-N Fatigue Properties of Pressure Boundary Materials in LWR Coolant Environments" [2]) has also recommended moderate environmental effects sub-factors, or Z factors, of 3 for carbon and low-alloy steel, and 1.5 for austenitic stainless steel.

At first, the NRC staff agreed with the modified PVRC recommendation [2] for a moderate environmental factor of 3 (instead of 4) for carbon and low-alloy steels, and a factor of 1.5 (instead of 2) for austenitic stainless steels. More recently, however, the NRC staff has stipulated that no moderate environmental effects factor greater than 1.0 can be credited at all, because of the presumably greater data scatter for laboratory-simulated reactor water environmental effects, relative to the scatter in the air data. While the scatter in the fatigue test data in air showed a scatter factor of about ± 2, the evaluations of scatter in the fatigue test data in simulated reactor water environments have claimed a scatter factor of about ± 5. The NRC staff relied heavily in this judgment on the arguments presented in NUREG/CR-6583 [5].

NUREG/CR-6583 [5] argued that the size effect portion of the factor of 20 is about 1.4; the surface finish factor is between 2.0 and 3.0, and potential errors in the application of Miner's Rule (loading history) introduces a factor of 1.5 to 2.5. With a data scatter factor of 2.5, the total adjustment ranges between 10.0 and 26.0. Any increase in data scatter beyond a factor of about 2.0 would cause the adjustment to be well above the available factor of 20 on cyclic life at the low-cycle end of the fatigue curves.

Recent evaluations of data from Japanese fatigue testing programs have supported this argument. For example, Tsutsumi et al. [6] have analyzed an extensive set of data on austenitic stainless steels, and have also argued that the data exhibit increased variability. This increased variability, if true, would not permit any allocation of the ASME Code factor of 20 to be assigned to moderate environmental effects because surface finish, specimen size effects, and other considerations account for the residual factor of 4. A similar argument on data variability has been made by Higuchi [7] for carbon and low-alloy steels. However, the data evaluations seem to be based on a logical inconsistency—the evaluation of data variability also includes varying environmental effects. That is, the data scatter assessment includes environmental effects variability that should be separated statistically from data scatter assessment within a particular water environment data set.

The topic of data scatter and its impact on moderate environmental effects margins in the ASME Code fatigue design curves is addressed in Section 5 of this report.

2.2 ASME Air Curve Laboratory Data

In June 1961, the ASME Sub-Task Group on Fatigue recommended [8] to the ASME Boiler and Pressure Vessel Committee's Special Committee to Review Code Stress Basis that the formula given below be used in low-cycle fatigue:

$$S = \frac{E}{4\sqrt{N}} \ln \frac{100}{100 - RA} + S_e, \qquad \textbf{Eq. 2-4}$$

where

S = elastic modulus x stain amplitude (psi)

E = elastic modulus (psi)

N = cycles-to-failure

RA = reduction of area in tensile test (percent)

S_e = endurance limit or fatigue strength at 10^7 cycles (psi)

The above formula was used to determine the low-cycle fatigue curves for carbon, low-alloy, and austenitic stainless steel. In each case, a best-fit curve obtained from the method of least squares was applied to the logarithms of the measured S and N values, with Equation 2-4 as the model. The room temperature modulus, E, was known in each case and the computer code gave the best-fit value for RA and S_e These values are shown on the curves reproduced in Figures 2-1, 2-2, and 2-3, taken from the ASME Code criteria document [4].

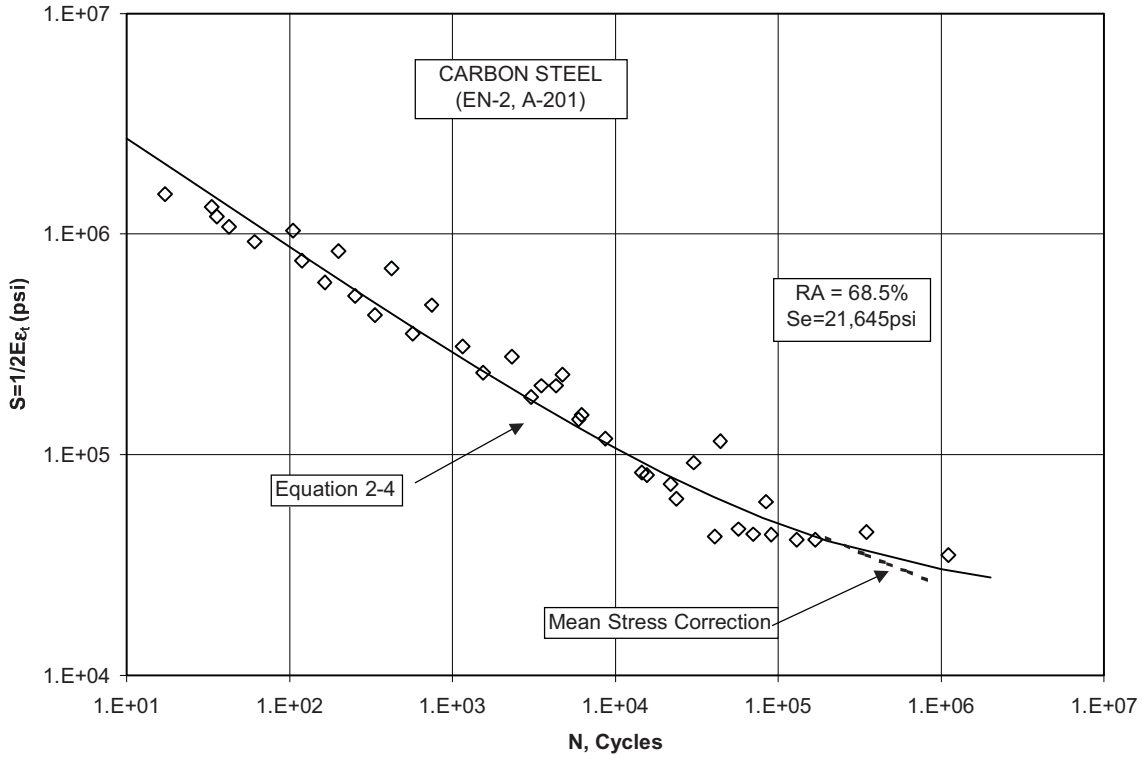

Figure 2-1
ASME Mean Air Fatigue Curve for Carbon Steel

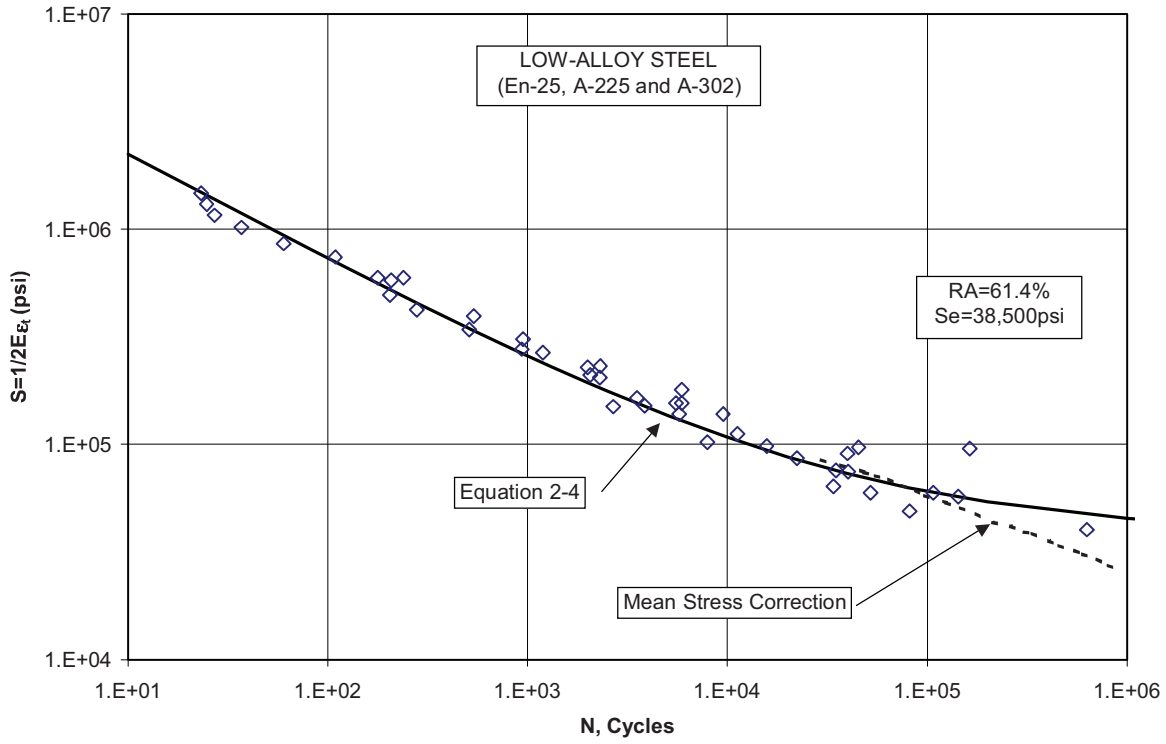

Figure 2-2
ASME Mean Air Fatigue Curve for Low-Alloy Steel

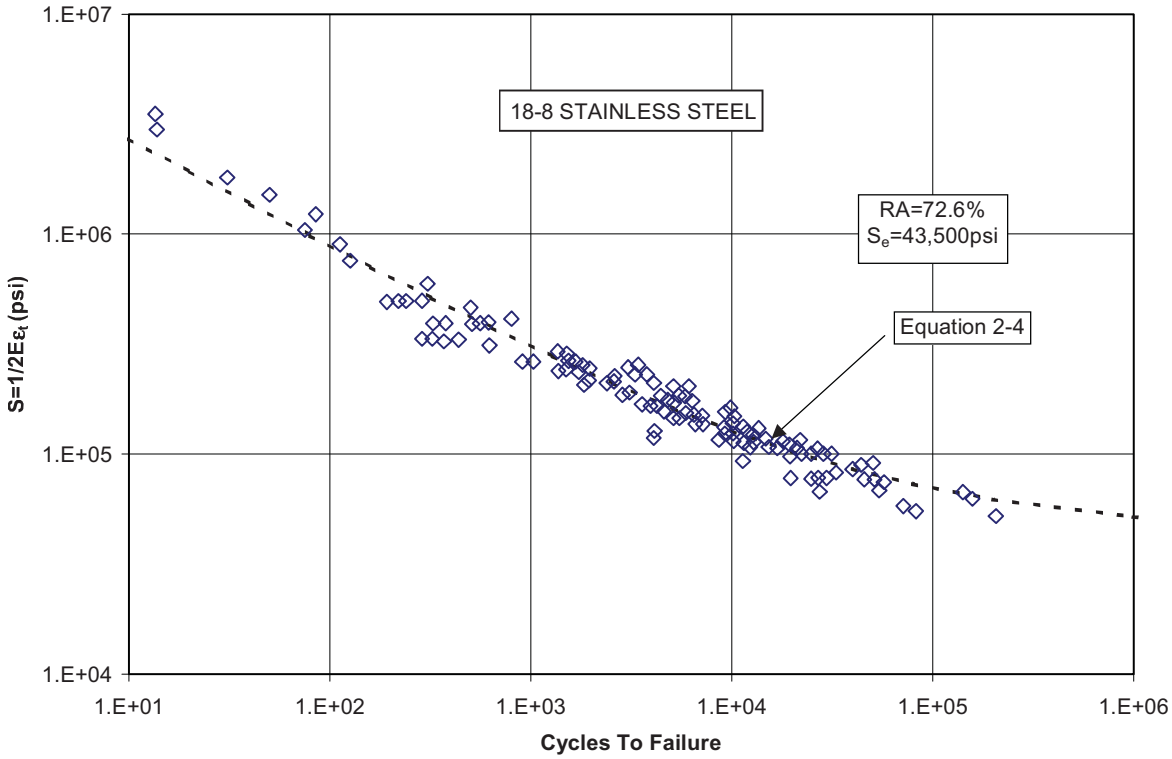

Figure 2-3
ASME Mean Air Fatigue Curve for Stainless Steel

These curves were then corrected for the maximum effect of mean stress using the formula below. This was derived from the Goodman diagram considering the change in the mean stress that is produced by yielding.

$$S' = S\left[\frac{S_u - S_Y}{S_U - S}\right] \text{ for } S < S_{y,} \qquad \textbf{Eq. 2-5}$$

where

S = value from curve
S' = adjusted S value
S_u = ultimate tensile strength
S_y = yield strength

The results from this correction for the mean stress are shown in Figures 2-1 and 2-2 as dotted lines. Due to their high endurance limit and low-yield strength, austenitic stainless steels cannot sustain a mean stress at a cyclic strain level that would produce failure (Figure 2-3). The best-fit lines, as expressed by Equation 2-4, appear to fit the data well. In these cases, all of the results are from strain-controlled experiments and the results are all in what is considered the low-cycle region.

2.3 ASME Austenitic Stainless Steel Air Curve Issue

Another issue has been identified relative to the mean air curves developed by the ASME Code bodies using Equation 2-4 and Equation 2-5. An apparent discrepancy exists between the ASME Code mean air curve for austenitic stainless steels [4] and the best-estimate data fit by Argonne National Laboratories (ANL) at the high-cycle end (above 10^4 cycles) for austenitic stainless steel fatigue data obtained in laboratory air environments [9].

This apparent discrepancy had been observed previously [10] and was the subject of considerable discussion during the mid-to-late 1970s within the ASME Code bodies concerned with fatigue [11]. At that time, the arguments for adjusting the ASME Code fatigue design curve to eliminate the apparent discrepancy were not deemed to be sufficiently persuasive. The major points made by the discussion participants who favored retaining the existing ASME Code mean air curve data fit were:

- The apparent discrepancy is insufficiently large to justify fine-tuning the high-cycle end of the existing ASME Code mean air curve.
- The apparent discrepancy might have been influenced by load-controlled results within the data set, in contrast with the ASME Code mean air curve that is strictly based on strain-controlled fatigue data.
- The forgiving nature of compositional differences and other metallurgical factors in the low-cycle (plastic strain) region, and the greater influence of these differences and factors in the high-cycle (elastic) region.
- The successful experience with stainless steel components, such as reactor internals, that are subjected to high-cycle, hot functional testing environments prior to service without fatigue failure.

More recently, ANL investigators have reintroduced the apparent discrepancies in the stainless steel, high-cycle, air environment fatigue data fits. NUREG/CR-5999 [9] states that:

> "In the early 1970s, additional data on the fatigue of stainless steels were collected by Jaske and O'Donnell, who developed a revised room-temperature fatigue design (curve). Comparison of the new curve developed by Jaske and O'Donnell with the original curve showed that (the) latter overestimated life for low strain ranges. However, the ASME Code Committee, because of relatively good in-plant experience, did not lower the corresponding portion of the design curve. In effect, the current curve is based on a factor of 1.5 on stress and 20 on cycles rather than the "2 on stress or 20 on cycles" originally proposed."

Several other items from these reports might be relevant for this discussion. U.S. Nuclear Regulatory Commission report GEAP-20244 [12] points out that, for evaluation of carbon and low-alloy steel fatigue data, seven tests in air and eight tests in water using hourglass specimens were excluded from the data set because the specimens yielded 20-30% longer fatigue life than did cylindrical-gauge-length specimens. In addition, the report claims that load-controlled tests in air at room temperature for SA 508, Class 2 forging material showed significantly longer fatigue lives than did strain-controlled tests on the same material.

The major questions to be answered regarding this issue are as follows:

First, are the apparent discrepancies significant? The ratio of alternating stress between 10^6 and 10^8 cycles for the 304 stainless steel air data fits is between 1.25 and 1.50. This implies that a component location with an alternating stress of 34 ksi (234.4 MPa) would be expected to fail at 10^8 cycles in the more conservative case, whereas the less conservative case would require an alternating stress of 42 ksi (289.6 MPa). The uncertainty in cyclic stress calculation, and in determining any stress intensification, might be of equal or greater significance.

Second, are there enough valid data points in the high-cycle life region above 10^6 cycles to justify the disputation of existing data fits that are heavily influenced by low-cycle data? The paucity of data in the very high-cycle end of the spectrum implies that any data fit in that region is relatively less robust than the data fit at lower cyclic lives.

Third, are the lower data points in the high-cycle region influenced by load-controlled data interspersed with strain-controlled data? The ASME Code intent is to rely on strain-controlled data because of the similarity to fatigue damage accumulation in actual component geometry. Load-controlled experiments should produce shorter fatigue lives, all other things being equal, by the very nature of specimen compliance. However, under high-cycle fatigue loading and essentially elastic specimen behavior, with little stress redistribution, the differences might not be significant.

Fourth, should cylindrical-gauge-length specimens be preferred in the high-cycle region where elastic behavior dominates? An argument could be made that hourglass fatigue specimens, which are preferred by many investigators, should be required for fatigue testing in the elastic range. Hourglass specimens guarantee that fatigue failure will occur at a specific location (that is, the narrowest portion of the hourglass shape), so that metallurgical variability effects are statistically minimized. A cylindrical-gauge-length specimen will be influenced by *weakest-link* effects because approximately the same level of stress exists over a substantial volume of material. Real component behavior is more similar to that of the hourglass specimen, with geometric and loading discontinuities or concentrations that tend to isolate fatigue damage. Large volumes of component material are not simultaneously subjected to high stresses.

Fifth, is the effective ASME Code fatigue margin of 1.5 adequate when the conservative approach used by ANL to obtain their best-estimate data fit is taken into account? When all of the above arguments are assembled, a Code margin of 2.0 seems to be applicable to purely strain-controlled, hourglass specimen data, while a Code margin of 1.5 arguably applies to a mix of strain-controlled and load-controlled data obtained from cylindrical-gauge-length specimens.

2.4 PVRC Database and Analysis

In 1992 the PVRC organized an activity to review the available information and make recommendations to the ASME BNCS on any modifications to the Code to reflect the new information on the effect of reactor water environments on fatigue life. In order to accomplish this objective, the first activity of the PVRC Working Group on S-N Curve Data Analysis was to collect all of the laboratory data available. As a result of inquiries and solicitation, a large amount of data, totaling nearly 2500 S-N test results in air and water environments, has been

received and compiled. A summary of the sources represented by the PVRC database, as categorized by material, test environment, and test parameters is presented in Table 2-1. This database has been used in the S-N data analysis presented in the tables and graphs in this report.

Table 2-1
PVRC Environmental Fatigue Database

Source	Reference	Material	Environment	Number of Tests
General Electric Company	[12]	Carbon Steel	Air and BWR	15
General Electric Company	[13]	Carbon Steel	BWR	160
Japanese	[14], [15], and [16]	Carbon Steel	Air, Water, PWR, BWR	950
		Low-Alloy Steel		
		304&316 SS		
		Inconel 600		
Japanese	[17]	316SS,Weld Metal	PWR, Water	96
Argonne National Laboratory	[9] and [17]	SS Steel	Air, PWR, BWR	100
		Carbon Steel		
		Low-Alloy Steel		
Babcock & Wilcox	[18]	Carbon Steel	Typical Fossil Power Plant	38
MEA	[19]	Carbon Steel	Air, Water	40
German	[20]	Carbon Steel	Air, Water	222
		Low-Alloy Steel		
Russian	[21]	Carbon Steel	Pure Water	69
		Low-Alloy steel		
Jaske & O'Donnell	[10]	Stainless Steels and Nickel-Based Alloys	Air	800

Carbon Steel

Figure 2-4 shows the room temperature air data for carbon steel that is included in the PVRC database. Figures 2-5, 2-6, and 2-7 show the PVRC carbon steel data in air at 250°C (482°F), 274°C (525°F), and 288°C (550°F), respectively. The figures also show the superposed ASME carbon steel mean air curve and the ASME Code carbon steel fatigue design curve.

The results of the PVRC S-N data review show that laboratory fatigue crack initiation data for carbon steels in an air environment at various temperatures are in good agreement with the ASME Code carbon steel mean air curve, with a data scatter factor of less than 3.

Figure 2-8 shows the PVRC data for carbon steels obtained under simulated PWR reactor water conditions. Figure 2-9 shows these same data after being shifted by the appropriate environmental factor, F_{en}. The environmental shift brings the data essentially back to the ASME mean air curve line, with slight under-shift at the low-cycle end of the curve and a slight over-shift at the high-cycle end of the curve. Figure 2-10 shows the same data after the shifted crack initiation points are adjusted by the moderate environmental effects factor, Z. All of the adjusted data points fall between the ASME mean air curve and the ASME design curve, except at the very high-cycle end of the curve. All of the laboratory fatigue crack initiation data for carbon steels satisfy the PVRC environmental parameter thresholds for moderate environmental effects, with no data points corrected by F_{en}/Z approaching the ASME Code carbon steel design fatigue curve.

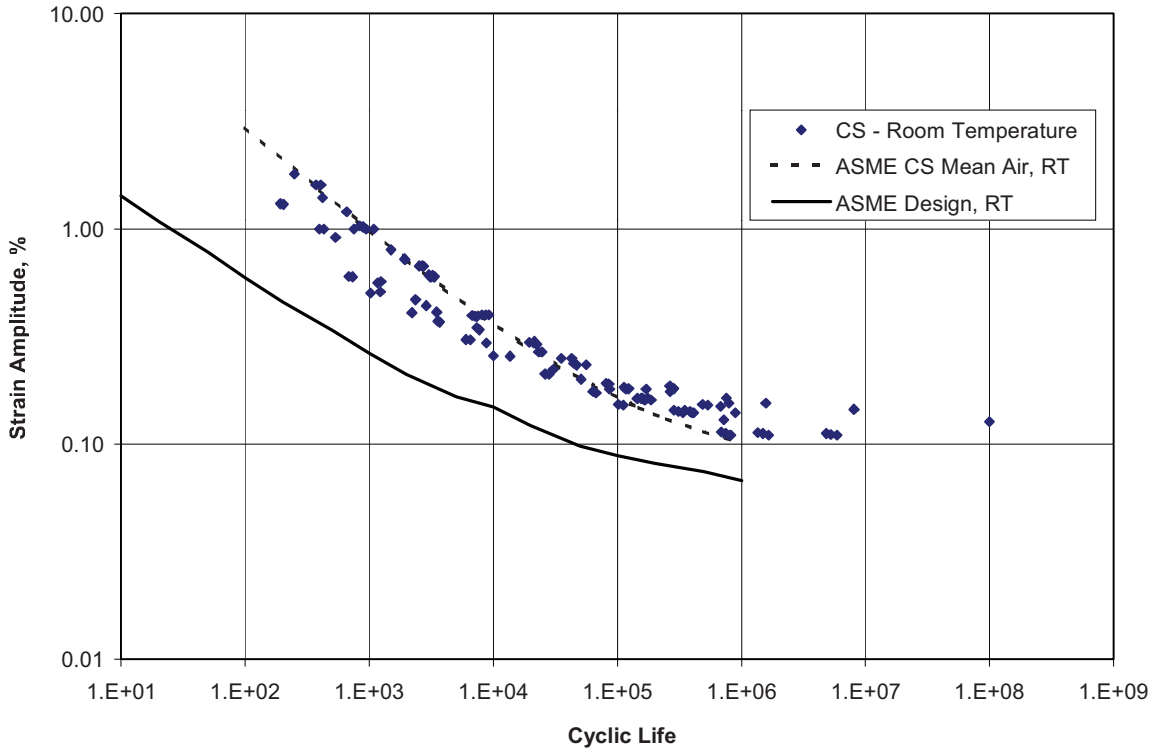

Figure 2-4
PVRC Room Temperature Air Data for Carbon Steel

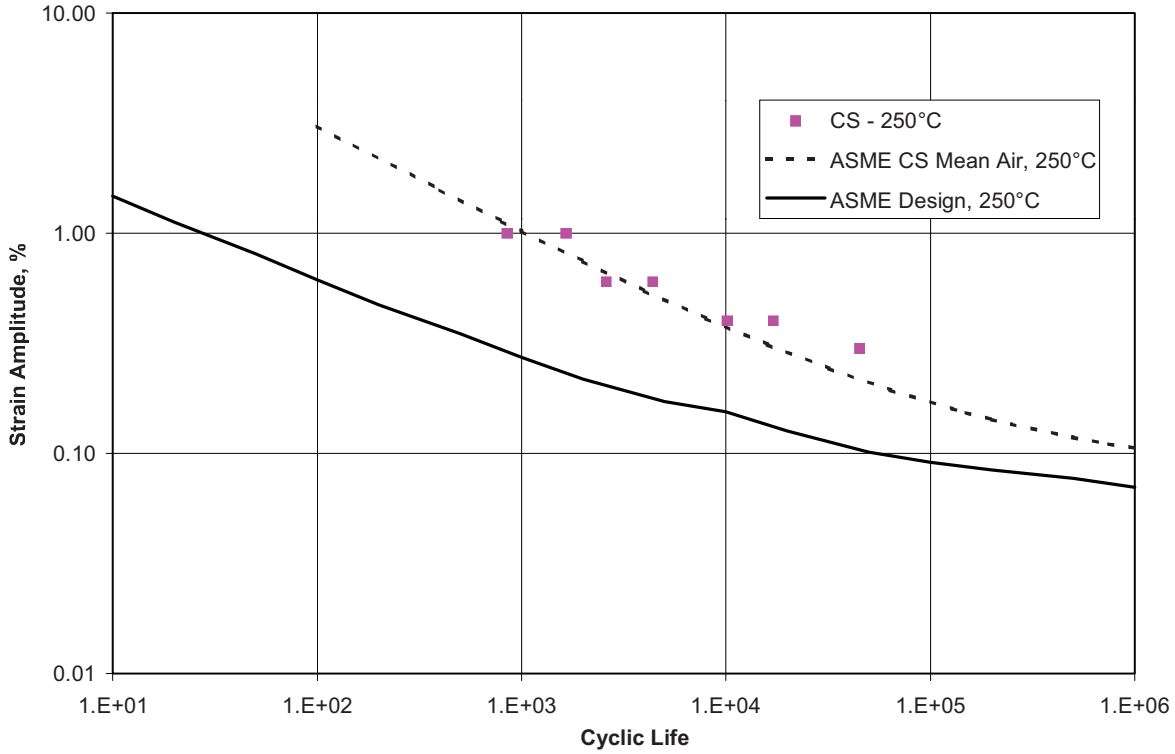

Figure 2-5
PVRC Air Data for Carbon Steel at 250°C (482°F)

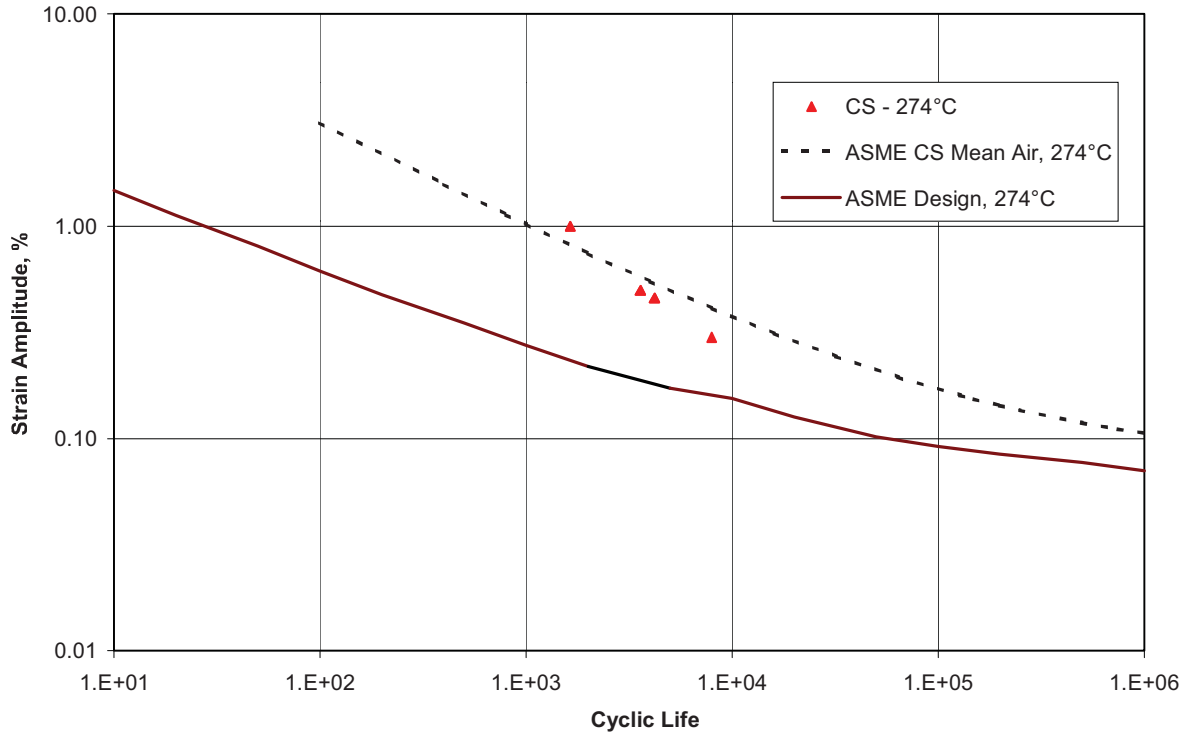

Figure 2-6
PVRC Air Data for Carbon Steel at 274°C (525°F)

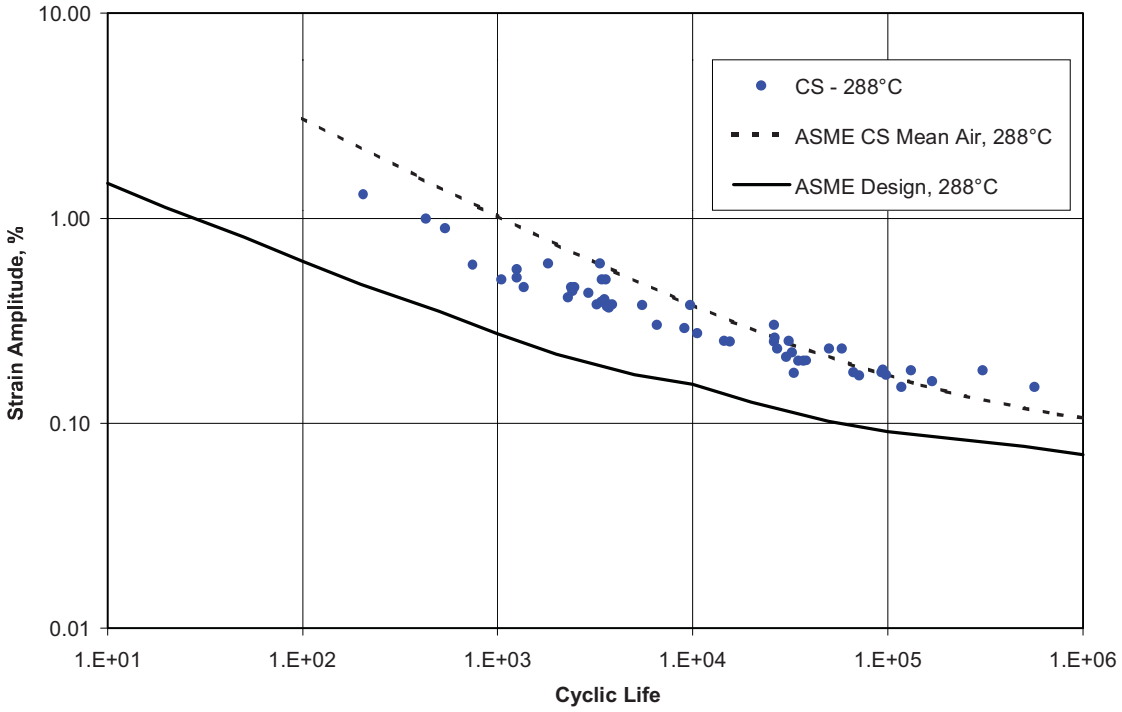

Figure 2-7
PVRC Air Data for Carbon Steel at 288°C (550°F)

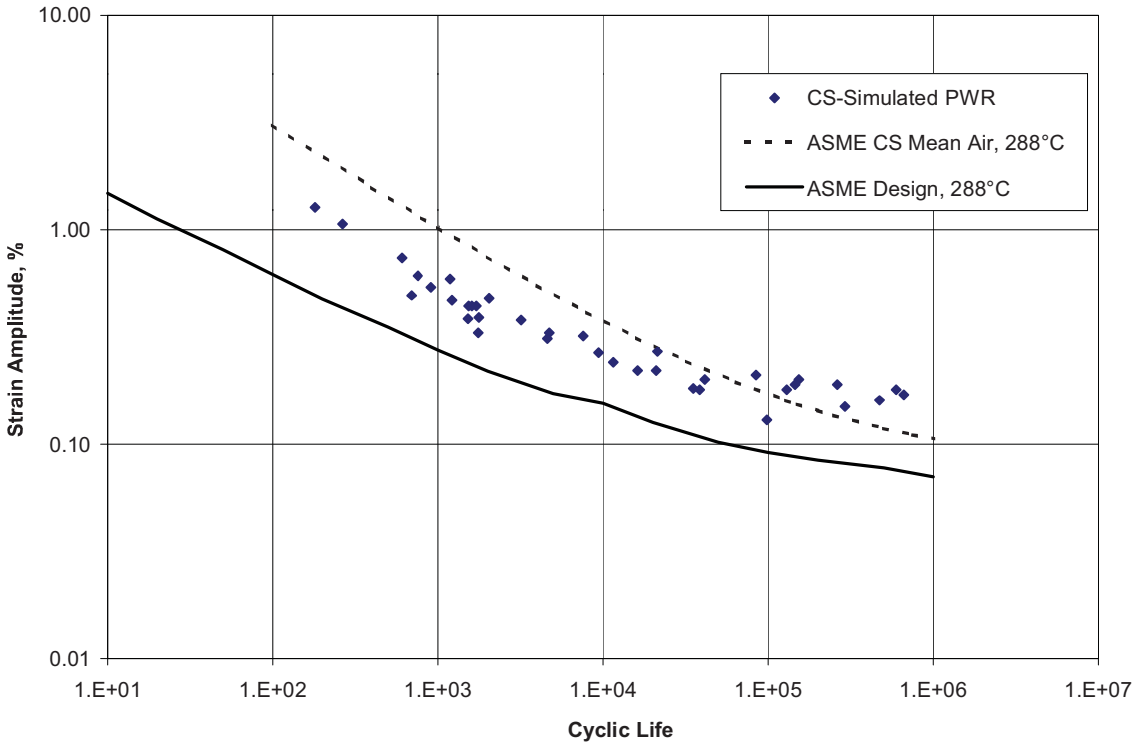

Figure 2-8
PVRC Data for Carbon Steels Obtained Under Simulated PWR Conditions

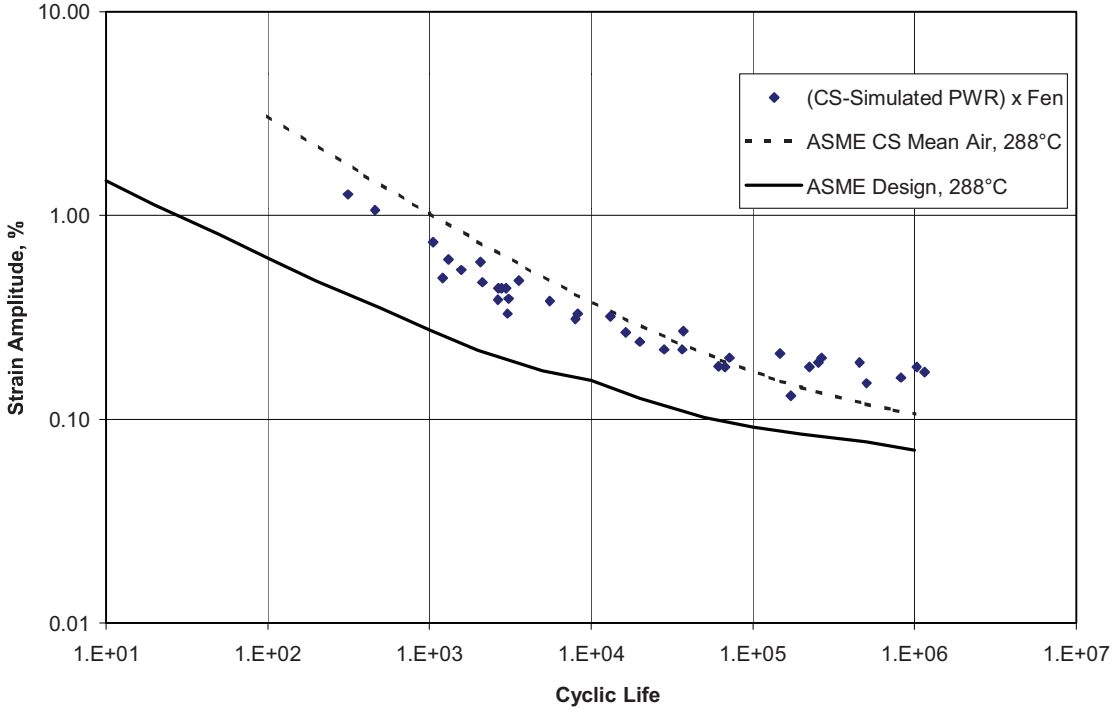

Figure 2-9
PVRC Data for Carbon Steels Obtained Under Simulated PWR Conditions and Corrected by F_{en}

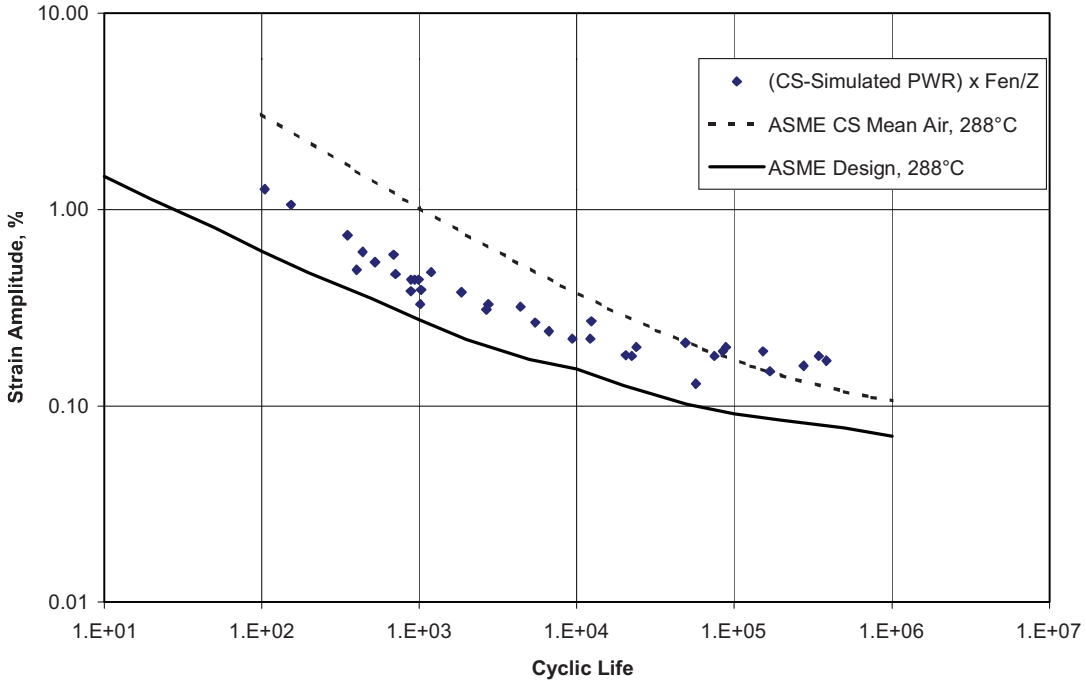

Figure 2-10
PVRC Data for Carbon Steels Obtained Under Simulated PWR Conditions, Corrected by F_{en}, and Adjusted by the Moderate Environmental Effects Factor, Z

In contrast, Figure 2-11 shows the complete set of laboratory data obtained under simulated BWR reactor water environments. The data scatter is very large. Figure 2-12 shows these same data after correction by the appropriate environmental shift, F_{en}. The data scatter is much smaller after correction for different environments and the shifted data points match well with the ASME mean air curve. Figure 2-13 shows these data after adjustment for moderate environmental effects. Note that the adjusted data points lie between the ASME mean air curve and the ASME Code design curve, except for the over-corrected points at the high-cycle end of the curve. A small number of adjusted data points approach the ASME Code carbon steel fatigue design curve.

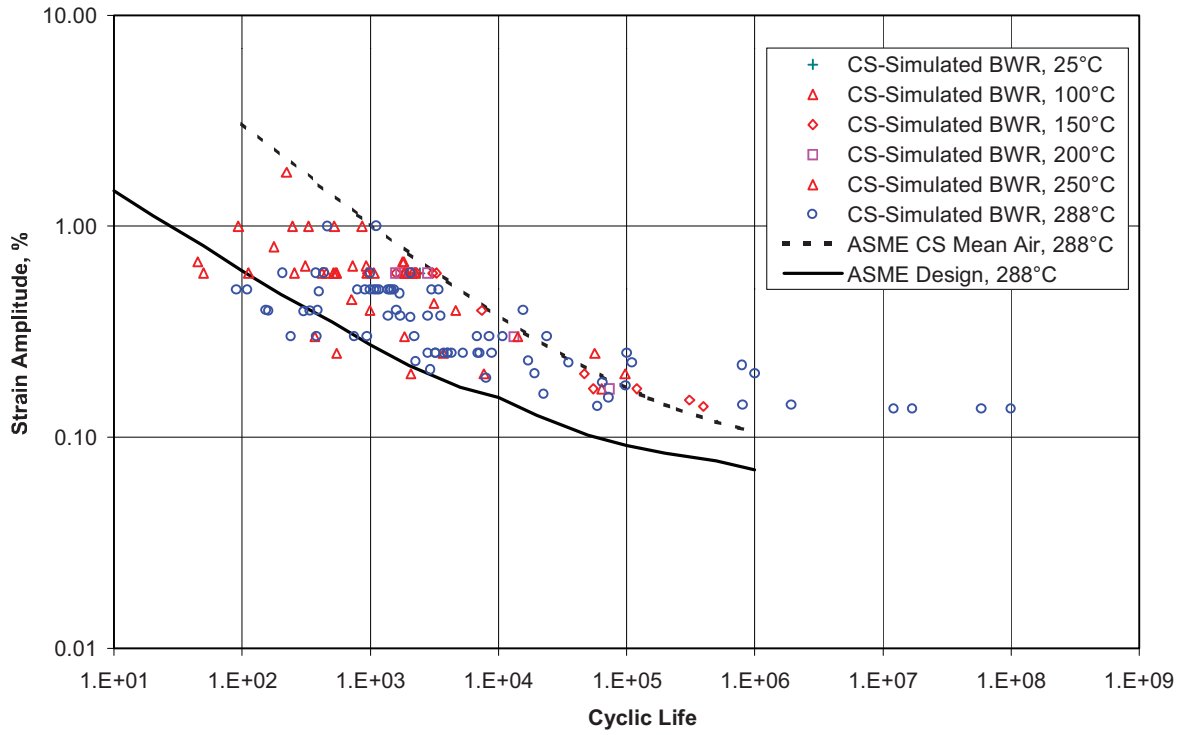

Figure 2-11
PVRC Laboratory Data Obtained Under Simulated BWR Reactor Water Environments

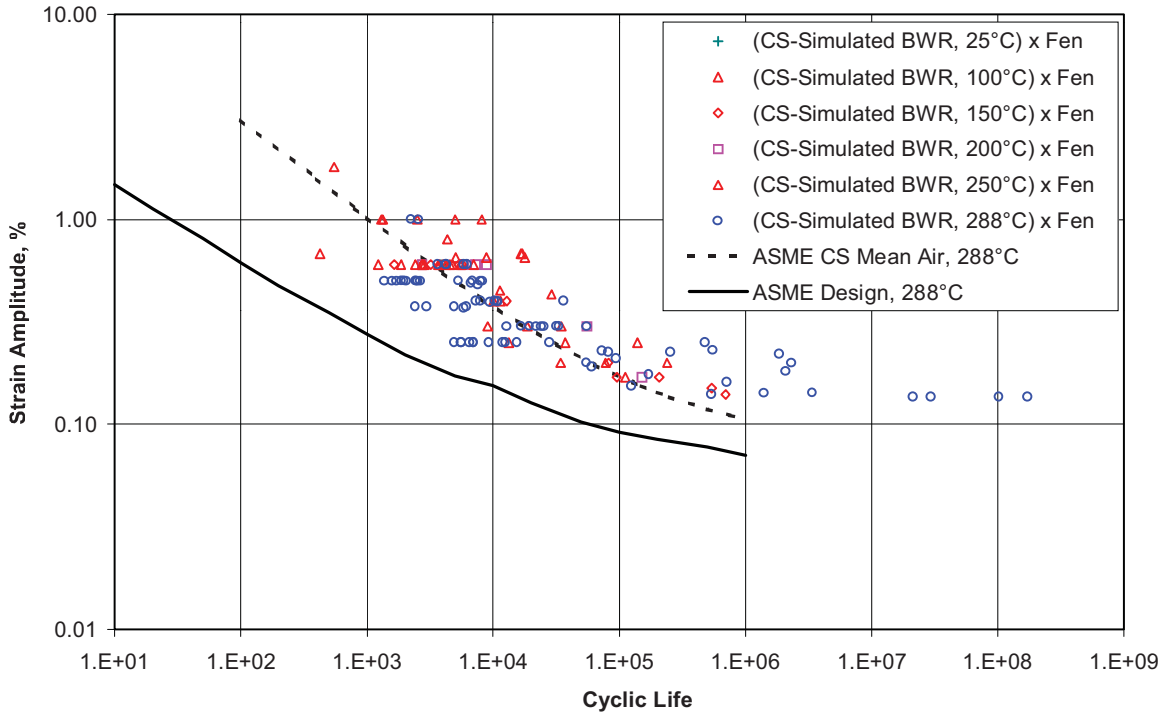

Figure 2-12
PVRC Laboratory Data Obtained Under Simulated BWR Reactor Water Environments and Corrected by F_{en}

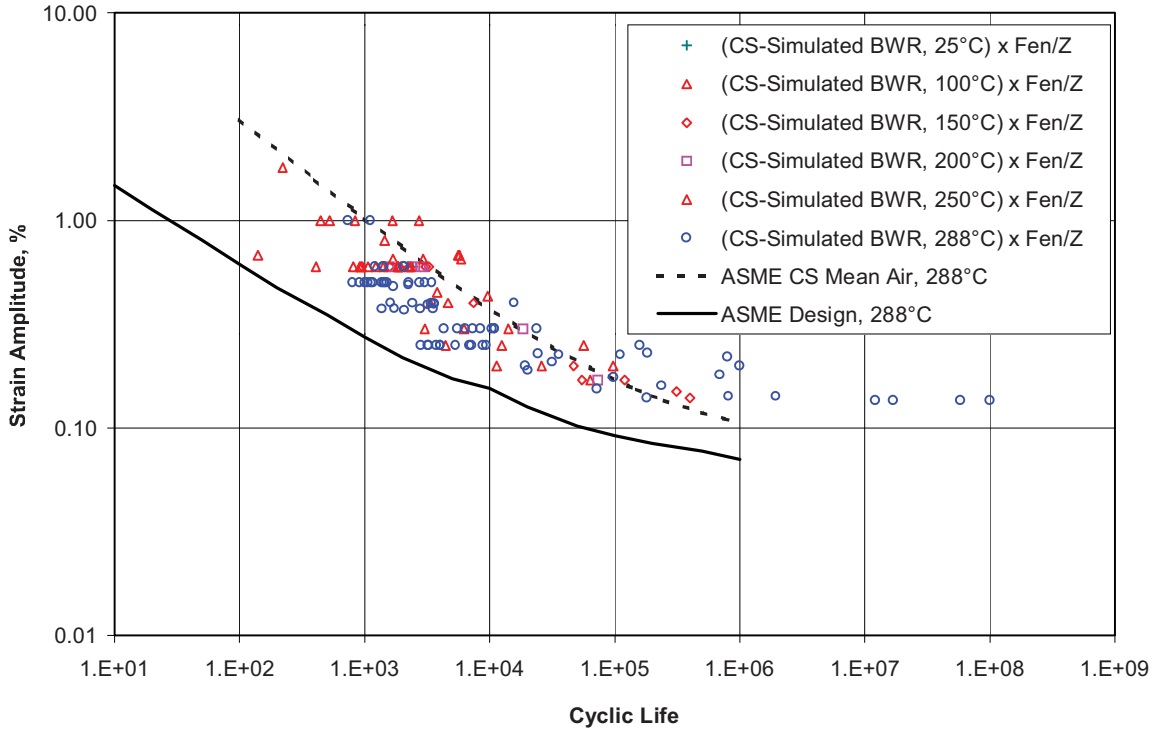

Figure 2-13
PVRC Laboratory Data Obtained Under Simulated BWR Reactor Water Environments and Corrected by F_{en} and Z

Low-Alloy Steel

Figure 2-14 shows the PVRC data set for low-alloy steels tested at room temperature, and the comparison with the ASME mean air curve and the ASME Code fatigue design curve for low-alloy steel. Figures 2-15, 2-16, and 2-17 show the PVRC low-alloy steel data set for testing in air at 150°C (302 °F), 200°C (392 °F), and 288°C (550 °F), respectively. In all cases, the laboratory air data are in excellent agreement with the ASME mean air curve with a data scatter of about a factor of 2.

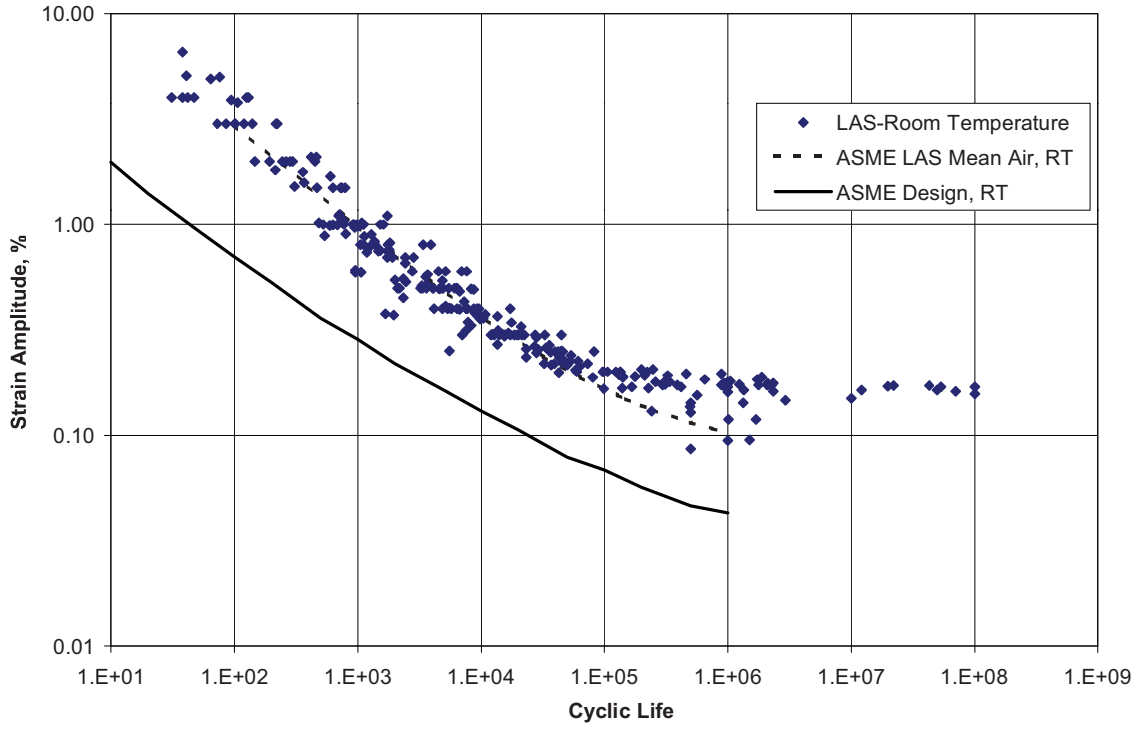

Figure 2-14
PVRC Data for Low-Alloy Steel at Room Temperature

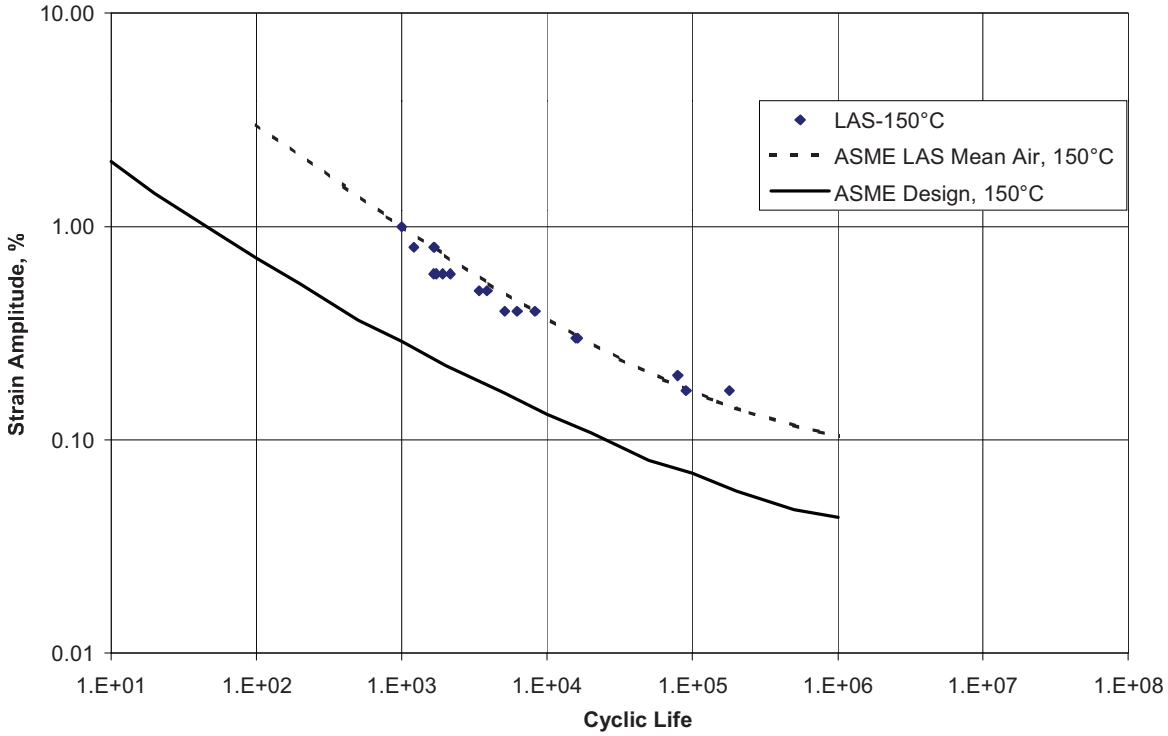

Figure 2-15
PVRC Data for Low-Alloy Steel at 150°C (302°F)

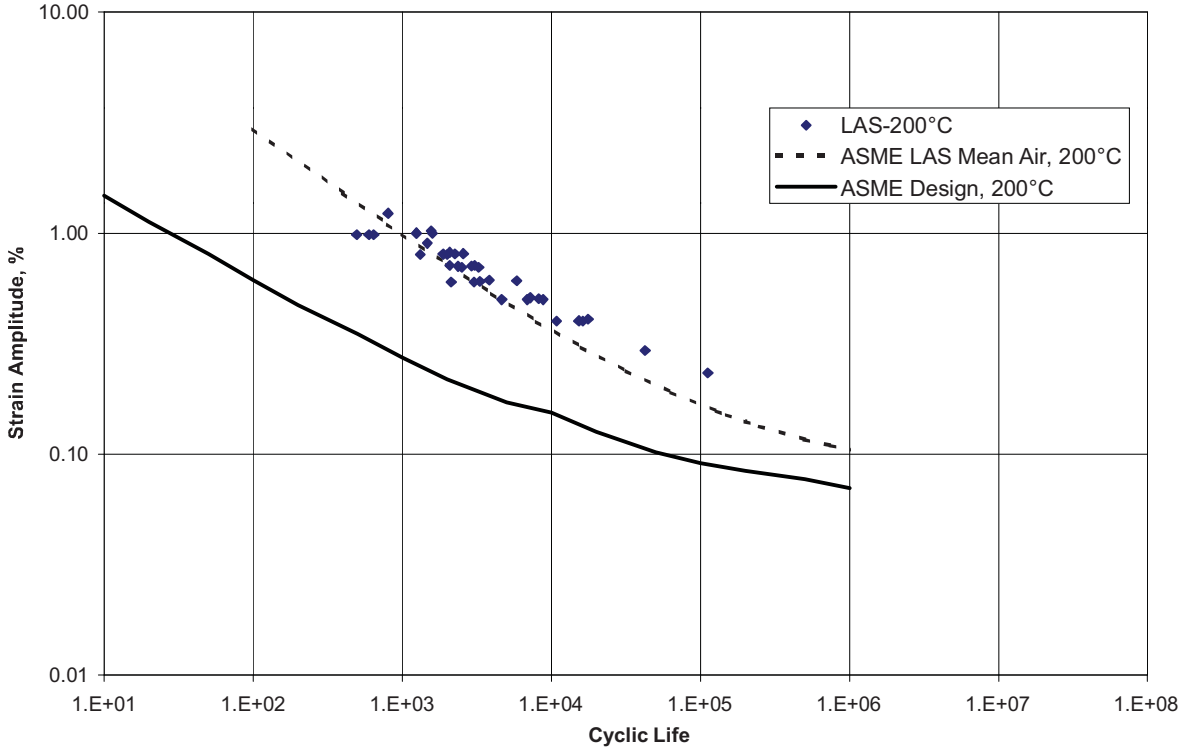

Figure 2-16
PVRC Data for Low-Alloy Steel at 200°C (392°F)

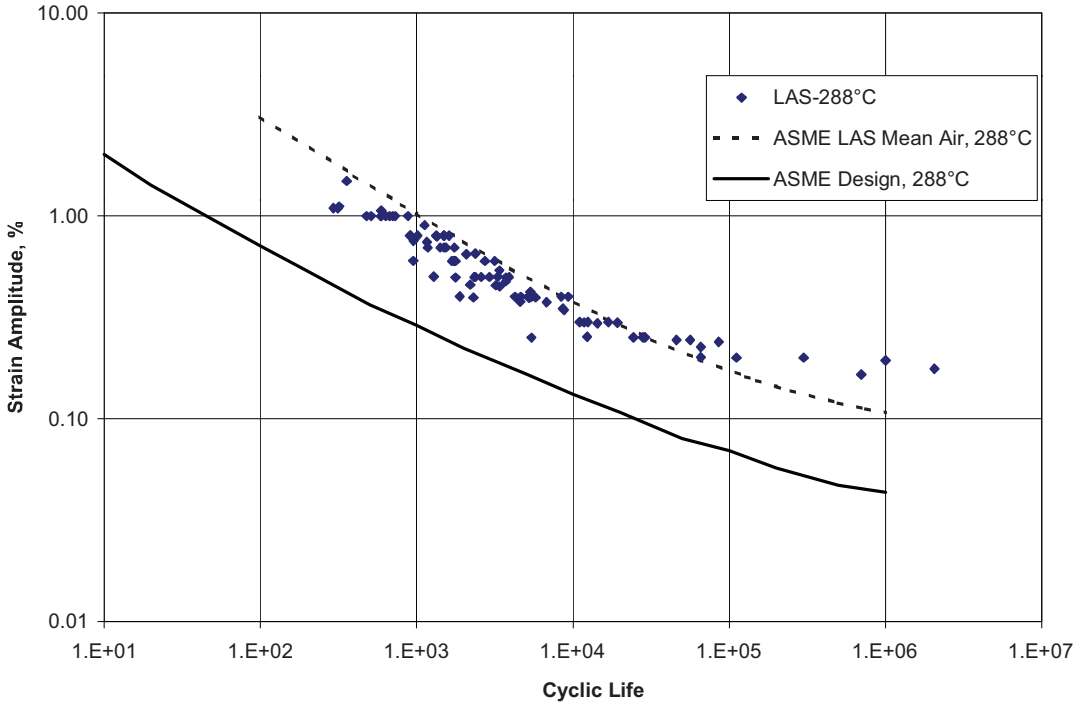

Figure 2-17
PVRC Data for Low-Alloy Steel at 288°C (550°F)

Figure 2-18 and Figure 2-19 show the PVRC data sets for simulated PWR and BWR reactor water environments, respectively. Also shown in Figure 2-18 and 2-19 are the ASME mean air curve for low-alloy steel and the ASME Code fatigue design curve for low-alloy steel. The light dashed line in the two figures is the ASME mean air curve reduced by a factor of 2. This dashed line illustrates the scatter in the data. There is very little scatter in the low-alloy steel data in a PWR environment, but considerable scatter in the low-alloy steel data in a BWR environment. The scatter in the BWR environmental data is much more pronounced at the low-cycle end of the data set. Laboratory fatigue crack initiation data for low-alloy steels in simulated PWR reactor water environments satisfy the PVRC environmental parameter thresholds for moderate environmental effects, with no need to correct the environmental data by F_{en}.

With the exception of a very few data points obtained at very high strain range (very low cycle fatigue), laboratory fatigue crack initiation data for low-alloy steels in simulated BWR reactor water environments satisfy the PVRC environmental parameter thresholds for moderate environmental effects. Figure 2-20 shows the BWR environmental data shifted by the appropriate F_{en}. Data points shifted by F_{en} are generally over-corrected relative to the ASME Code low-alloy steel mean air curve, especially above a cyclic life of 10,000 cycles. However, a few data points approach the ASME Code low-alloy steel fatigue design curve at the low-cycle end of the data after correction by F_{en}/Z (see Figure 2-21).

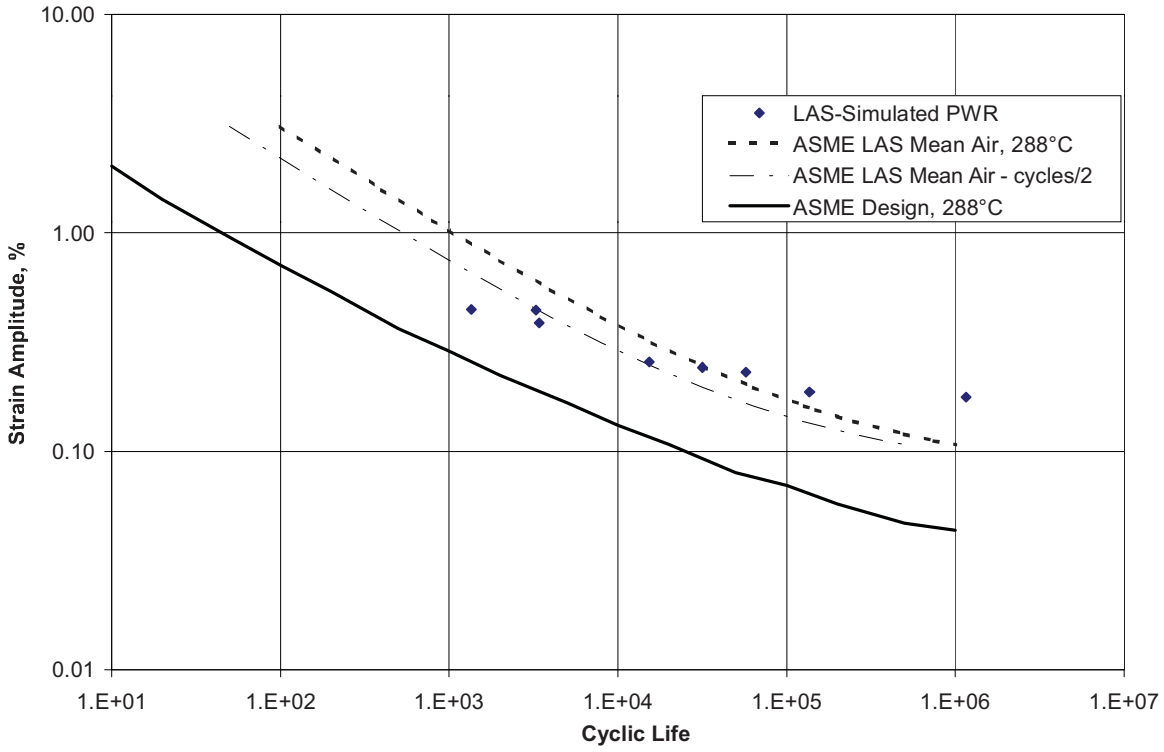

Figure 2-18
PVRC Data for Low-Alloy Steel Obtained Under Simulated PWR Conditions

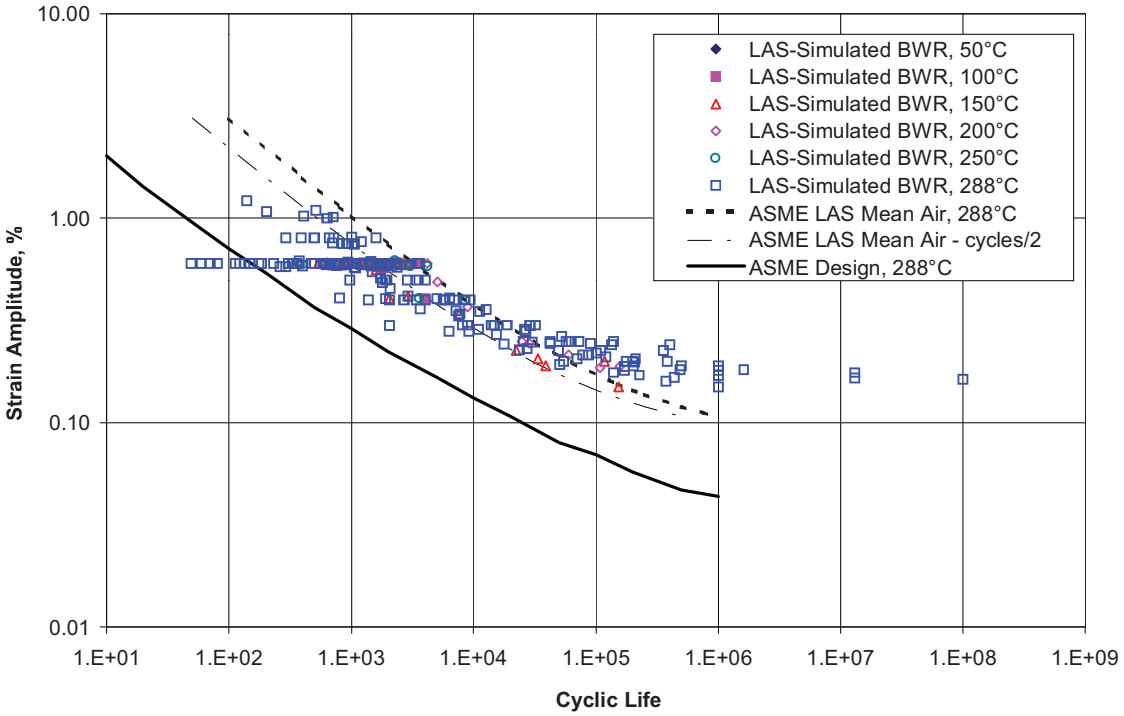

Figure 2-19
PVRC Data for Low-Alloy Steel Obtained Under Simulated BWR Conditions

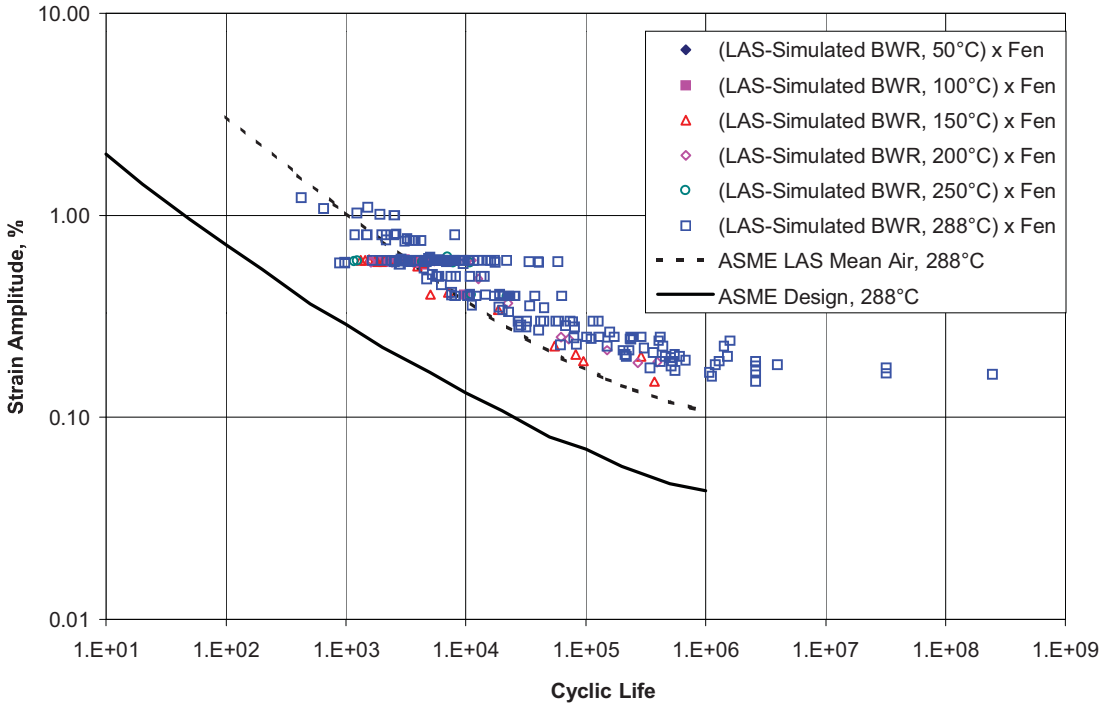

Figure 2-20
PVRC Data for Low-Alloy Steel Obtained Under Simulated BWR Conditions and Corrected by F_{en}

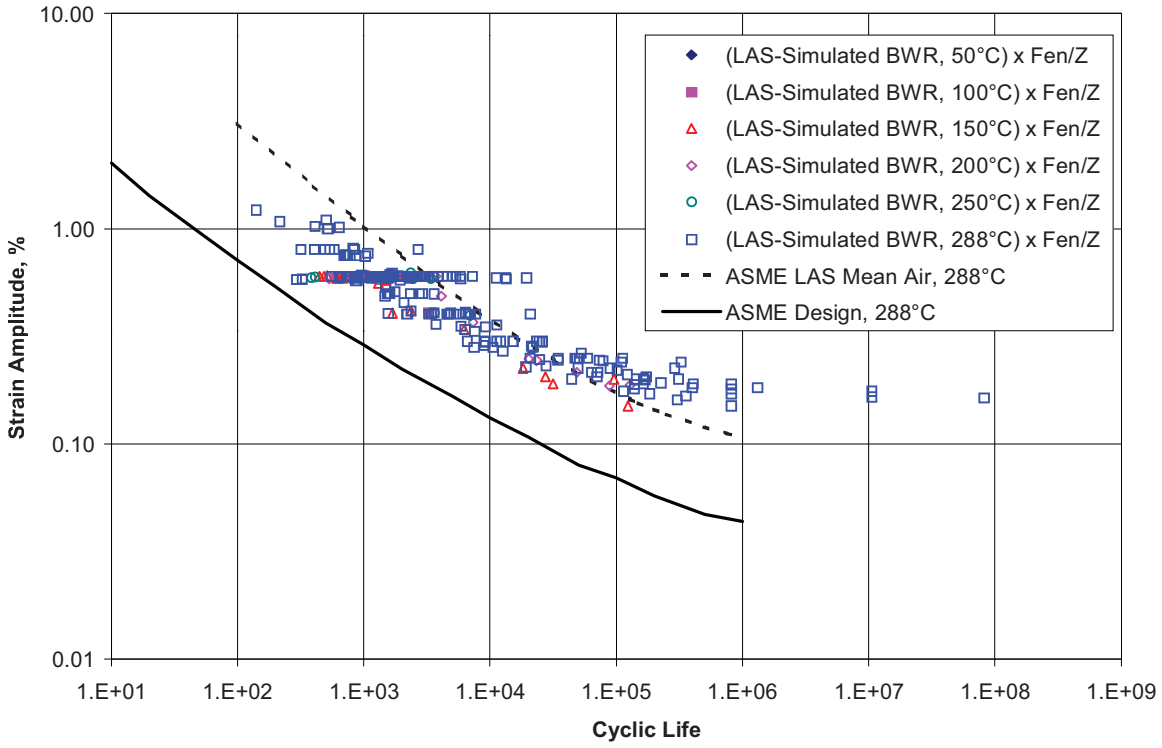

Figure 2-21
PVRC Data for Low-Alloy Steel Obtained Under Simulated BWR Conditions and Corrected by F_{en} and Z

Austenitic Stainless Steel

Figure 2-22 shows the PVRC data set for austenitic stainless steel tested in an air environment at room temperature. Also shown on the figure are the ASME mean air curve and the ASME Code fatigue design curve for austenitic stainless steel. Figure 2-23 shows the data set for austenitic stainless steel in an air environment at room temperature with the data from Jaske and O'Donnell [10] added. Note that the scatter in the data is much greater in Figure 2-23 than in Figure 2-22. Figure 2-24 and Figure 2-25 show the PVRC data set and the PVRC data set augmented by the Jaske and O'Donnell data in air environments at 288°C (550°F). As can be seen from all four of these figures, laboratory fatigue crack initiation data for austenitic stainless steels in an air environment at various temperatures do not agree very well with the ASME Code mean air curve. More than half of the data lie below the air curve data fit. The ANL mean air curve data fit, shown on the room temperature plots, is in much better agreement, confirming criticism of the ASME Code mean air curve from the late 1970s. However, the strain control versus load control characteristics of much of the Jaske and O'Donnell data set cannot be determined. Load-controlled test results would tend to provide data below strain-controlled test results.

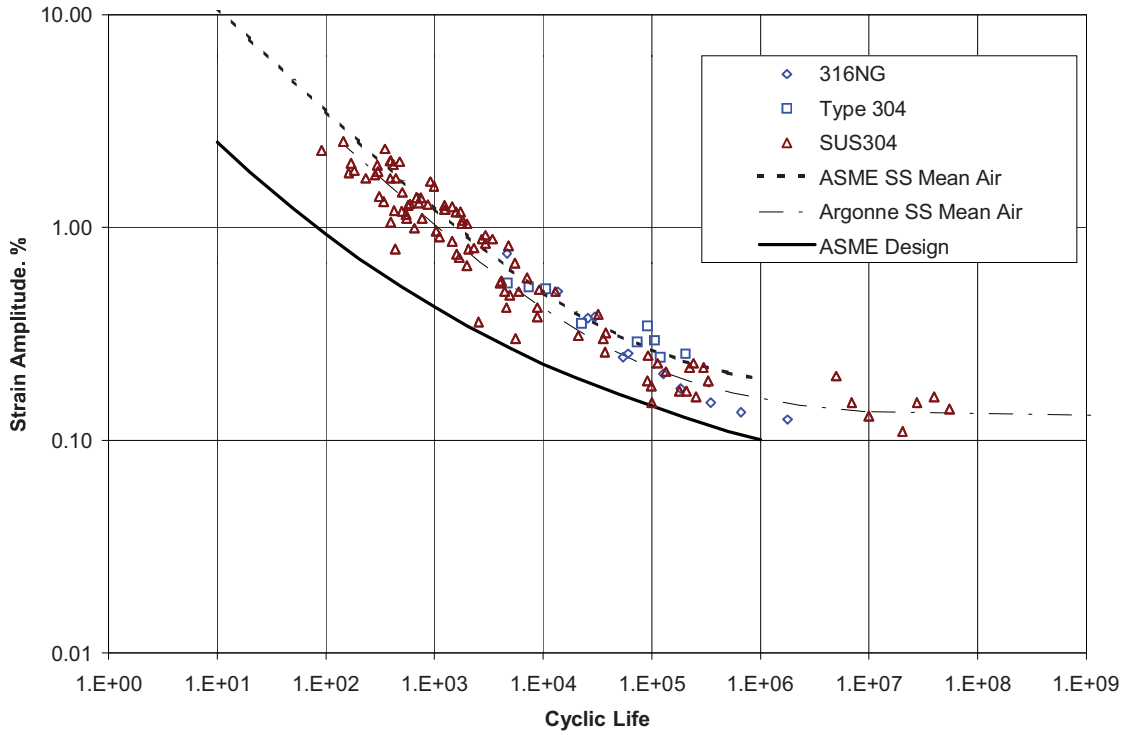

Figure 2-22
PVRC Data for Austenitic Stainless Steel in Air at Room Temperature

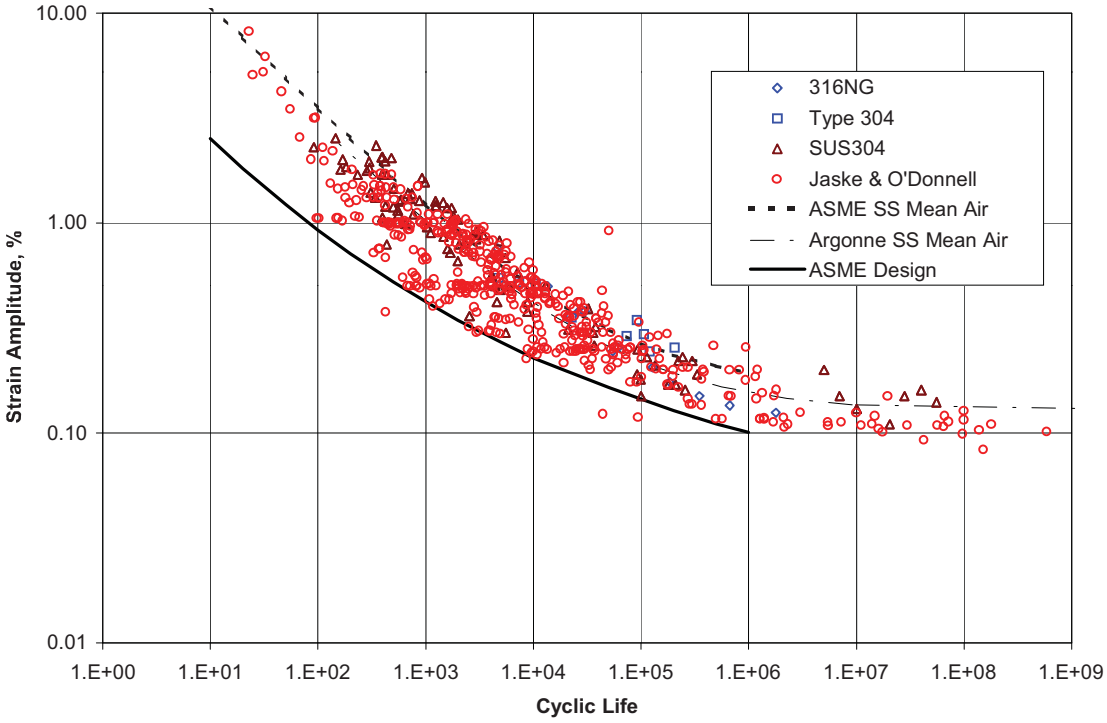

Figure 2-23
PVRC Data for Austenitic Stainless Steel in Air at Room Temperature with Data From Jaske and O'Donnell

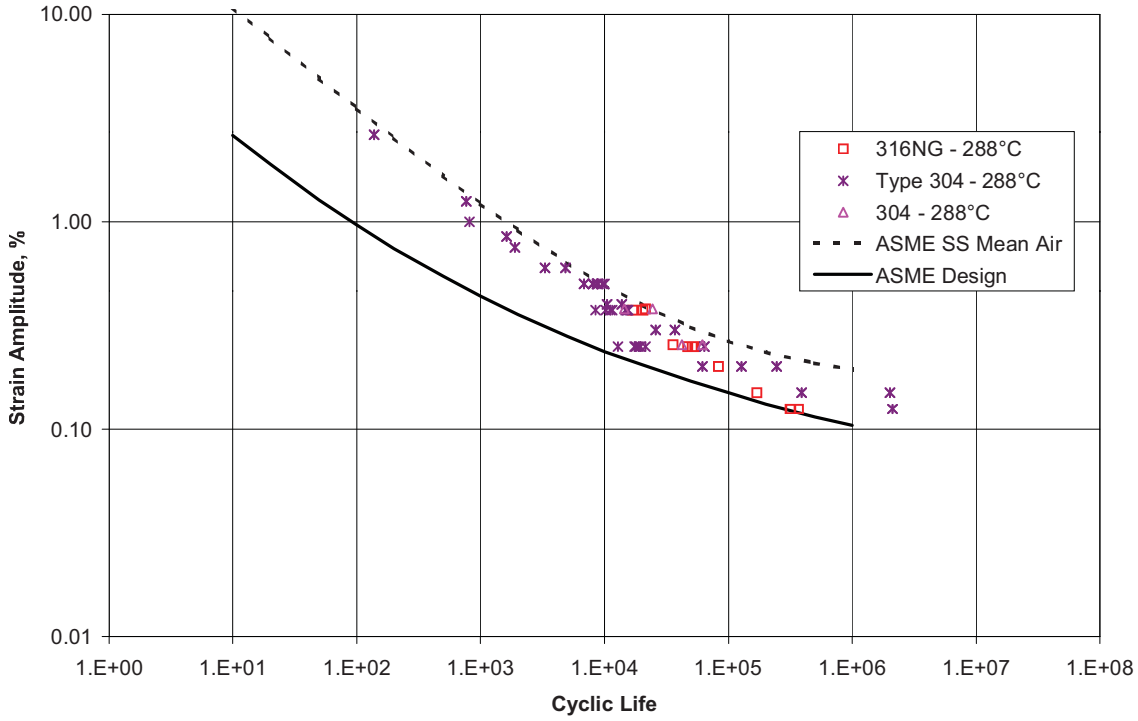

Figure 2-24
PVRC Data for Austenitic Stainless Steel in Air at 288°C (550°F)

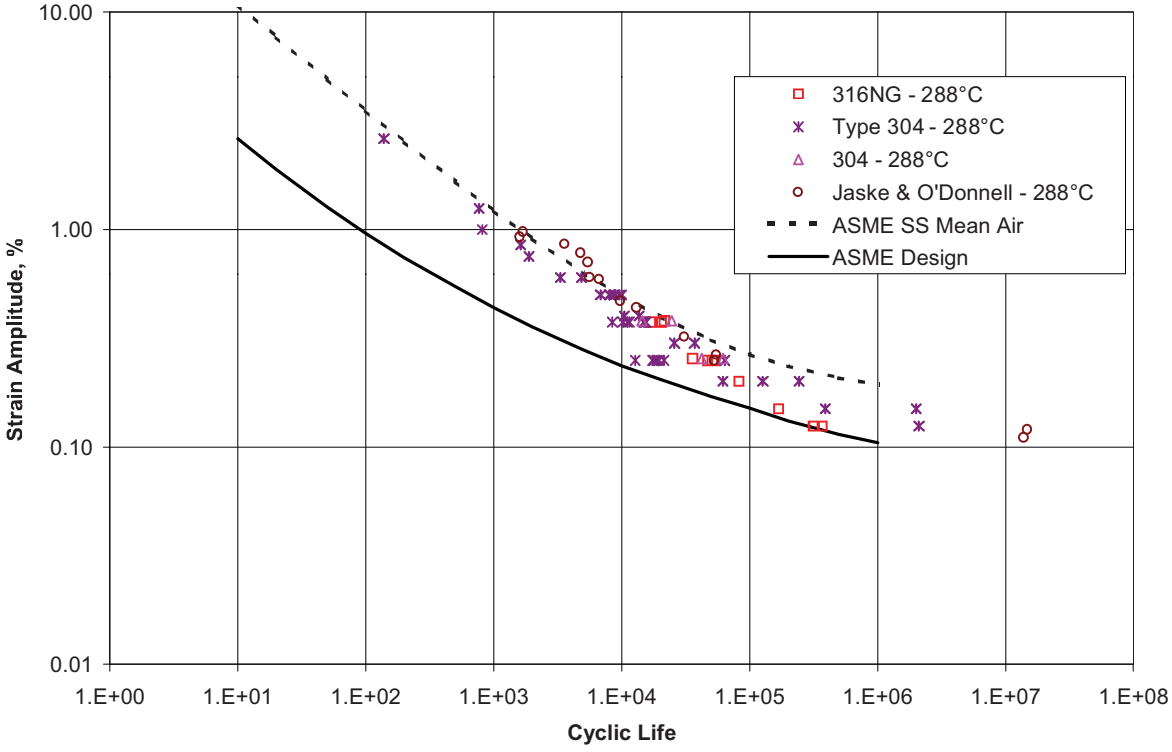

Figure 2-25
PVRC Data for Austenitic Stainless Steel in Air at 288°C (550°F) With Data From Jaske and O'Donnell

Figure 2-26 shows the PVRC data set for austenitic stainless steel specimens tested under simulated PWR reactor water environmental conditions. Figure 2-27 shows these same data after appropriate F_{en} environmental correction, and Figure 2-28 shows the data after the moderate environmental effects factor, Z, is taken into account. The data scatter appears to be large but, as discussed later in Section 5 of this report, the apparent data scatter is a function of combining results obtained under quite different environmental conditions. Figure 2-27 illustrates that simulated PWR reactor water environmental fatigue data, after environmental correction, shift to the ANL mean air curve for the austenitic stainless steels. Figure 2-28 shows that there is no need for any environmental correction except for recognizing moderate environmental effects. A modest tendency to under-correct for the environmental conditions can be observed at the high-cycle end of the data set.

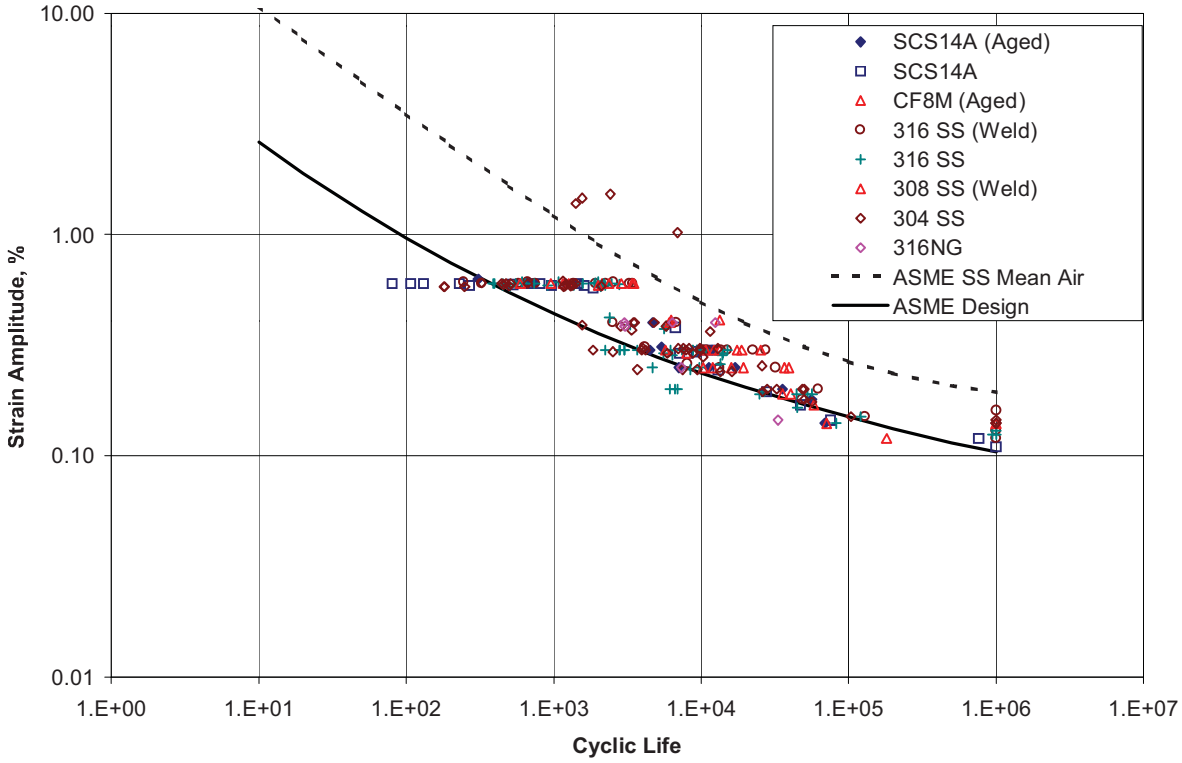

Figure 2-26
PVRC Data for Austenitic Stainless Steel Obtained Under Simulated PWR Conditions

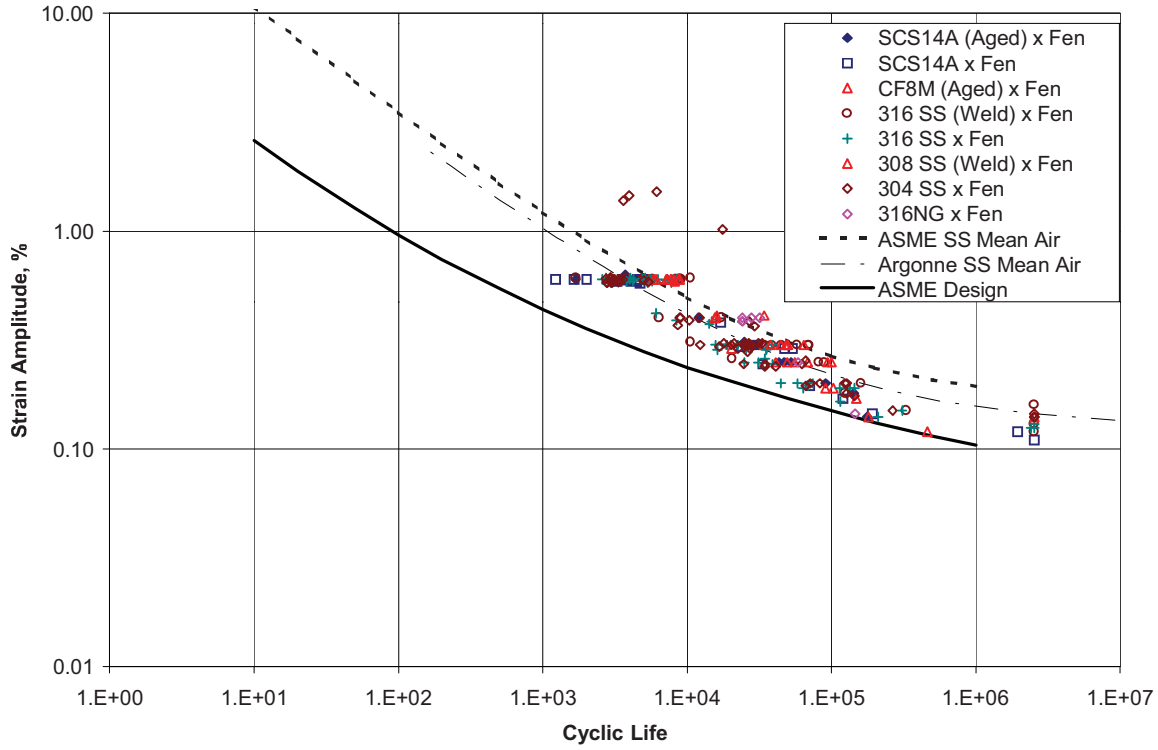

Figure 2-27
PVRC Data for Austenitic Stainless Steel Obtained Under Simulated PWR Conditions and Corrected by F_{en}

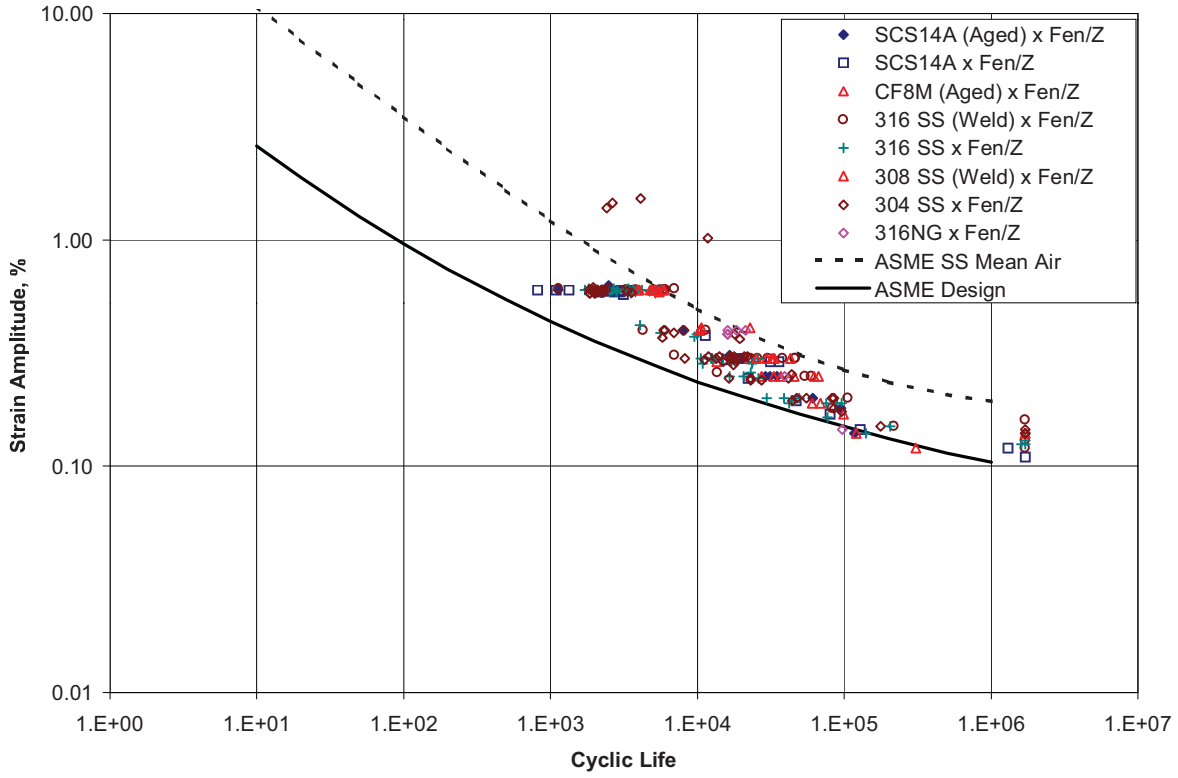

Figure 2-28
PVRC Data for Austenitic Stainless Steel Obtained Under Simulated PWR Conditions and Corrected by F_{en} and Z

Figures 2-29, 2-30, and 2-31 show a much smaller data set for nuclear grade 316 stainless steel tested in a simulated BWR oxygenated reactor water environment at temperature, both before (Figure 2-29) and after environmental correction (Figure 2-30) and moderate environmental effects adjustment (Figure 2-31). The data scatter is small and similar conclusions are seen for this material in a BWR environment as was seen for all stainless steels in a PWR environment. Again, a slight tendency for environmental effects under correction is observed at the high-cycle end of the data set.

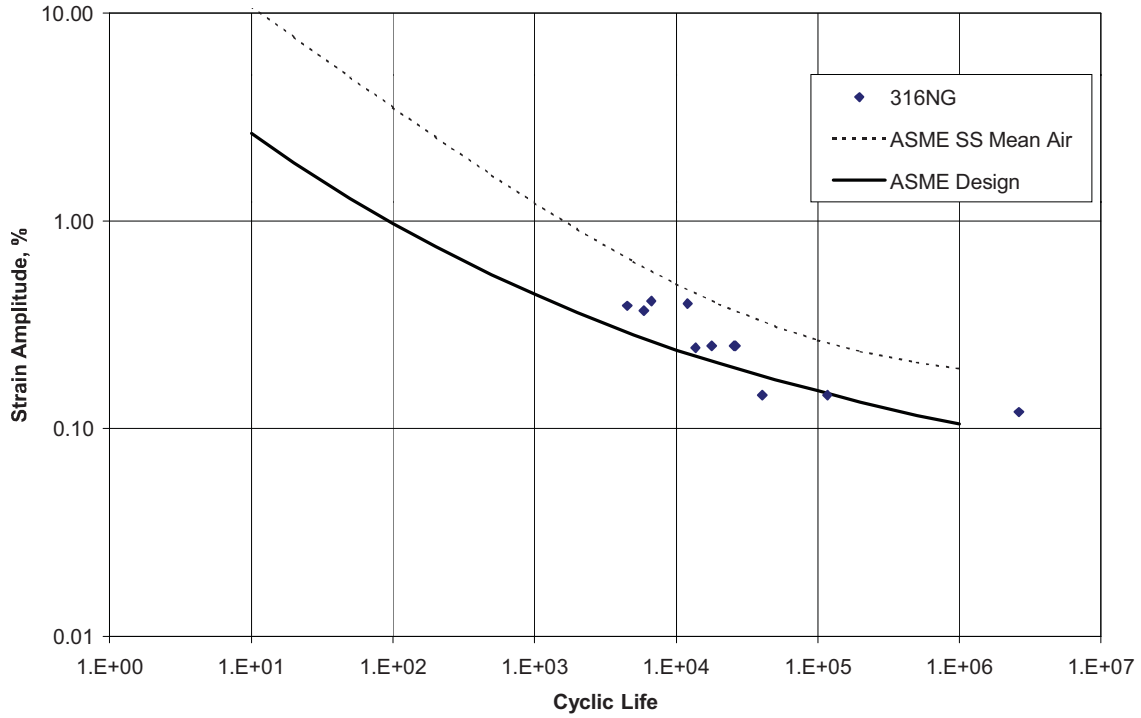

Figure 2-29
Data for 316 NG Stainless Steel Obtained Under Simulated BWR Conditions

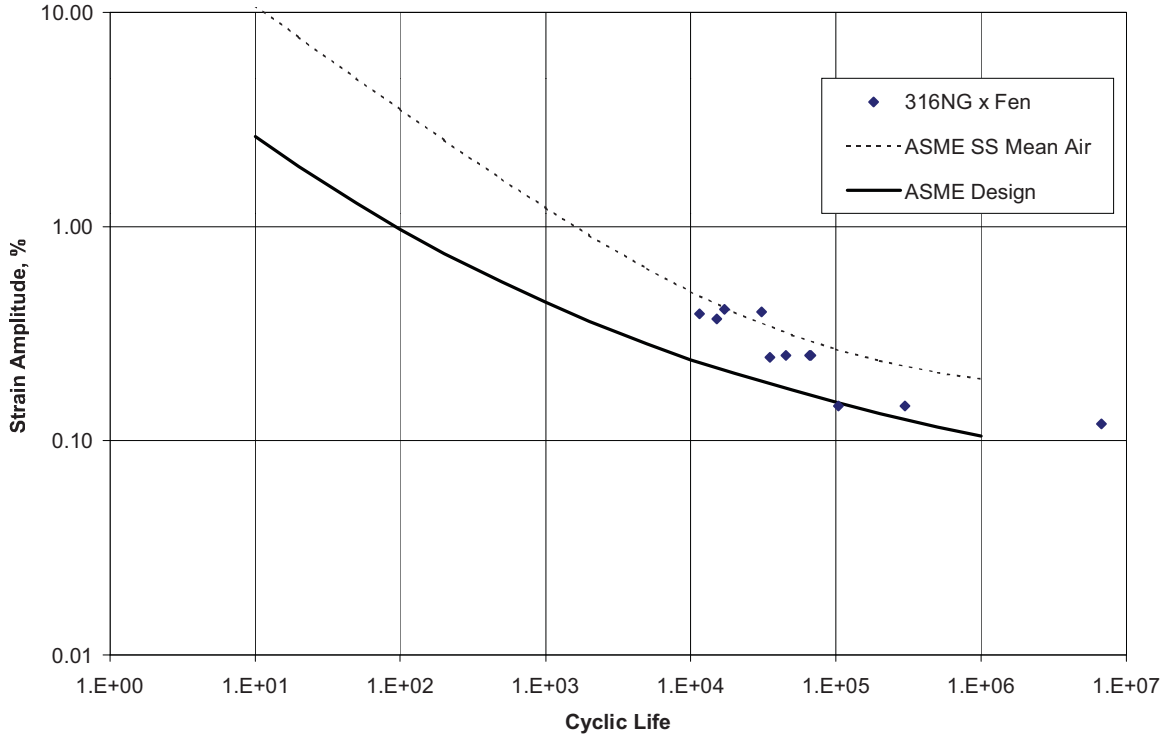

Figure 2-30
Data for 316 NG Stainless Steel Obtained Under Simulated BWR Conditions and Corrected by F_{en}

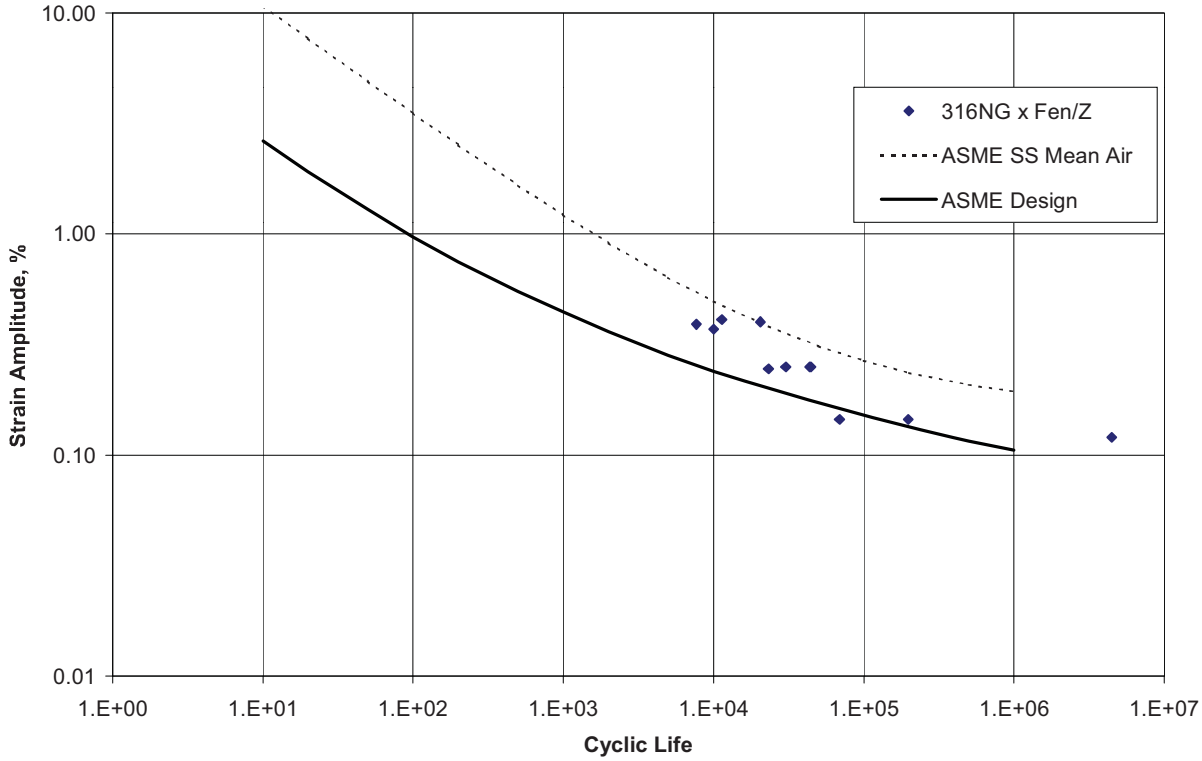

Figure 2-31
Data for 316 NG Stainless Steel Obtained Under Simulated BWR Conditions and Corrected by F_{en} and Z

The findings are quite different for 304 stainless steel in simulated BWR oxygenated reactor water environments. Figures 2-32, 2-33, and 2-34 show these data both before (Figure 2-32) and after environmental correction (Figure 2-33) and moderate environmental effects adjustment (Figure 2-34). Figure 2-33 shows that the F_{en} correction shifts many of the data points toward and, in some cases, beyond, the mean air curve. However, many other data points are not shifted sufficiently to approach the mean air curve. The data scatter is very large both before and after the attempted environmental correction.

For the purposes of this evaluation, a Z factor of 1.5 was used. No PVRC moderate environmental effects thresholds were applied in the F_{en} process.

The laboratory fatigue data evaluated in this section of the report will be further evaluated in terms of applicability to actual component operating conditions in Section 3. The capability of the environmental fatigue models to characterize the complete range of laboratory data is addressed in Section 4. Data scatter is evaluated in terms of the environmental fatigue models in Section 4 and in Section 5.

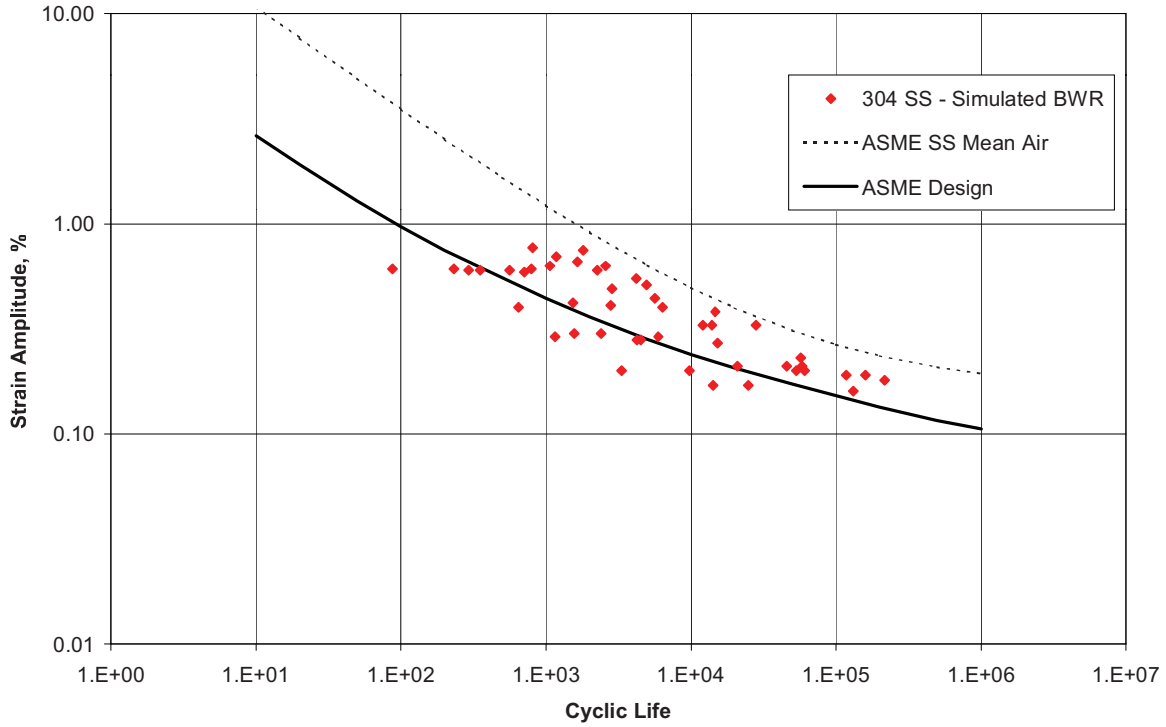

Figure 2-32
Data for 304 Stainless Steel Obtained Under Simulated BWR Conditions

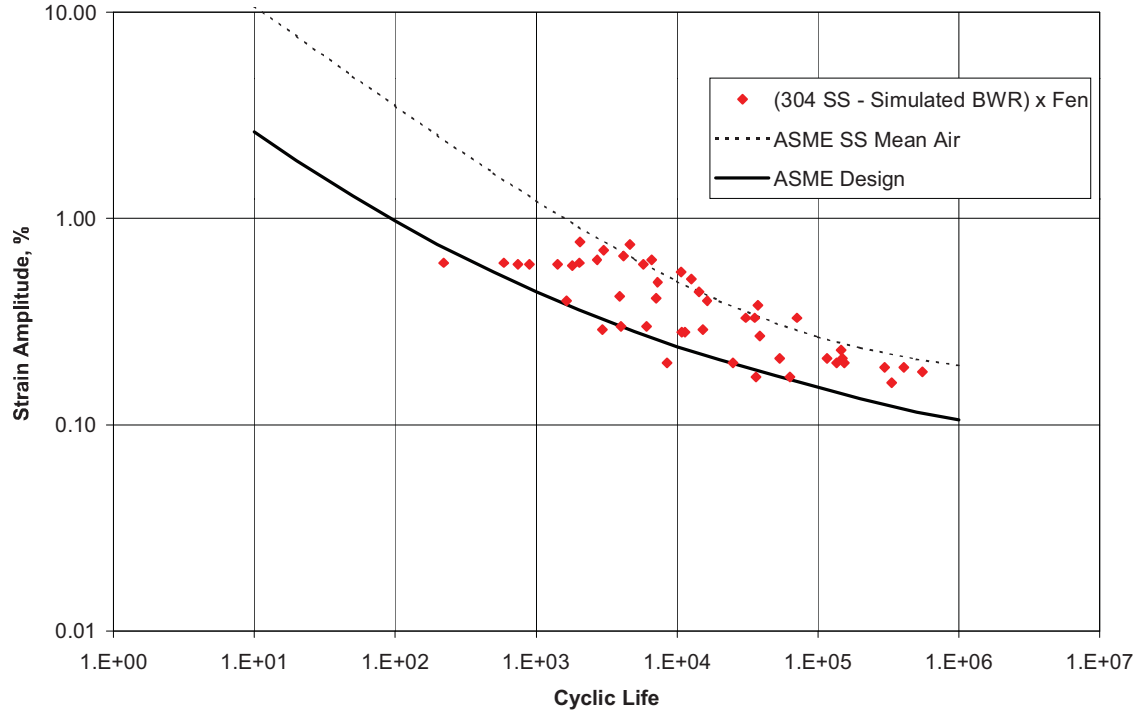

Figure 2-33
Data for 304 Stainless Steel Obtained Under Simulated BWR Conditions and Corrected by F_{en}

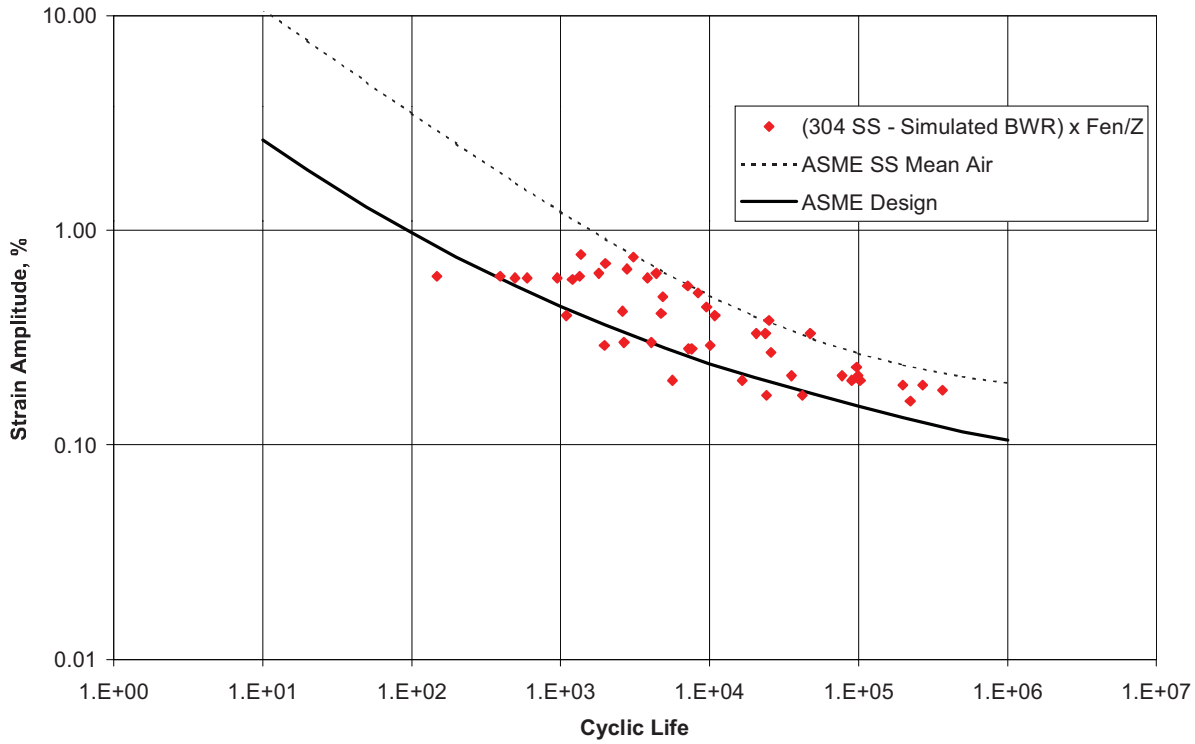

Figure 2-34
Data for 304 Stainless Steel Obtained Under Simulated BWR Conditions and Corrected for F_{en} and Z

2.5 Structural Test Results

Information has been collected and analyzed for this report on fatigue tests that have been performed on structures in a water environment. The results from such tests are extremely valuable for the purpose of evaluating the proposed PVRC F_{en} procedure for consideration of the impact of the environment on the fatigue properties of structures. The ASME Code fatigue design curves are based on laboratory test results from smooth, polished laboratory specimens. Because of concerns about the differences between the fatigue properties of laboratory specimens and actual structures in service environments, the ASME Code added the factors of 2 or 20 to the laboratory data. As has been discussed earlier, these factors were used to shift the mean crack initiation data from laboratory specimens to develop a design curve that was to represent the best estimate of the mean curve for the initiation of cracks in the structure under service conditions.

If the factors are correct, the design curve should be the mean crack initiation data from fatigue tests conducted on actual structures in a water environment. This should be the case because all of the differences between the test specimen and the structure have been eliminated when actual structures are tested. However, other conservatisms exist in the design assumptions of the ASME fatigue analysis that do not exist in actual structure testing. These include the use of actual rather than calculated strain levels, mean stress effects, and actual rather than assumed cycles definitions.

Three sets of experiments have been identified that can be used for evaluating the proposed PVRC approach to include environmental effects in the fatigue analysis. These include fatigue tests performed on pressure vessels at Southwest Research Institute (SWRI) in the early 1960s for the PVRC and the former Atomic Energy Commission (AEC), tests performed by General Electric Company on butt-welded piping, and tests preformed in Germany (KWU) on tubing.

2.5.1 PVRC Pressure Vessel Tests

In this program, a total of six carbon or low-alloy pressure vessels were tested under fatigue loading. Six vessels each of A-201 carbon steel and A-302 low-alloy steel were tested. The pressure vessels consisted of a cylindrical shell 7-ft (2.13 m) long with a 36-inch (91.44 cm) inside diameter and a 2-inch (50.80 mm) thick wall. The vessels had hemispherical heads, with one head containing a 15-inch (38.10 cm) manway. The vessels contained a number of different nozzle openings and blind holes. Details of the vessel design can be found in *Low Cycle Fatigue Research on Full-Size Pressure Vessels* [22]. The vessels were fatigue loaded by cycling the pressure in the vessel by pumping water into the vessels. Extensive stress analyses were performed on the vessels both experimentally with strain gages and by analysis to define the stress and strain ranges at the various locations in the vessels. The vessels were cycled until leakage or failure. In some cases, leaks were repaired and the cycling continued.

The results from these twelve tests were reported in a Welding Research Supplement and the ASME Code Criteria [4,22] and are shown in Figures 2-35 and 2-36. The carbon steel vessel results are shown in Figure 2-35 and the low-alloy steel vessel results in Figure 2-36. While some of the crack initiation results approach the ASME Code fatigue design curve, none of the cycles to crack initiation were less than the design curve. Because the intent of the ASME Code fatigue design curves is to predict the mean line for crack initiation in actual vessels, these tests demonstrate that the margins used by the ASME in developing the design curves are conservative, even with exposure of vessel inner surfaces to oxygenated water.

These tests were conducted at room temperature with water, most likely air saturated, as the pressurizing medium. The PVRC threshold would predict that the environmental effects under these conditions would be moderate and that F_{en} correction would not be needed under these conditions. This is demonstrated to be true because the numbers of cycles to initiation are all greater than the ASME design curve. However, the fact that the PVRC thresholds predict a moderate environmental effect does not mean that there was no environmental effect in these tests. The MITI Guidelines in Japan, which do not include thresholds, would assign a F_{en} value of 6.6 to the analysis of this vessel under these conditions. Figures 2-37 and 2-38 show the results from these experiments corrected with this F_{en} value. In these figures, the crack initiation values fall slightly to the left of the ASME mean data line, while the vessel failure points (vessel leakage) fall to the right of the mean data lines. Considering that these results are for actual pressure vessels that include realistic vessel sizes, typical surface finishes, actual stress levels etc., the MITI procedures appear to be overly conservative.

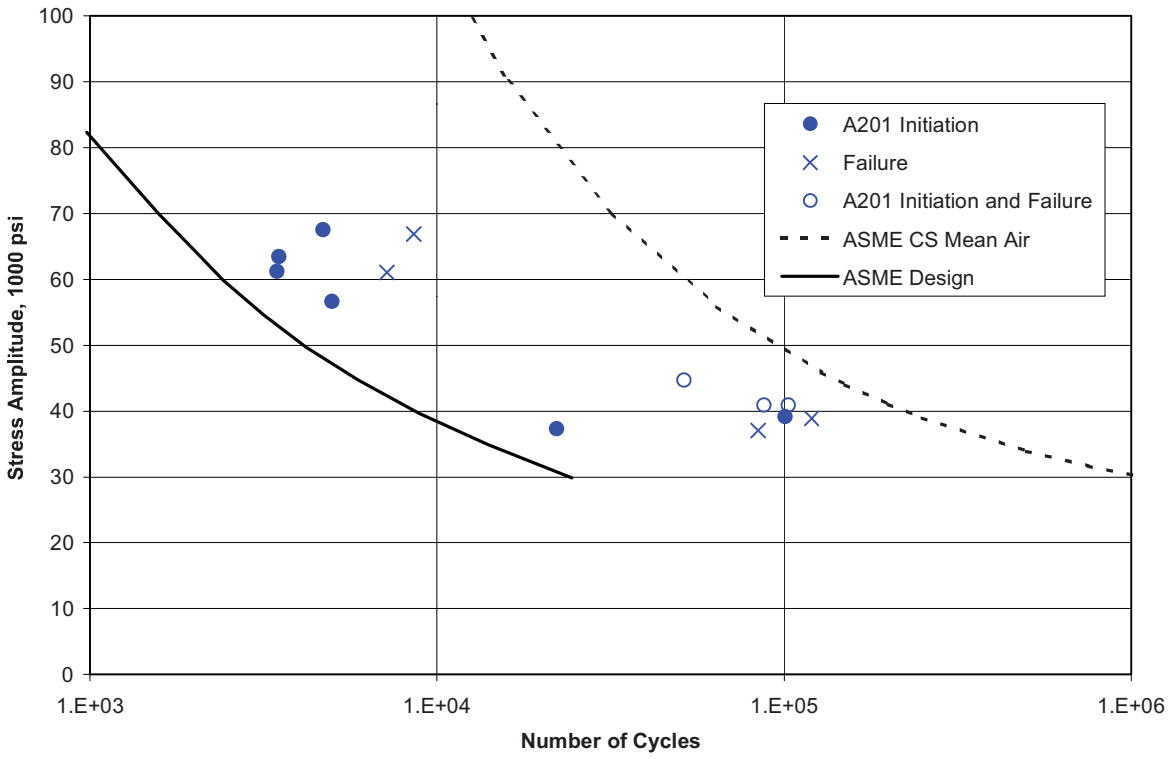

Figure 2-35
Results From the PVRC Fatigue Testing of Full Size Carbon Steel Pressure Vessels

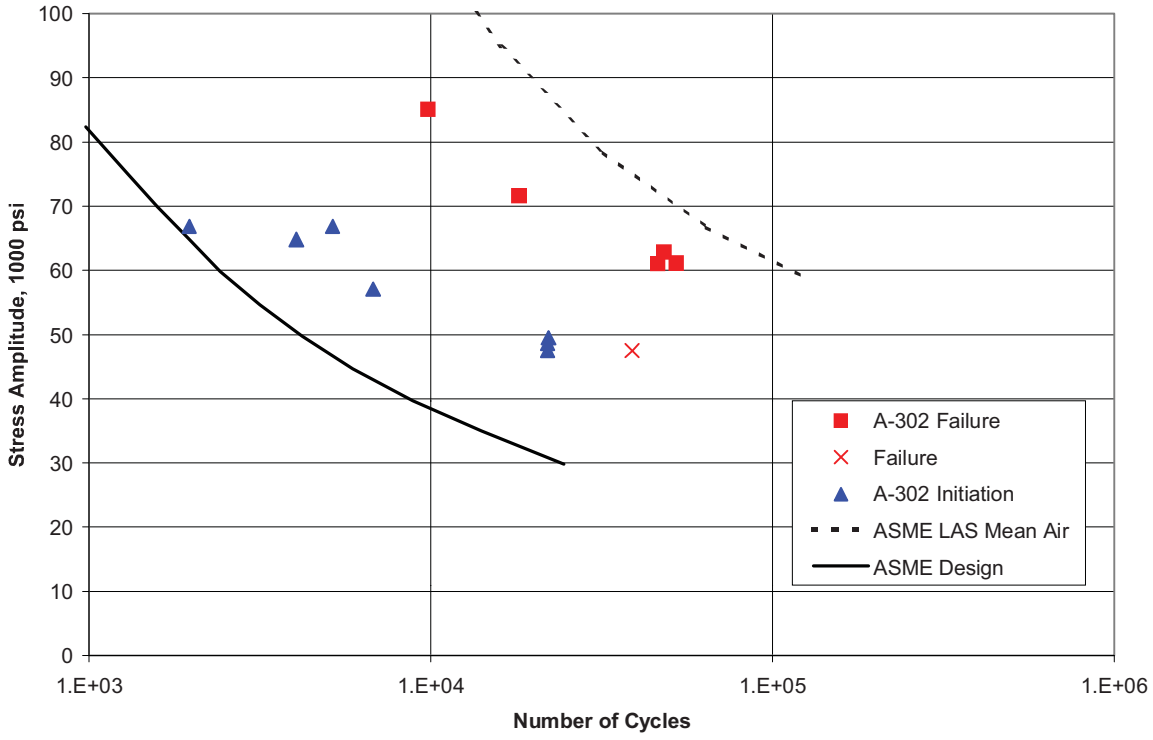

Figure 2-36
Results From the PVRC Fatigue Testing of Full Size Low-Alloy Steel Pressure Vessels

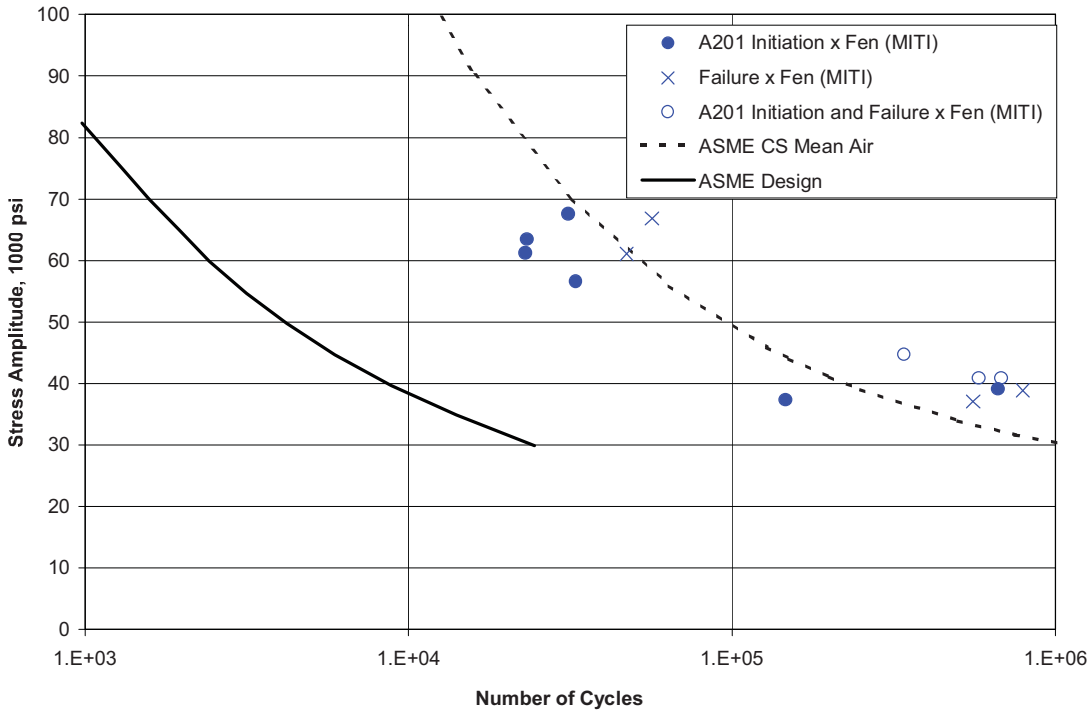

Figure 2-37
Results From the PVRC Fatigue Testing of Full Size Carbon Steel Pressure Vessels Corrected by MITI F_{en}

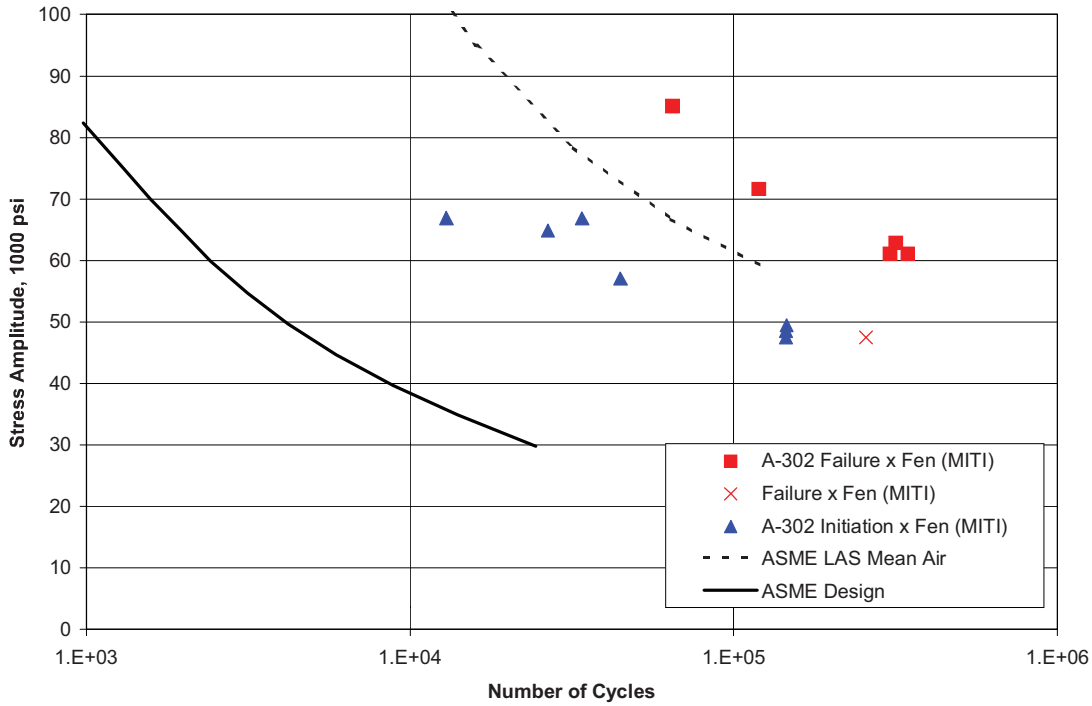

Figure 2-38
Results From the PVRC Fatigue Testing of Full Size Low-Alloy Steel Pressure Vessels Corrected by MITI F_{en}

2.5.2 General Electric Company Tests on Butt-Welded Piping

In the early 1980s, the General Electric Company conducted a combined experimental and analytical program on the fatigue crack initiation behavior of carbon steel components [23,24]. Included in the program were a series of fatigue experiments on butt-welded pipes in simulated BWR reactor coolant environments. The test specimens were 4-in. (101.60-mm), Schedule 80 welded pipe. The test section was about 4 ft. (1.22 m) long and contained 11 butt welds in series spaced about one diameter apart. The welding parameters were typical of those used in the field, and the welds were post-weld ground to reproduce typical field conditions on the inside diameter. The pipes contained 1200 psig (8.3 MPa) water on the inside and were subjected to an externally applied axial stress. In addition to the external load, the pipe welds also experienced welding residual stresses. The pipe tests were conducted in 288°C (550°F) air and in 0.2 (nominal BWR conditions) and 8 ppm (saturated) oxygenated water, under zero-tension load control with trapezoidal wave shapes at 183 μHz. The recirculating test loop had an internal volume flow rate of 12 gal/min (45.4 l/min) through the nominal 4-inch (101.6 mm) diameter piping specimens, implying a velocity of about 25 in/s (0.6 m/s).

The results are shown in Figures 2-39, 2-40, and 2-41. These figures show the actual fatigue life measured in the experiments (Figure 2-39), the measured fatigue life corrected with F_{en} (Figure 2-40), and the fatigue life as corrected with F_{en}/Z (Figure 2-41). The fatigue life, without correcting for the effects of the environment, were all less than the life predicted by the ASME Code fatigue design curve. The F_{en} correction moved these points into the region between the ASME mean air curve and the ASME Code fatigue design curve. The F_{en}/Z correction moved the data back towards the design fatigue curve. One data point fell slightly to the left of the Code fatigue design curve. The major reason for the measured cyclic life to be low is the bounding nature of the test program. When the first of the eleven butt welds failed, the test was terminated, in spite of the fact that ten other butt welds had longer, and perhaps much longer, lives. Therefore, these test results must be viewed with the perspective that a complete set of failure points for all of the butt welds would produce a considerably different statistical picture. This is confirmed by the *apparent* scatter in the failure data from these bounding failure points and those points from specimens (with 11 butt welds in series) for which no fatigue failure was observed.

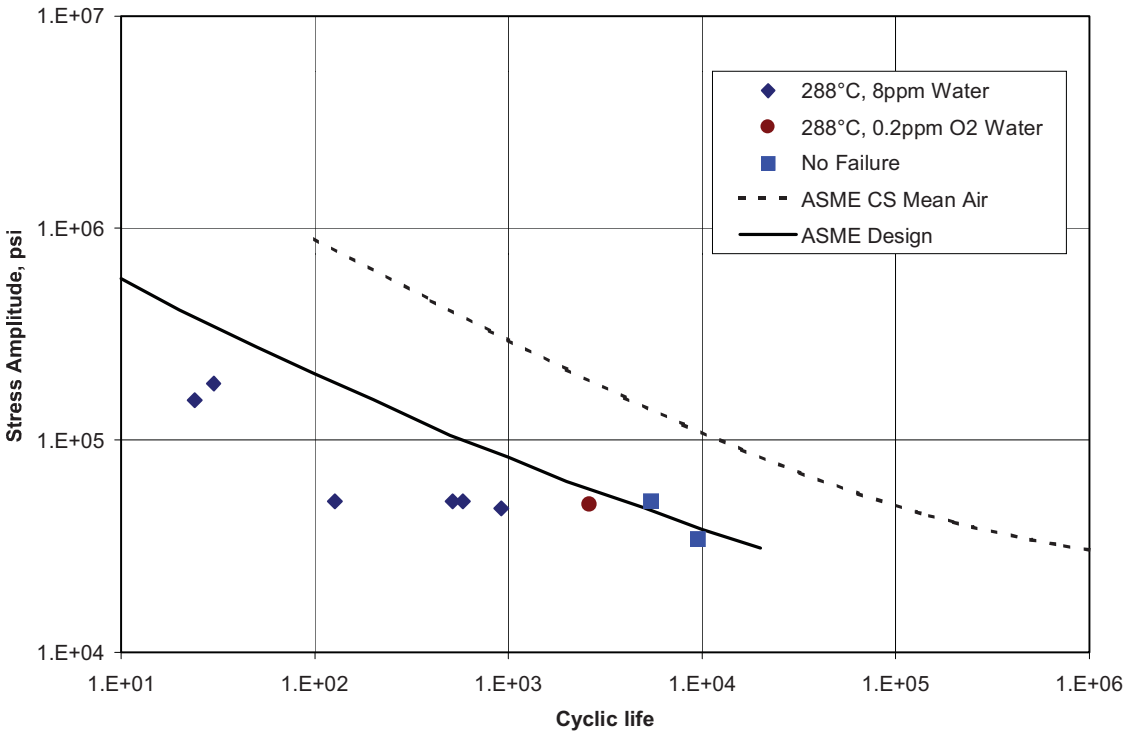

Figure 2-39
Results From Fatigue Testing of Butt-Welded Pipe Under Simulated BWR Conditions

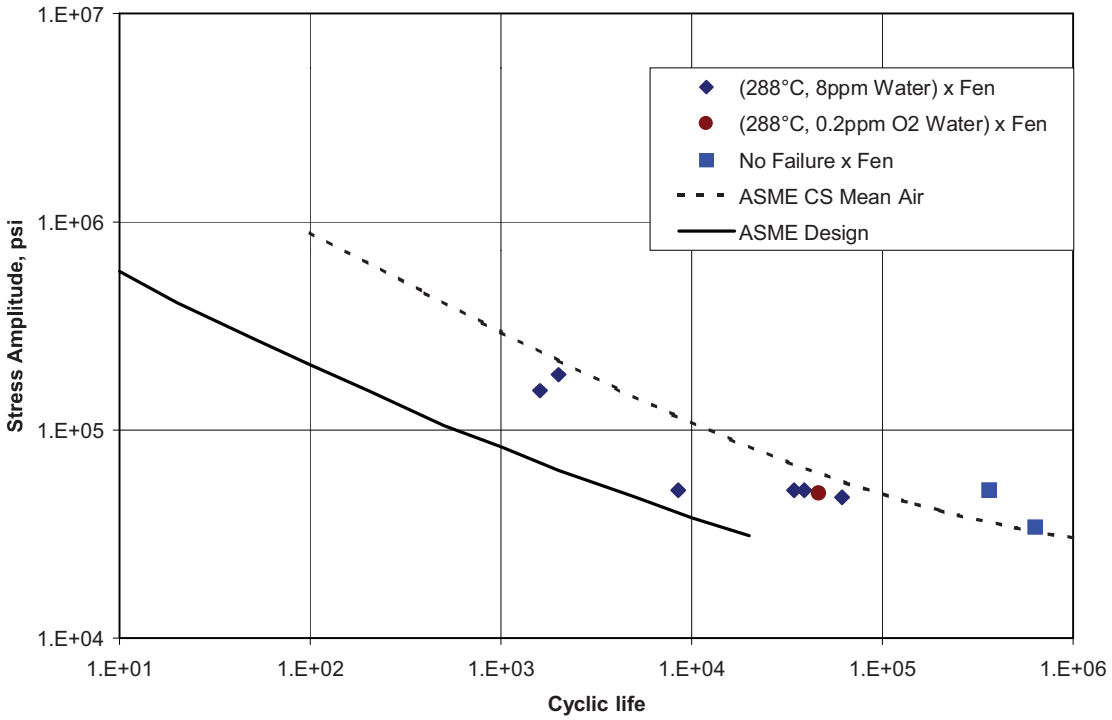

Figure 2-40
Results From Fatigue Testing of Butt-Welded Pipe Under Simulated BWR Conditions and Corrected by F_{en}

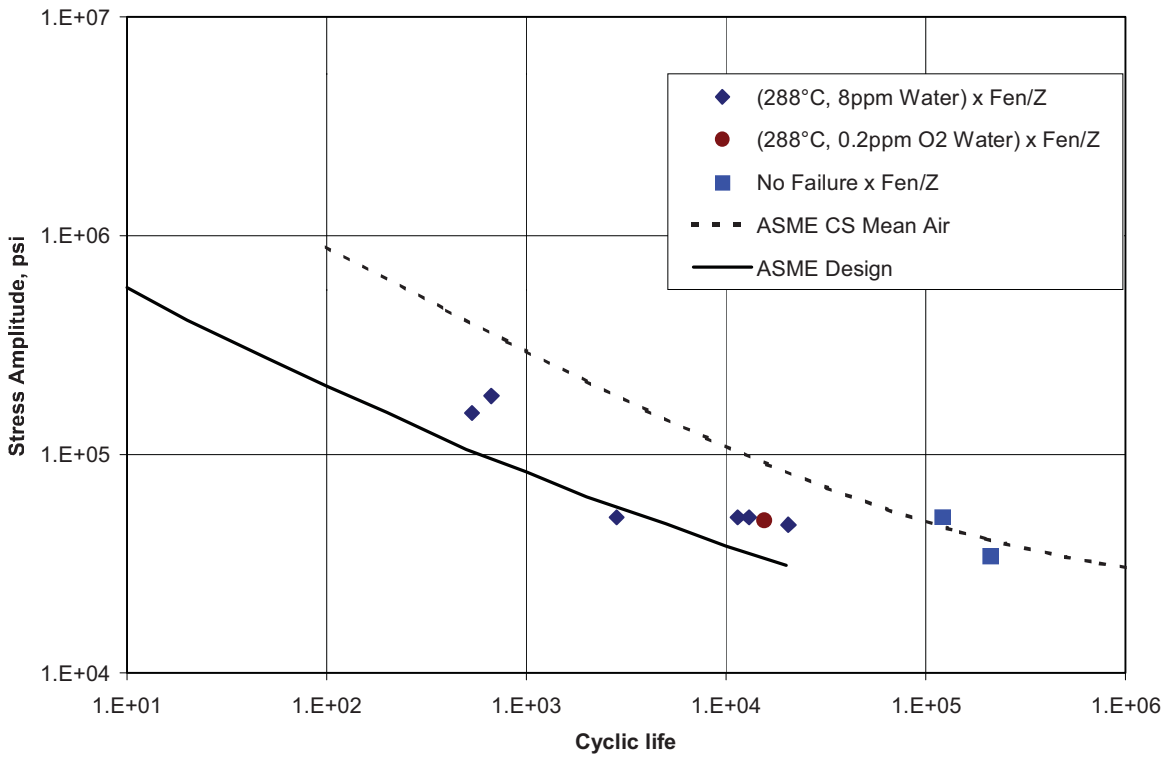

Figure 2-41
Results From Fatigue Testing of Butt-Welded Pipe Under Simulated BWR Conditions and Corrected by F_{en} and Z

For this reason, the scatter in fatigue life shown in Figure 2-39 is much greater than the scatter generally seen in fatigue results from laboratory specimens. This is particularly evident at the lowest stress level tested. At this stress level, one pipe section cracked after 127 cycles, while two other pipe sections did not crack after 5000 cycles and termination of testing. In addition, the environmental conditions under which most of these tests were conducted were more severe than is typical of a BWR environment. Typical oxygen contents in BWR coolant are 0.2 ppm for normal water chemistry and 0.05 ppm for hydrogen water chemistry. Most of these tests were conducted with 8ppm oxygen. Only one test was conducted with 0.2 ppm oxygen. That one test exhibited a relatively long fatigue life and the F_{en}/Z procedure resulted in a life of approximately five times the ASME Code fatigue design curve prediction. It would be expected that the other tests display similar behavior in the actual BWR oxygenated environment.

As stated earlier, the ASME Code Fatigue design curve is intended to be an estimate of the mean line for crack initiation in a structure. However, considering the extreme conservatism of these test results, with failure defined as the weakest butt weld out of eleven butt welds in series and the conservative dissolved oxygen used, the results are not surprising. One point out of 9 test results slightly to the left of the curve is not unexpected, especially when the bounding nature of the test results and the excessive oxygen in most of the tests is taken into account.

These results support the use of a Z factor for the moderate environmental effects recommended in the PVRC procedure. Without the use of the Z factor, the F_{en} correction for the environment causes an overly conservative estimate of the life of the components.

2.5.3 Stainless Steel Component Fatigue Tests

A large amount of component/structural fatigue test data is available for carbon steel and austenitic stainless steel piping components tested under conditions where one surface is exposed to stagnant, high-oxygen water. For many of these tests, measurements and analyses are available that can be used to confirm the applicability of the ASME Code fatigue design process, and to determine the significance of exposure to oxygenated water environments. An excellent summary of the then existing component/structural fatigue test data was prepared in 1979 by Mayfield, Rodabaugh, and Eiber [25].

The Mayfield, Rodabaugh, and Eiber data [25] were examined closely in this report, in order to determine the influence of the oxygenated water environment on the ASME Code margins.

Heald and Kiss [26] reported the results for 26 fatigue tests of girth butt welds, elbows, and tee junctions. Fifteen of the tests were carried out at room temperature, all of which involved internal hydraulic pressure. Two of the fifteen tests involved cyclic internal hydraulic pressure and cyclic in-plane bending of 304 austenitic stainless steel elbows.

Stainless steel elbow tests CSLS-5 and CSLS-7 from Heald and Kiss [26] had measured lives of 3990 and 2531 cycles under test conditions, compared to 23 and 24 cycles predicted by ASME Code analysis procedures. These points are also well above the ASME mean air curve. The predictions included a K_e of 3.33, which is conservative, but not overly conservative. For the S_p calculation, $K_1 = K_2 = 1.0$, but $C_1 = 1.27$ and $C_2 = 2.27$. That is, the pressure in Test CSLS-5 is 1375 psi (9.5 MPa), with M/Z = 49.9 ksi (344.0 MPa), while the pressure for Test CSLS-7 is 2800 psi (19.3 MPa), with M/Z = 44.7 ksi (308.2 MPa). The higher pressure in the second test is only bumped up by a factor of 1.27, while the higher moment loading in the first test is bumped up by 2.27. When K_e is figured in, the total multiplier is 4.23 for the higher pressure term versus 7.56 for the higher bending moment. The total alternating stress was almost the same. Even with the essentially identical alternating stress, the higher pressure test failed quite a bit earlier, but not by a factor of 2.

The loading was such that surface strains were well into the plastic range, with S_p calculated to be 260 to 264 ksi (1792.6 MPa to 1820.2 MPa), and S_{alt} calculated to be 433 to 440 ksi (2985.4 MPa to 3033.7 MPa). For one of these identical elbows, the hydraulic pressure cycled between 100 psi and 1475 psi (0.7 MPa to 10.2 MPa), while, for the other identical elbow, the hydraulic pressure cycled between 100 and 2900 psi (0.7 MPa to 20.0 MPa). The cyclic in-plane bending load was adjusted to make the peak fatigue stress essentially the same for the two tests. In other words, one of the combined load tests had peak surface strains that were fairly uniform because of the dominance of cyclic internal pressure. The other combined load test had peak surface strains that were much more localized because of the dominance of ovalization from in-plane bending. The combined load test dominated by cyclic pressure loading withstood about 2500 full amplitude cycles before the first initiated crack was detected ultrasonically, and it withstood 2531 full amplitude cycles before leakage was observed. The combined load test, dominated by cyclic in-plane bending, only withstood about 250 full amplitude cycles before the first initiated crack was detected ultrasonically, but it withstood 3990 full amplitude cycles before leakage was observed.

The results were consistent with experience. The localized bending strains caused initiation first, but the state of stress was somewhat less conducive to propagation of the initiated crack across the elbow wall thickness. The more uniform surface strains from the pressure-dominated test were less conducive to crack initiation, but the state of stress caused more rapid crack propagation across the elbow wall. The oxygenated water environment seemed to have little or no effect. The predicted cyclic life to initiation was calculated to be 23 or 24 cycles, which means that the ideal cyclic life (that is, no size effect, no surface roughness effect, no environmental effect) would be of the order of 500 cycles. In the test dominated by cyclic in-plane bending, initiation was observed at about 250 cycles. This is consistent with the PVRC tests reported above. In the test dominated by cyclic internal hydraulic pressure, the ratio of design life to actual life is of the order of 100, well above the factor of 20. There would appear to be no environmental effect on austenitic stainless steel under high oxygen, room temperature conditions.

Udoguchi and Asada [27] reported on the low-cycle fatigue testing of austenitic stainless steel piping tees and curved pipe subjected to various cyclic in-plane and out-of-plane bending loads, thrust loads, and pulsating internal pressure. Twenty different tests were carried out, four of which involved tee junctions loaded by cycling the internal pressure supplied hydraulically.

For the four tee junction tests, Mayfield et al. [25] calculated the alternating stress using $C_1 = 2.0$ and $K_1 = 1.7$, for a multiplier of 3.4 on the pressure stress, in order to obtain the peak stress. The plastic strain correction multiplier, K_e, was 3.33 for the first three tests and 3.063 for the last test. Therefore, the ASME Code design inelastic strain range estimate was about 1.36% for the first test, 1.17% for the second test, 1.10% for the third test, and 0.89% for the fourth test. The predicted fatigue lives were 34 cycles (680 cycles on the ASME mean air curve), 45 cycles (900 cycles on the ASME mean air curve), 53 cycles (1060 cycles on the ASME mean air curve), and 80 cycles (1600 cycles on the ASME mean air curve). If the ASME mean air curve formula is used, it can be shown that, for 680 cycles, the strain range is about 1.39%. This compares very well with the inelastic strain range estimate of 1.36%. The mean air curve strain range for 1600 cycles is 0.96%, compared to 0.89%, which also compares very well. The other Code estimates compare equally well.

The total actual strain range (as opposed to Code estimated strain range) was determined by placing strain gauges in the crotch region of the tees. The actual strain ranges measured by Udoguchi and Asada were reported as 0.576% for the first test, 0.467% for the second test, 0.456% for the third test, and 0.388% for the fourth test. Therefore, the Code estimated plastic strains are about a factor of 2 too high, which is reasonable for the stress index approach to fatigue design. All of the actual failure points are well above the ASME mean air curve line by factors of between 8 and 18.

For the four tests, failure occurred as the result of cracks initiating at the internal surface of the intersection between the run pipe and the branch pipe. The number of full-range cycles before failure was 5806 cycles, 16642 cycles, 18206 cycles, and 20000 cycles, respectively.

All four of the failure points for the Udoguchi-Asada tee junction tests, and both of the failure points for the Heald-Kiss elbow tests, lie above the ASME mean air curve line (see Figure 8 from Udoguchi-Asada and Figure 3 from Heald-Kiss), based on ASME Code analysis procedures. All of these tests were conducted at room temperature with the internal surfaces in

contact with oxygenated water. Therefore, the shift from room temperature air to room temperature water is about 3.6 if the ASME mean air curve is used, or about 2.5 if the ANL mean air curve is used. The actual environmental data at relatively low temperature [100 °C (212°F)] is sparse, but a shift of about 3.5 to 5.0 is probably fairly accurate for high strain amplitude, very low strain rate, high dissolved oxygen, and room temperature conditions.

These test data on stainless steel components show that:

- Any size effect is completely overshadowed by the conservatism in the ASME Code estimated plastic strain concentration process.
- Any surface finish effect is also overshadowed by the ASME Code plastic strain concentration conservatism, but is also at least partially mitigated by a passivation layer that eliminates any surface roughness effect.
- The Code plastic strain conservatism for elbows and fittings is about a factor of 2 higher than actual measurements, with most of the conservatism due to K_e.

The combination of structural test results on carbon, low-alloy, and austenitic stainless steel described in this section provide a convincing demonstration that ASME Code fatigue design margins adequately compensate for reactor water environmental effects. Attempts to superimpose reactor water environmental effects penalties to the ASME Code design process, such as those proposed in Japan, cause excessive conservatism. A few structural tests lead to results that appear to compromise ASME Code fatigue design margins. However, even in the General Electric Company butt-welded pipe tests, the bounding nature of the experimental results and the conservatism in the dissolved oxygen concentration provide confirmation of the ASME Code fatigue design process. Finally, for the case of austenitic stainless steel components, laboratory test results in simulated reactor water environments are not borne out by structural tests. Two factors appear to be responsible for the observed differences. First, the strain that ruptures the passivation layer for an actual structural component is very localized, unlike the uniform surface strains in the cylindrical laboratory specimens. Second, the estimated localized strains from ASME Code fatigue design procedures appear to be conservative by about a factor of 2, or a conservatism of about a factor of 30 on fatigue life. This conservatism more than compensates for reactor water environmental effects observed in the laboratory.

2.6 References

1. W. A. Van Der Sluys and S. Yukawa, “Status of PVRC Evaluation of LWR Coolant Environmental Effects on the S-N Fatigue Properties of Pressure Boundary Materials,” *PVP.* Vol. 306*,* pp. 47-58, ASME PVP 1995, Honolulu, HI (July 23-27, 1995).

2. W. A. Van Der Sluys and S. Yukawa, “S-N Fatigue Properties of Pressure Boundary Materials in LWR Coolant Environments,” *PVP.* Vol. 374, pp. 269-276, ASME PVP 1998 (July 24-28, 1998).

3. *An Environmental Factor Approach to Account for Reactor Water Effects in Light Water Reactor Pressure Vessel and Piping Fatigue Evaluations.* EPRI, Palo Alto, CA and General Electric Company, San Jose, CA: December 1995. TR-105759.

4. *Criteria of the ASME Boiler and Pressure Vessel Code for Design by Analysis in Sections III and VIII, Division 2.* The American Society of Mechanical Engineers, New York, 1969.

5. O. K. Chopra and W. J. Shack, *Effects of LWR Coolant Environments on Fatigue Design Curves of Carbon and Low-Alloy Steels.* NUREG/CR-6583 (ANL-97/18), Argonne National Laboratory, Argonne, IL, March 1998.

6. K. Tsutsumi, H. Kanasaki, T. Umakoshi, T. Nakamura, S. Urata, H. Mizuta, and S. Nomoto, "Fatigue Life Reduction in PWR Water Environment for Stainless Steels," *PVP*. Vol. 410-2, pp. 23-34, ASME PVP 2000, Seattle, WA (July 24-27, 2000).

7. M. Higuchi, "An Updated Method to Evaluate Reactor Water Effects on Fatigue Life for Carbon and Low Alloy Steels," Proceedings, International Conference on Fatigue of Reactor Components, Napa, CA (July 31-August 2, 2000).

8. Letter from B. F. Langer, plus attachment, to Members, Special Committee to Review Code Stress Basis, "Report of Sub-Task Group on Fatigue," ASME Boiler and Pressure Vessel Code, June 19, 1961.

9. Majumdar, S., Chopra, O. K., and Shack, W. J., *Interim Fatigue Design Curves for Carbon, Low-Alloy, and Austenitic Stainless Steels in LWR Environments.* NUREG/CR-5999 (ANL-93/3), Argonne National Laboratory, Argonne, IL, April 1993.

10. C. E. Jaske and W. J. O'Donnell, "Fatigue Design Criteria for Pressure Vessel Alloys," ASME Transactions*, Journal of Pressure Vessel Technology.* Vol. 99, No. 4, pp. 584-592 (November 1977).

11. W. F. English, R. L. Greene, D. A Hughes, and R. I. Post; L. F. Coffin, M. J. Manjoine, and D. R. Diercks, Discussion: "Fatigue Design Criteria for Pressure Vessel Alloys," ASME Transactions, *Journal of Pressure Vessel Technology*, Vol. 100, No. 2, pp. 236-243 (May 1978).

12. U.S. Nuclear Regulatory Commission, D. A. Hale, S. A. Wilson, E. Kiss, and A. J. Giannuzzi, *Low Cycle Fatigue Evaluation of Primary Piping Materials in a BWR Environment*. GEAP-20244, September 1977.

13. S. Ranganath, J. N. Kass, and J. D. Heald, "Fatigue Behavior of Carbon Steel Components in High-Temperature Water Environments," ASTM STP 7780, Edited by C. Amzallog, B. N. Leis, and P. Rabbe, American Society for Testing and Materials, Philadelphia, PA, pp. 436-459 (1982).

14. N. Nagata, S. Sato, and Y. Katada, "Low-Cycle Fatigue Behavior of Low-Alloy Steels in High-Temperature Pressurized Water." Transactions, 19th International Conference on Structural Mechanics In Reactor Technology, Vol. F, Edited by A. H. Hadjian, International Association for Structural Mechanics in Reactor Technology, Anaheim, CA (1989).

15. M. Higuchi and K. Iida, "Fatigue Strength Correction Factors for Carbon and Low-Alloy Steels in Oxygen-Containing High-Temperature Water," *Nuclear Engineering and Design.* Vol. 129, pp. 293-306 (1991).

16. "Environmental Effects in Nuclear Applications," Welding Research Council Symposium Proceedings, Vols. 1 and 2, Clearwater Beach, FL (January 20-21, 1992), Welding Research Council, New York, New York.

17. O. K. Chopra and W. J. Shack, *Effects of LWR Coolant Environments on Fatigue Design Curves of Austenitic Stainless Steels.* NUREG/CR-5704 (ANL-98/31), Argonne National Laboratory, Argonne, IL, April 1999.

18. L. A. James, L. D. Paul, and M. T. Miglin, "Low Cycle Fatigue Initiation in SA-2 IO AI Carbon Steel Boiler Tubing in Contaminated Boiler Water," *PVP.* Vol. 195, Edited by W. H. Bamford, C. Becht, S. B. Framatonne, J. D. Gilman, L. A. James, and M. Prager, ASME PVP 1990, New York, pp. 13-19 (1990).

19. J. B. Terrell, "Effect of Cyclic Frequency on the Fatigue Life on ASME SA-106-B Piping Steel in PWR Environments," Transactions ASME, *Journal of Materials Engineering.* Vol. 10, pp. 193-203 (1988).

20. J. Hickling, Minutes of the ICGEAC, Switzerland (March 1992).

21. B. Timofeev, Personal Communication. Prometey Institute, St. Petersburg, Russia.

22. L. F. Kooistra and M.M. Lemcoe, "Low Cycle Fatigue Research on Full-Size Pressure Vessels," Welding Research Supplement (July 1962).

23. S. Ranganath, J. N. Kass, and J. D. Heald, "Fatigue Behavior of Carbon Steel Components in High-Temperature Water Environments," *Low-Cycle Fatigue and Life Prediction*, ASTM STP 770, Edited by C. Amzalliag, B. N. Leis, and P. Rabbe, American Society for Testing and Materials (1982).

24. D. Weinstein, *BWR Environmental Cracking Margins for Carbon Steel Piping.* EPRI, Palo Alto, CA: May 1982. NP-2406, Project 1248-1.

25. M. E. Mayfield, E. C. Rodabaugh, and R. J. Eiber, "A Comparison of Fatigue Test Data on Piping with the ASME Code Fatigue Evaluation Procedure," 3rd U. S. National Congress on Pressure Vessels and Piping, San Francisco, CA (June 25-29, 1979). Paper No. 79-PVP-92.

26. J. D. Heald and E. Kiss, "Low Cycle Fatigue of Nuclear Pipe Components," ASME Transactions, *Journal of Pressure Vessel Technology.* Vol. 96, No. 3, pp. 171-176 (August 1974).

27. T. Udoguchi and Y. Asada, "Investigation on Low-Cycle Fatigue Strength of Piping Components," 2nd International Conference on Pressure Vessel Technology, San Antonio, TX (1973). Proceedings, pp. 773-783.

3
RELEVANCE OF LABORATORY DATA

The six independent environmental parameters that govern the significance of reactor water environmental effects are applied strain amplitude, applied strain rate, dissolved oxygen concentration in the reactor water coolant, component metal temperature, component metal sulfur content, and reactor water flow rate. Thresholds for four of the six independent environmental parameters are discussed and justified in Section 2 of this report. No threshold for steel sulfur content has been implemented. The threshold given in Van Der Sluys and Yukawa [1], a metal sulfur content less than or equal to 0.003%, is less than the maximum permissible sulfur limits for reactor coolant system vessel and piping materials (for example, 0.030% for SA 376 stainless steel piping). No threshold for reactor water flow rate has been implemented. The threshold given in Van Der Sluys and Yukawa [1]—a water flow velocity greater than 3 m/sec (120 in/sec)—was thought to depend upon an insufficient amount of data.

If any one of the other four environmental parameters satisfies the remaining thresholds, the effects of the reactor water environment are considered to be moderate.

In this section, the laboratory conditions under which reactor water environments have been simulated are compared to the conditions experienced under actual plant operation. The objective is the determination of the laboratory data that should be considered relevant to actual plant operation.

3.1 Review of Operating Experience

3.1.1 Component Metal Temperature

Operating temperatures for PWR reactor coolant system and BWR primary coolant pressure boundary components are in the range of 550°F (290°C), with excursions up to 650°F (340°C) as the design-basis for some components (for example, pressurizers). The simulation of nominal light-water reactor coolant temperatures is not an issue with respect to applicability of laboratory results.

3.1.2 Applied Strain Amplitude

Design-basis transient severity is nominally based on sudden discontinuities (that is, step changes) in temperature. It is not unusual for a plant thermal transient to be described by a step change in temperature of the order of 450°F (232°C) and a corresponding strain amplitude of 2 to 3%, including the effect of plastic strain concentrations. In actuality, these calculated strain amplitudes are very conservative because the actual transient severity (see *Use of On-Line*

Fatigue Monitoring of Nuclear Reactor Components as a Tool for Plant Life Extension [2]) is much less in both the temperature change and its temporal variation. Applied strain amplitudes are typically an order of magnitude less than those calculated from full-amplitude step changes in temperature.

In addition, plastic strains tend to be very localized in regions of geometric discontinuity, with the effects of strain concentration causing strain amplitudes of the order of 0.2% to 0.5% in the worst cases. Laboratory testing has emphasized low-cycle fatigue testing in simulated reactor water environments at peak applied strain amplitudes ranging from 0.1% to 1%. Such peak strain amplitudes are appropriate. However, an issue of some concern is the distribution of the plastic strain.

Because the distribution of plastic strain is very localized in actual components, the ASME Code fatigue design curve and the underlying fatigue data are based on strict strain control. For that reason, laboratory test specimens should be subjected to strain control, as opposed to load control, so that locally high stresses have the opportunity to be redistributed, similar to the behavior of actual components in service. Also, while both cylindrical and hourglass-shaped specimens are valid fatigue test geometries, hourglass-shaped specimens are more representative of actual components in service than cylindrical-shaped specimens, because the high stress (strain) field is truly localized and the stresses can be redistributed in two dimensions rather than one. The entire gauge length of the uniform cylindrical-shaped test specimen is subjected to the applied cyclic strain and environmental conditions. In contrast, only a small location with a stress concentration such as root of a groove or fillet weld or the crotch of an elbow is subjected to such strain cycling in actual components in service. It is speculated that increasing the length of the gauge section increases the likelihood of a spot where a local small defect could serve as a fatigue crack initiator. Thus, the smooth specimen is more likely to overstate the fatigue effects. For example, it was noted in NUREG/CR-6237 [3] that the hourglass-shaped test specimens generally yielded 20 to 30% longer lives than uniform gauge-length samples.

This observation on localized strain is also confirmed by the fatigue life data on notched specimens tested in LWR environments [4]. Figures 3-1 and 3-2 illustrate the data. (These are Figures 5 and 6 from *Effect of Loading Rate on the Fatigue Strength of Notched Carbon Steel in High Temperature Water* [4].) Although the strain rates in specimens with different K_t do not match exactly, the trend in fatigue life is very clear. For the same stress (Figure 3-1) or strain (Figure 3-2) amplitude, the fatigue life of the specimen with a higher K_t value is longer, compared to the specimen with $K_t = 1.0$. This observation is further confirmed by Hickling [5], who cited German design requirements on the allowable surface strain for low-alloy steel components exposed to water. These surface strain limits are intended to avoid disruption of the protective magnetite film and/or separation of the film from the underlying metal surface.

Therefore, the issue of strict strain control versus load control, and the related issue of a test specimen shape that promotes localized plastic straining, is of significant concern for the laboratory simulation of conditions that actually occur in service.

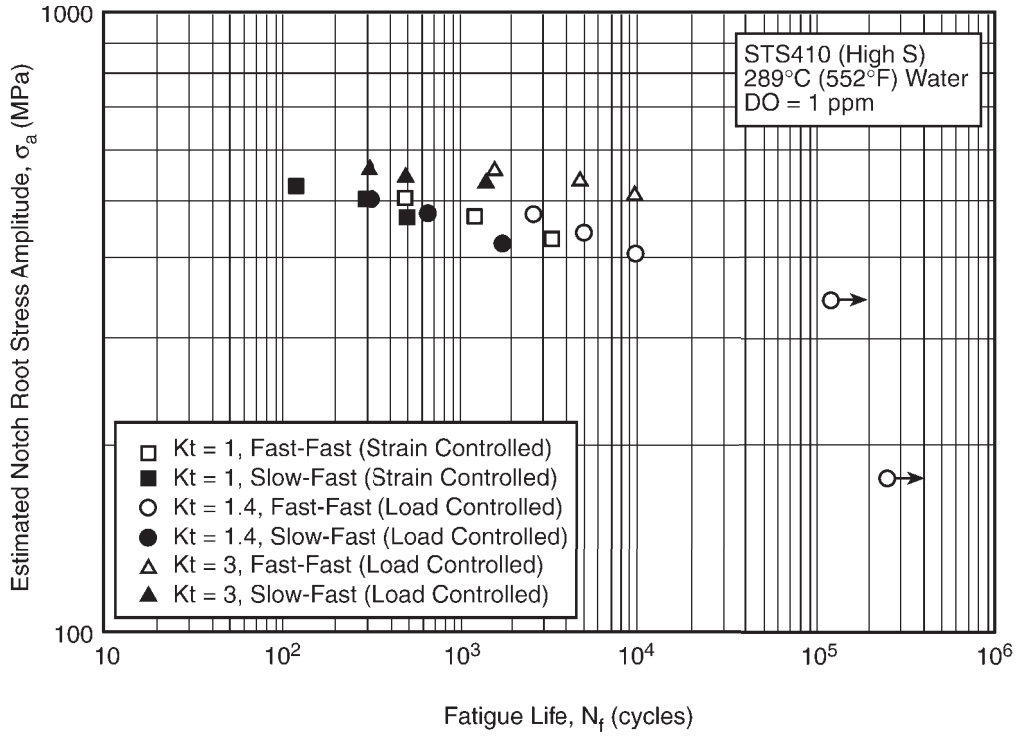

Figure 3-1
Relationship Between Estimated Notch Root Stress Amplitude by Neuber's Rule and Fatigue Life

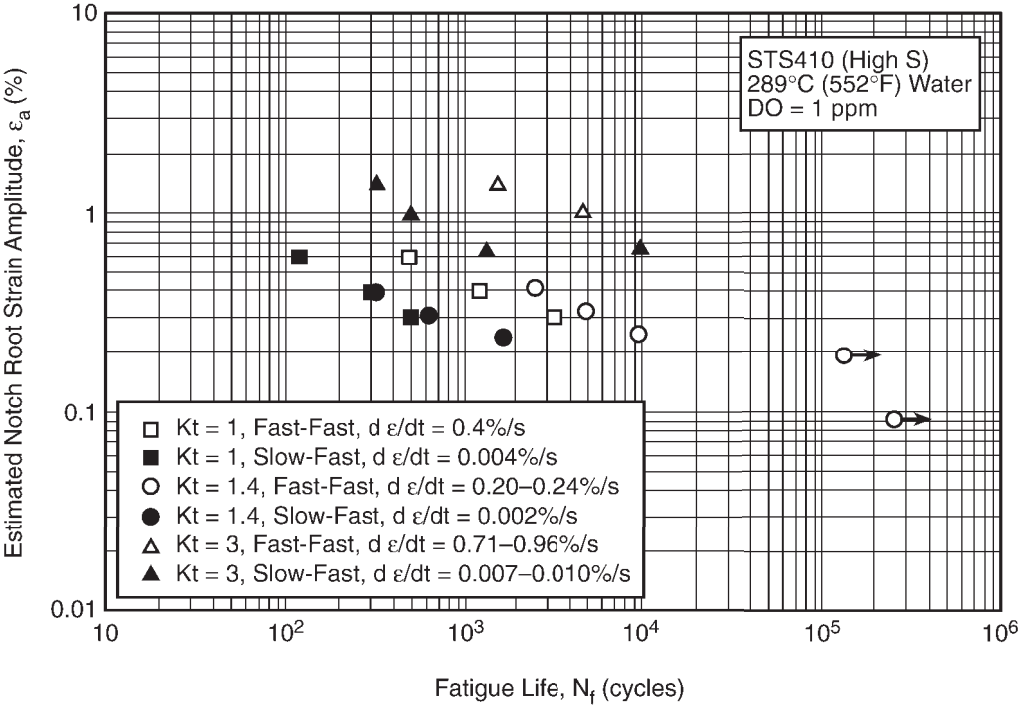

Figure 3-2
Relationship Between Estimated Notch Root Strain Amplitude by Neuber's Rule and Fatigue Life

3.1.3 Applied Strain Rate

Because of the difference between design-basis transient severity and actual plant transients, the calculation of the theoretical applied strain rate is not conservative. Design-basis plant thermal transients with large ramp changes in temperature cause applied strain rates of 0.1%/sec to 0.5%/sec, while actual plant thermal transients cause applied strain rates that are one order of magnitude less. When the ramp change in temperature is reduced (for example, 10% power change, rather than shutdown), the actual applied strain rate could be reduced by two orders of magnitude. For slower temperature changes, applied strain rates can approach the lower end of the range of strain rates measured in the laboratory. The strain rates measured in laboratory fatigue tests that simulate reactor water environments cover the range of expected strain rates in service, as well as theoretical strain rates from design-basis transients.

3.1.4 Dissolved Oxygen Content

Reactor coolant chemistry is controlled during normal plant operation to maintain prescribed dissolved oxygen content and other oxidizing species. For PWRs, the nominal dissolved oxygen levels in the reactor coolant system during normal plant operation is of the order of 0.01 to 0.02 ppm, well below the threshold level for carbon and low-alloy steels. These levels also apply for BWRs using hydrogen water chemistry. For other BWRs, the primary coolant pressure boundary is maintained at dissolved oxygen levels of 0.05 to 0.2 ppm during normal plant operation. During plant shutdown, when the reactor coolant system or the primary coolant pressure boundary might be open to atmospheric conditions, it is possible for the dissolved oxygen to reach saturation levels (that is, 8 ppm). The plant returns quickly to normal operating chemistry during startup and before the plant reaches significant power levels.

The simulated reactor water chemistry ranges used in laboratory fatigue testing tend to meet either PWR normal operating levels or saturated conditions. The full range of reactor water chemistry of interest is covered.

The only issue of any concern is the oxidizing potential of the simulated reactor water coolant at the flow rates used in most laboratory tests. That issue is discussed in detail below.

3.2 The Effect of Reactor Water Coolant Flow Rate

No flow rate thresholds have been implemented in the F_{en} procedure. However, it should be pointed out that the effect of reactor water flow rate has been evaluated for carbon steels in both the laboratory and in large-scale component tests, and has been found to be a critical environmental parameter.

Typical reactor coolant velocities are of the order of 25 to 200 in/s (0.6 to 5 m/s). On the other hand, flow velocities in the laboratory, under simulated reactor water conditions, are much lower. As an example, the apparatus used by Argonne National Laboratory (ANL) for their simulated fatigue crack initiation experiments has a volume flow rate of 10 ml/min, with an autoclave volume of 12 mL. Using a length of 2 inches (50 mm) between the inlet and outlet to the autoclave, and ignoring the volume occupied by the specimen, the average flow velocity is

about 0.028 in/s (0.0007 m/s), approaching stagnant flow. Of course, not all simulated reactor water velocities are that low. The recirculating test loop used by General Electric Company for the butt-welded piping tests reported in *Effect of Loading Rate on the Fatigue Strength of Notched Carbon Steel in High Temperature Water* [4] had a volume flow rate of 12 gal/min (45.4 l/min) through the NPS 4 piping specimens, implying a velocity of about 25 in/s (0.6 m/s). However, much of the experimental data generated over the past two decades has been obtained at flow rates that are virtually stagnant. These low flow rates, when combined with very low dissolved oxygen, expose the test specimens to extremely low oxidizing potential that could introduce problems at strain amplitudes sufficient to rupture protective oxide or passivated surfaces.

In this regard, Hickling [5] has reported on German experience for both PWR and BWR environments. For BWR environments, he found that:

> "An important common feature in almost all cases of damage was lack of flow; the lines were operated only intermittently and usually contained stagnant medium. Furthermore, damage was observed almost exclusively in piping where the oxygen concentration in the water film adjacent to the steel wall was relatively high (typically > 0.3 ppm)."

Hickling also found that, for PWRs:

> "Limited work carried out in Germany on this effect shows that higher flow rates are always more beneficial, but that it is difficult to separate out the influence on crack initiation and on subsequent crack growth. A direct comparison with WB 35 steel (SSRT in pure water with 0.4 ppm oxygen at 240 $^{\circ}$C and a strain rate of 10^{-6} s^{-1}) showed the same ductile behavior as in air at a linear flow rate of 3.6 m/s, but a 90% drop in the measured area to fracture of an identical tensile specimen under quasi-stagnant conditions."

Hickling [5] goes on to describe component scale tests carried out in Germany to confirm operating experience. He introduced the discussion by observing that:

> "Further work on flow rates was carried out in the KWU laboratories using 180 $^{\circ}$ bends of carbon steel tubing (S = 0.025%) where internal flow rates of up to 0.6 m/s were established. The results at low flow rates show very clear environmental effects, except at the lowest oxygen level tested (0.01 ppm). However, establishment of flowing conditions reduced or even eliminated the influence of corrosion on fatigue crack initiation."

The raw data from the KWU test program are plotted in Figure 3-3. Note that four different experimental conditions were used—high dissolved oxygen/low flow, very low dissolved oxygen/low flow, 0.2 ppm dissolved oxygen/low flow, and 0.2 ppm dissolved oxygen/moderate flow. With the exception of the very low dissolved oxygen/low flow, all of the low flow data lies close to, or below, the ASME Code fatigue design curve for carbon steel at temperature. For very low dissolved oxygen, approximating stagnant flow in a PWR reactor water environment, the data points are similar to previous component test results from PVRC testing. The effect of even a moderate flow rate is to largely eliminate the environmental effect. When the test data are adjusted by F_{en}, in accordance with the current formulas, all of the data except the very low dissolved oxygen data points are shifted well above the ASME mean air curve (Figure 3-4). When the F_{en} adjustment is compensated by the moderate environmental effects factor Z, the tendency for over-correction remains (Figure 3-5).

This component-scale data evaluation provides the following conclusions:

- Higher flow rate fatigue tests for large-scale carbon steel piping components in environment show significantly less environmental reduction in fatigue life than stagnant flow tests.
- Very low dissolved oxygen fatigue tests for large-scale carbon steel piping components that approximate PWR environments show significantly less environmental reduction, even with stagnant flow.
- The F_{en} adjustment procedure, even when compensated by a moderate environmental effects factor, Z, overcorrects for the environment, even for stagnant flow conditions and 0.2 ppm dissolved oxygen.

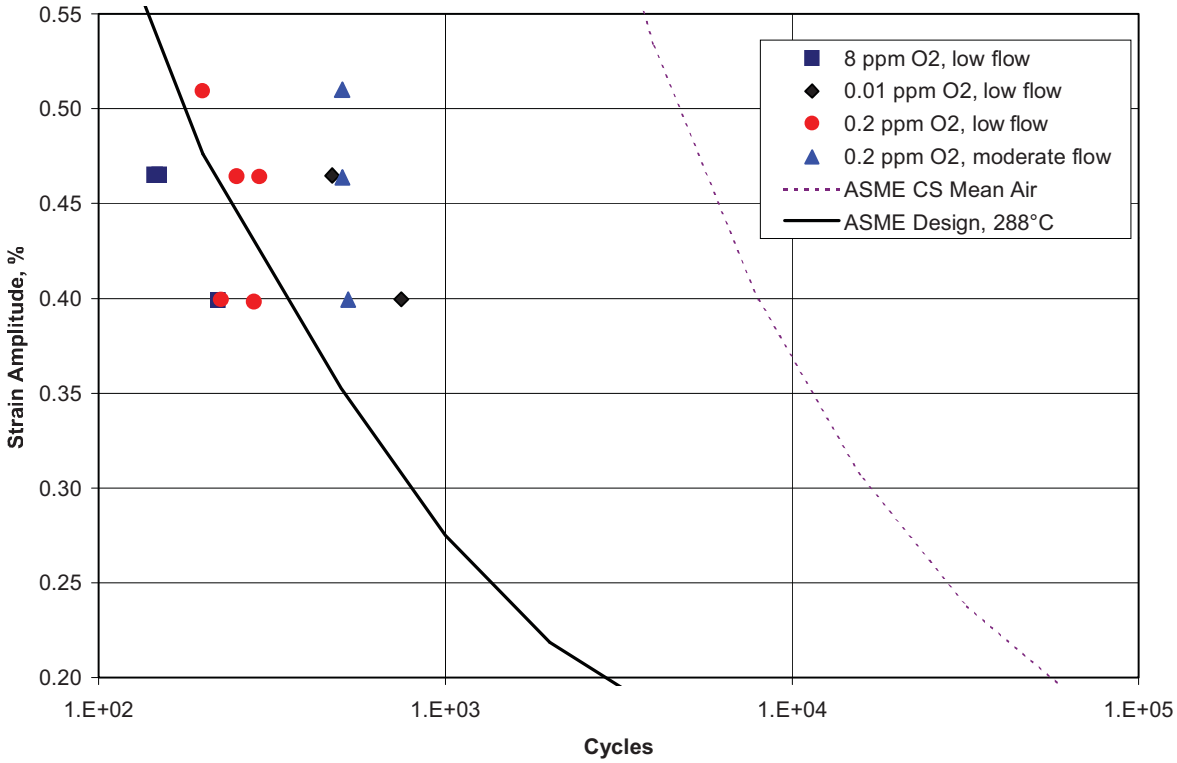

Figure 3-3
KWU Component Scale Test Results for Carbon Steel

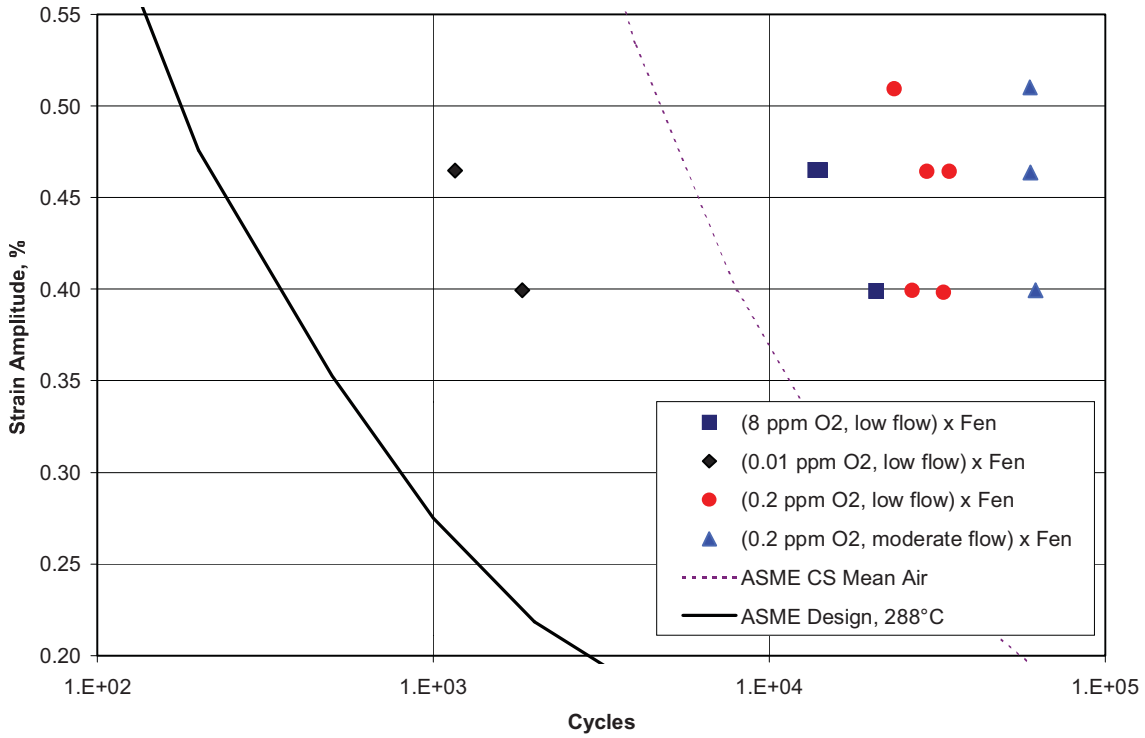

Figure 3-4
KWU Component Scale Test Results for Carbon Steel Corrected by F_{en}

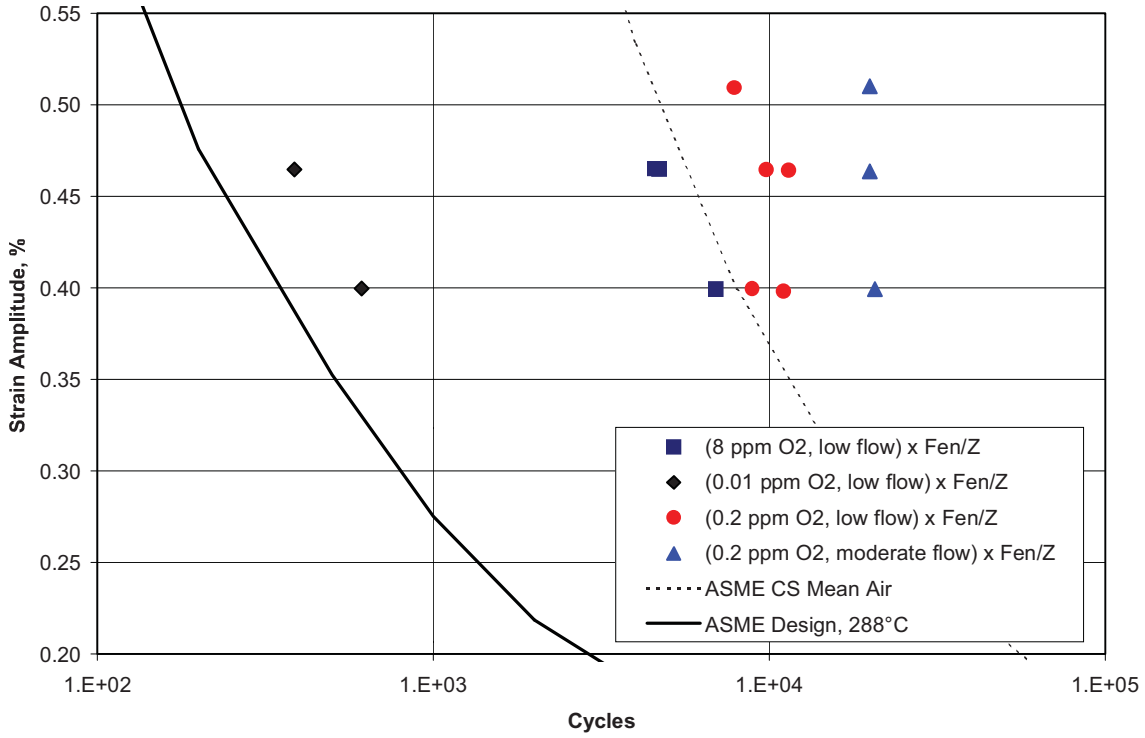

Figure 3-5
KWU Component Scale Test Results for Carbon Steel Corrected by F_{en} and Z

Therefore, these results appear to be consistent with the General Electric Company piping component tests, which were carried out at 8 ppm dissolved oxygen. **No environmental correction is needed for carbon steels except possibly for stagnant flow, very high dissolved oxygen conditions. This same conclusion would also seem likely to apply to low-alloy steels.**

Recent laboratory data obtained by Hirano, et al. [6,7], have helped to clarify the effect of coolant flow rate on environmental fatigue life reduction. Hirano et al. examined the effects on environmental fatigue life reduction at four different flow rates—0.1 m/sec (4 in/sec), 0.3 m/sec (12 in/sec), 4.3 m/sec (170 in/sec), and 7 m/sec (275 in/sec). Two of these flow rates are above and two are below the original threshold established by PVRC [1]. The material studied was typical carbon steel used for nuclear power plant piping. All tests were conducted at 289°C (552°F), nominal reactor coolant temperature at operating conditions, with a fully reversed strain amplitude of 0.3%. Three levels of dissolved oxygen were used—0.05 ppm, 0.2 ppm, and 1 ppm. One of these levels is below and two levels are above the PVRC dissolved oxygen threshold for carbon and low-alloy steels. One fairly low strain rate (0.01%/sec) and one fairly high strain rate (0.4%/sec) were used to evaluate the effect of strain rate.

The first major finding in the study was that, for tests at the fairly high strain rate (0.4%/sec), no effect of coolant flow rate on fatigue life was observed. These results are shown in Figure 3-6 (Figure 3 from *Effects of Water Flow Rate on Fatigue Life of Carbon Steel in High Temperature Pure Water Environment* [6]). This result was expected because the time available for attacking the carbon steel surface is limited following oxide layer rupture, and ample amounts of dissolved oxygen are available for reoxidation during strain reversal, even at 0.05 ppm dissolved oxygen.

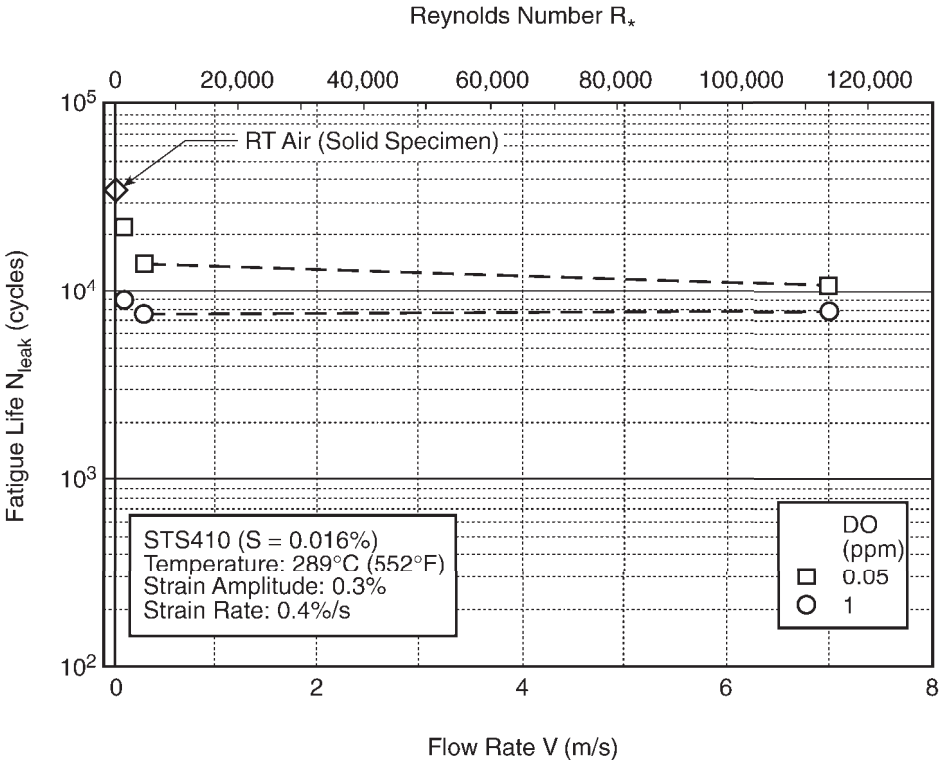

Figure 3-6
Effects of Water Flow Rate on Fatigue Life Tested at the Strain Rate of 0.4%/sec

For testing at the relatively low strain rate (0.01%/sec), the effect of coolant flow was significant, with much less fatigue life reduction at the higher flow rates. This effect is shown in Figure 3-7 (Figure 4 from *Effects of Water Flow Rate on Fatigue Life of Carbon Steel in High Temperature Pure Water Environment* [6]). In addition, and perhaps as important, the reduction in fatigue life is considerably less for the lower levels of dissolved oxygen. This is an expected finding but one that has been thrown into some confusion by data generated by Argonne National Laboratory (ANL). For example, the ratio of fatigue life at a coolant flow rate of 7 m/sec (275 in/sec) to that at a coolant flow rate of 0.1 m/sec (4 in/sec) is about a factor of 5 or 6 for dissolved oxygen of 0.05 ppm. This same ratio at a dissolved oxygen level of 1 ppm, is only about a factor of 3. Again, such a result is to be expected. At the relatively low strain rate, some surface attack is observed following oxide layer rupture; however, the higher flow rates offer ample dissolved oxygen for reoxidation during strain reversal. The surface attack is a function of the dissolved oxygen concentration, with higher dissolved oxygen levels causing greater reductions in fatigue life.

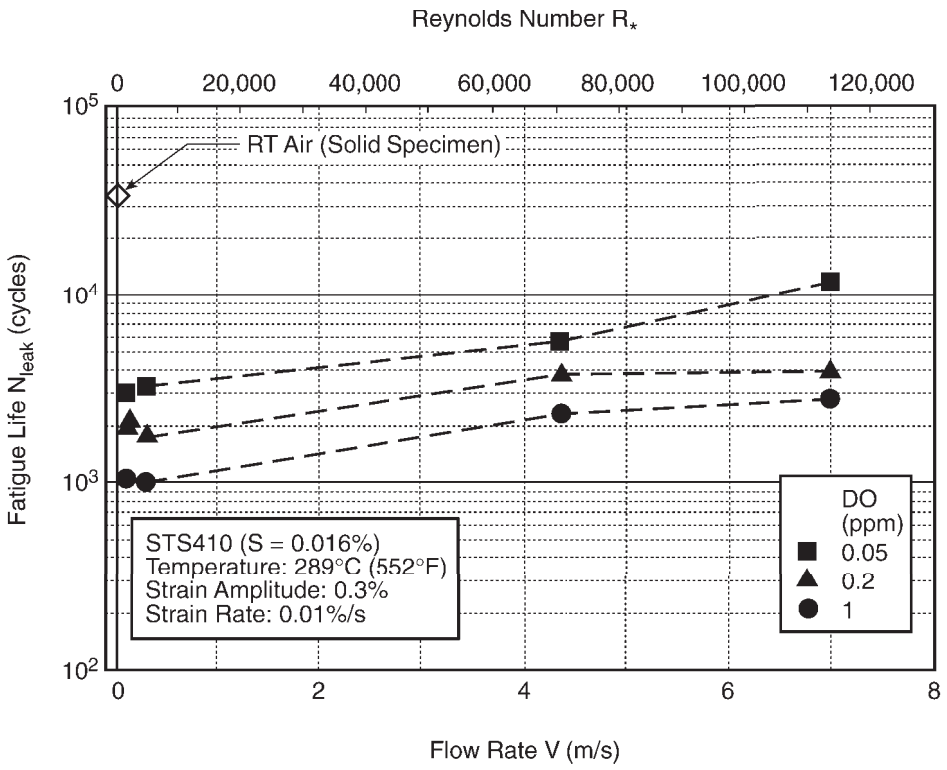

Figure 3-7
Effects of Water Flow Rate on Fatigue Life Tested at the Strain Rate of 0.01%/sec

This surface attack is also confirmed by noting that, for the highest coolant flow rate of 7 m/sec (275 in/sec), the fatigue life reduction over that in an air environment is about a factor of 3 for a dissolved oxygen level of 0.05 ppm. This ratio is about a factor of 10 for a dissolved oxygen level of 1 ppm. At the lowest coolant flow rate of 0.1 m/sec (4 in/sec), these fatigue life reductions are about 10 for a dissolved oxygen level of 0.05 ppm, and 35 for a dissolved oxygen level of 1 ppm. The fatigue life reduction at low strain rate, high coolant flow rate, and low dissolved oxygen is essentially equivalent to the fatigue life reduction at high strain rate.

From these data and their interpretation, we conclude that:

- For strain rates above the original PVRC threshold, the effect of coolant flow rate on fatigue life at temperature is not significant. The reduction in fatigue life (from that in air) is approximately a factor of 2 to 4 at the higher strain rates, with the factor of 2 applicable to low dissolved oxygen levels and the factor of 4 applicable to high dissolved oxygen levels.
- For strain rates below the original PVRC threshold, the effect of coolant flow rate is essentially equivalent to the effect of strain rate; that is, the high flow rate–low strain rate reductions in fatigue life are essentially equivalent to high strain rate fatigue life reductions. The latter are independent of the coolant flow rate.

3.3 References

1. W. A. Van Der Sluys and S. Yukawa, "Status of PVRC Evaluation of LWR Coolant Environmental Effects on the S-N Fatigue Properties of Pressure Boundary Materials." *PVP.* Vol. 306, pp. 47-58, ASME PVP 1995, Honolulu, HI (July 23-27, 1995).

2. G. L. Stevens and S. Ranganath, "Use of On-Line Fatigue Monitoring of Nuclear Reactor Components as a Tool for Plant Life Extension," Transactions ASME*,Journal of Pressure Vessel Technology*. Vol. 113, No. 3, pp. 349-357 (August 1991).

3. Keisler, J., Chopra, O. K., and Shack, W. J., *Statistical Analysis of Fatigue Strain-Life Data for Carbon and Low-Alloy Steels.* NUREG/CR-6237 (ANL-95/21), August 1994.

4. Itani, M., Iida, K., and Ogawa, K., "Effect of Loading Rate on the Fatigue Strength of Notched Carbon Steel in High Temperature Water." *PVP*. Vol. 374, pp. 261-268, ASME PVP 1998 (July 1998).

5. J. Hickling, *Low-Cycle Corrosion Fatigue of Unalloyed and Low-Alloy Steels in LWR Systems: Review of German Experience.* Report prepared for EPRI, Palo Alto, CA: January 1997.

6. A. Hirano, et al., "Effects of Water Flow Rate on Fatigue Life of Carbon Steel in High Temperature Pure Water Environment." *PVP*. Vol. 410-2, pp. 13-18, presented at ASME PVP 2000, Seattle, WA (July 24-28, 2000).

7. A. Hirano, et al., "Effects of Water Flow Rate on Fatigue Life of Carbon Steel in Simulated LWR Environment Under Low Strain Rate Conditions." *PVP*. Vol. 419, pp. 111-114, presented at ASME PVP 2001, Atlanta, GA (July 23-27, 2001).

4
REVIEW OF S-N MODELS

A variety of models have been used in the development of the S-N analysis procedures described in this report. Fatigue models were used in the development of the original fatigue curves in ASME Section III. Models have also been developed to describe the effect of the primary coolant environment on the S-N fatigue properties of the pressure boundary materials. These various models will be described and comparisons made between the predictions from the models and the available fatigue data in order to gain a better understanding of the accuracy of these models.

4.1 ASME Code S-N Models

In June 1961, the ASME Sub-Task Group on Fatigue recommended [1] to the ASME Boiler and Pressure Vessel Committee's Special Committee to Review Code Stress Basis that the formula given below be used for modeling low-cycle fatigue data:

$$S = \frac{E}{4\sqrt{N}} \ln \frac{100}{100 - RA} + S_e, \qquad \text{Eq. 4-1}$$

where

S = elastic modulus x stain amplitude (psi)

E = elastic modulus (psi)

N = cycles-to-failure

RA = reduction of area in tensile test (percent)

S_e = endurance limit or fatigue strength at 10^7cycles (psi)

Langer [2] applied Equation 4-1 to determine the low-cycle fatigue curves for carbon steel, low-alloy steel, and austenitic stainless steel. A best-fit curve was obtained by using the method of least squares, as applied to the logarithms of the measured S and N values, with Equation 4-1 as the model. The modulus, E, was known in each case and the computer code gave the best-fit value for RA and S_e. These values are shown on the curves reproduced as Figures 4-1, 4-2, and 4-3.

These best-fit curves were then corrected for the maximum effect of mean stress using the formula below. This was derived from the Goodman diagram considering the change in the mean stress that is produced by yielding.

$$S' = S\left[\frac{S_u - S_Y}{S_U - S}\right] \text{ for } S < S_y, \qquad \textbf{Eq. 4-2}$$

where

S = value from curve
S' = adjusted S value
S_u = ultimate tensile strength
S_y = yield strength

The results from this correction for the mean stress are shown in Figures 4-1 and 4-2 as dotted lines. Because of their high endurance limit and low-yield strength, austenitic stainless steels cannot sustain a mean stress at a cyclic strain level that would produce failure (Figure 4-3).

The best-fit lines, developed by Langer [2], appear to fit the data well. It must be pointed out that all of these data were obtained from strain-controlled experiments and that all of the results lie in what is considered the low-cycle region.

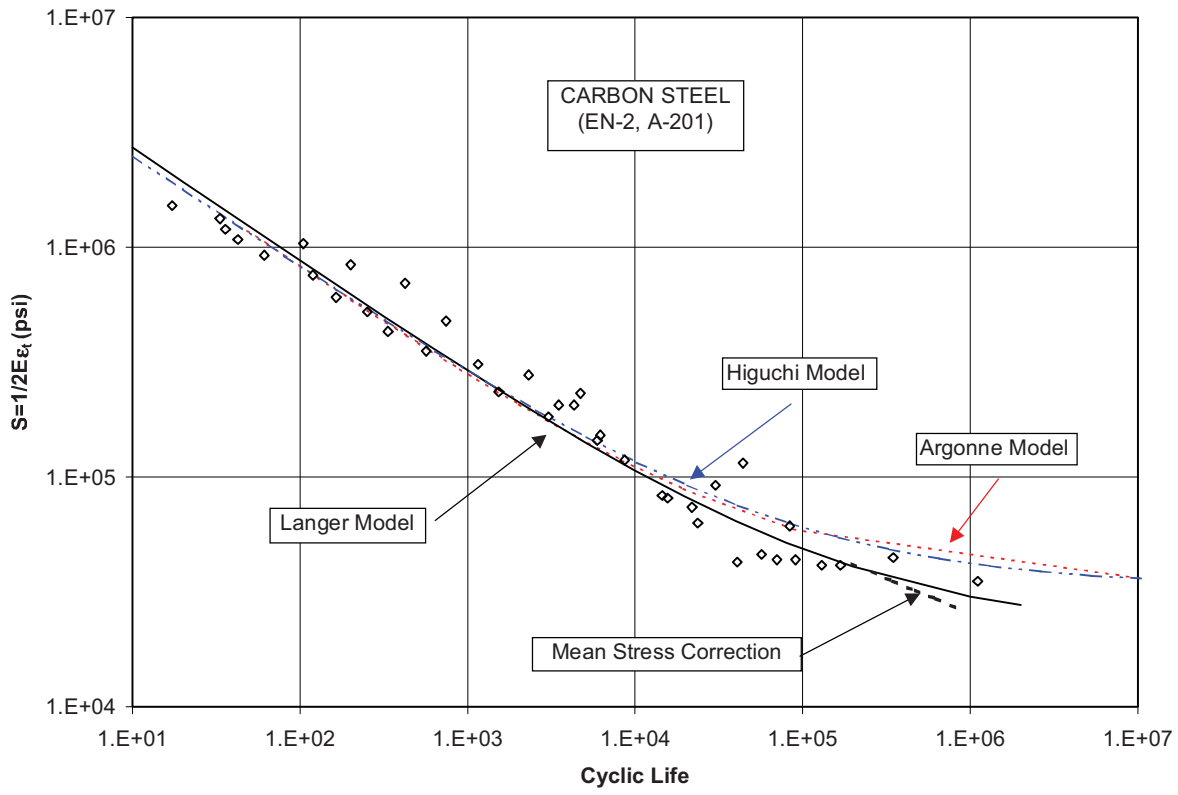

Figure 4-1
Carbon Steel Data in Room Temperature Air Used in the Development of the ASME Procedure Compared With the Predictions From the Three Models

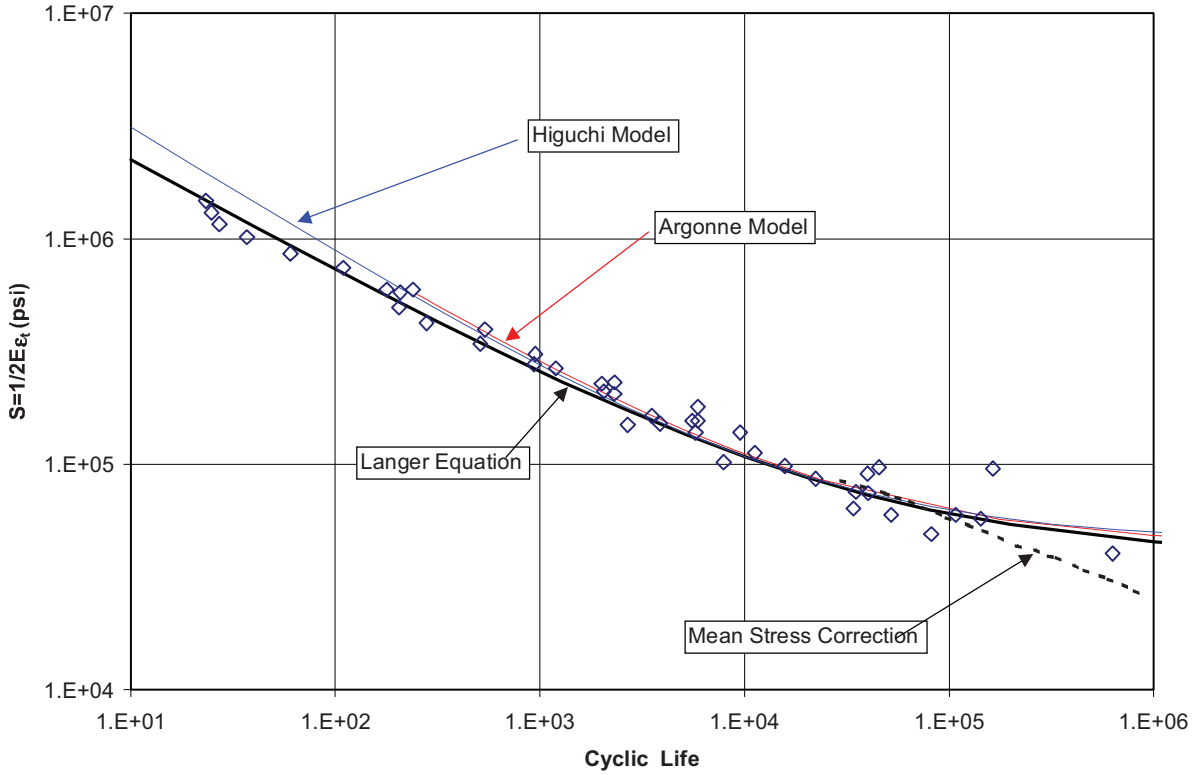

Figure 4-2
Low-Alloy Steel Data in Room Temperature Air Used in the Development of the ASME Procedure Compared With the Predictions From the Three Models

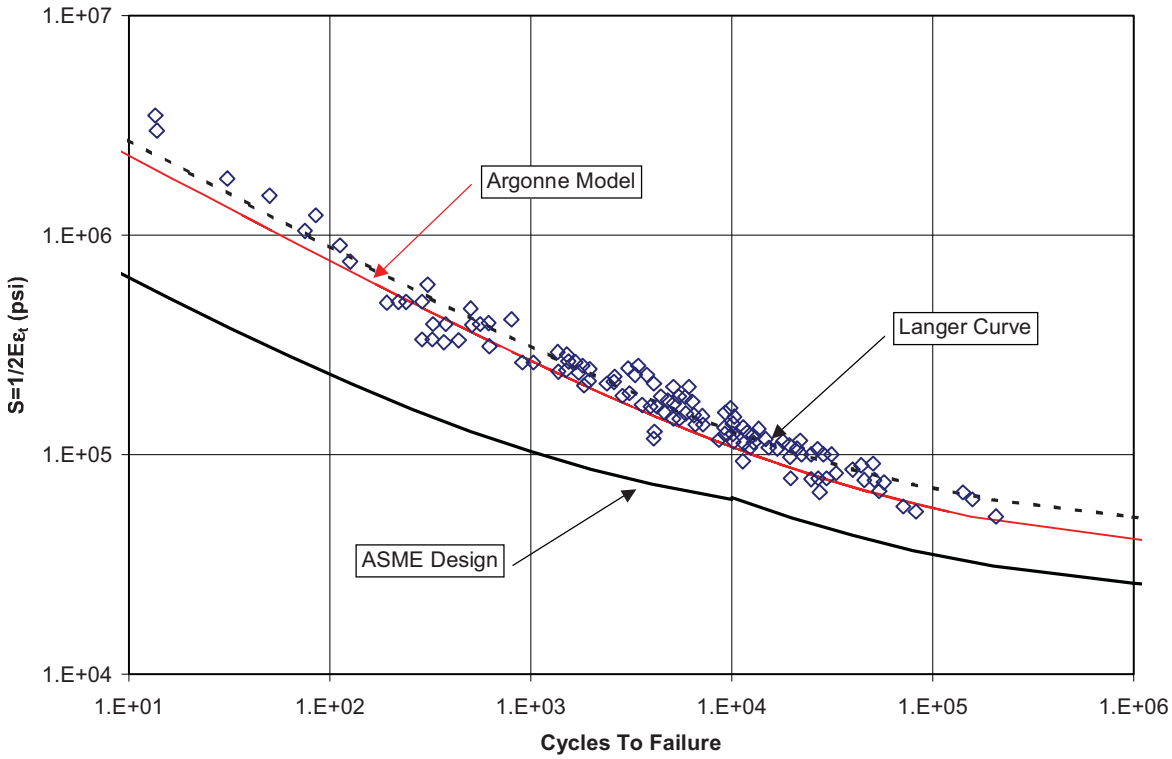

Figure 4-3
Austenitic Stainless Steel Data in Room Temperature Air Used in the Development of the ASME Procedure Compared With the Predictions From the Langer Equation and the Argonne Model

4.2 Argonne National Laboratory Air Fatigue Data Models

There are a number of recent reports from Argonne National Laboratory (ANL) [3,4] with alternative equations that have been used to fit the available data. The equations that ANL has developed for carbon, low-alloy, and austenitic stainless steel are as follows:

Carbon Steel

$$\ln(N) = 6.564 - 1.975\ln(\varepsilon_a - 0.113) - 0.00124T \qquad \textbf{Eq. 4-3}$$

Low-Alloy Steel

$$\ln(N) = 6.627 - 1.808\ln(\varepsilon_a - 0.151) - 0.00124T \qquad \textbf{Eq. 4-4}$$

In Equations 4-3 and 4-4

ε_a =strain amplitude (%)

T = temperature (°C)

Austenitic Stainless Steel (Types 304 and 316)

$$\ln(N) = 6.703 - 2.30\ln(\varepsilon_a - 0.126) \qquad \textbf{Eq. 4-5}$$

Austenitic Stainless Steel (Type 316 NG)

$$\ln(N) = 7.422 - 21.671\ln(\varepsilon_a - 0.126) \qquad \textbf{Eq. 4-6}$$

In Equations 4-5 and 4-6

ε_a =strain amplitude (%)

The predictions of the fatigue lives from the ANL model equations are also shown in Figures 4-1, 4-2, and 4-3.

4.3 Japanese Air Fatigue Data Models

The results from similar air fatigue data models developed in Japan [5,6] are shown below. These model results, as well as the ANL model results, are also shown in Figures 4-1 and 4-2.

Carbon Steel

$$\varepsilon_a = 25.71 N^{-0.490} + 0.113 \qquad \textbf{Eq. 4-7}$$

Low-Alloy Steel

$$\varepsilon_a = 38.44 N^{-0.562} + 0.155 \qquad \textbf{Eq. 4-8}$$

4.4 Comparison of Model Predictions for Air Fatigue Data

The ANL air fatigue data models and those developed in Japan produce very similar results. In the case of carbon steel, these two models are almost identical and somewhat above the Langer prediction in the high-cycle life region of the curves. The carbon steel data used by Langer also appear to follow the predictions made by Langer better than those made by the two newer models.

All three of the models that predict the fatigue properties of the low-alloy steels produce essentially the same curve.

Figure 4-3 compares the Langer model with the ANL model for the prediction of the fatigue properties of austenitic stainless steel. The ANL prediction is somewhat below the Langer curve and the data, although scattered, appears to support the Langer curve as a curve representative of the mean of the data.

Figures 4-4, 4-5, and 4-6 show the corresponding three previous data and curves, with the addition of the new test results from the database collected by the PVRC. Figure 4-4 presents the carbon steel data. The data from the PVRC database appear to have a slightly higher fatigue limit than the ASME data. The ANL and Japanese models appear to over-predict the mean of the properties in the vicinity of the fatigue limit. The newer carbon steels from which the PVRC data were obtained have slightly higher strengths than the materials used to obtain the ASME data. This would cause a higher fatigue limit.

The low-alloy steel data follow the predictions of all three models, as shown in Figure 4-5. Little difference is seen between the original ASME data, the PVRC data, and the three predictions.

The stainless steel data are shown in Figure 4-6. There appears to be little difference between the ASME data and the PVRC data in the low-cycle fatigue region. The ASME data do not extend past a life of 2 x 10^5 cycles. The PVRC data extend to fatigue lives of 5.5 x 10^7 cycles. All of the fatigue results in this figure were conducted under strain range control. The ANL model does appear to predict the mean fatigue properties in the 10^5 to 10^7 cycles region better than Equation 4-1.

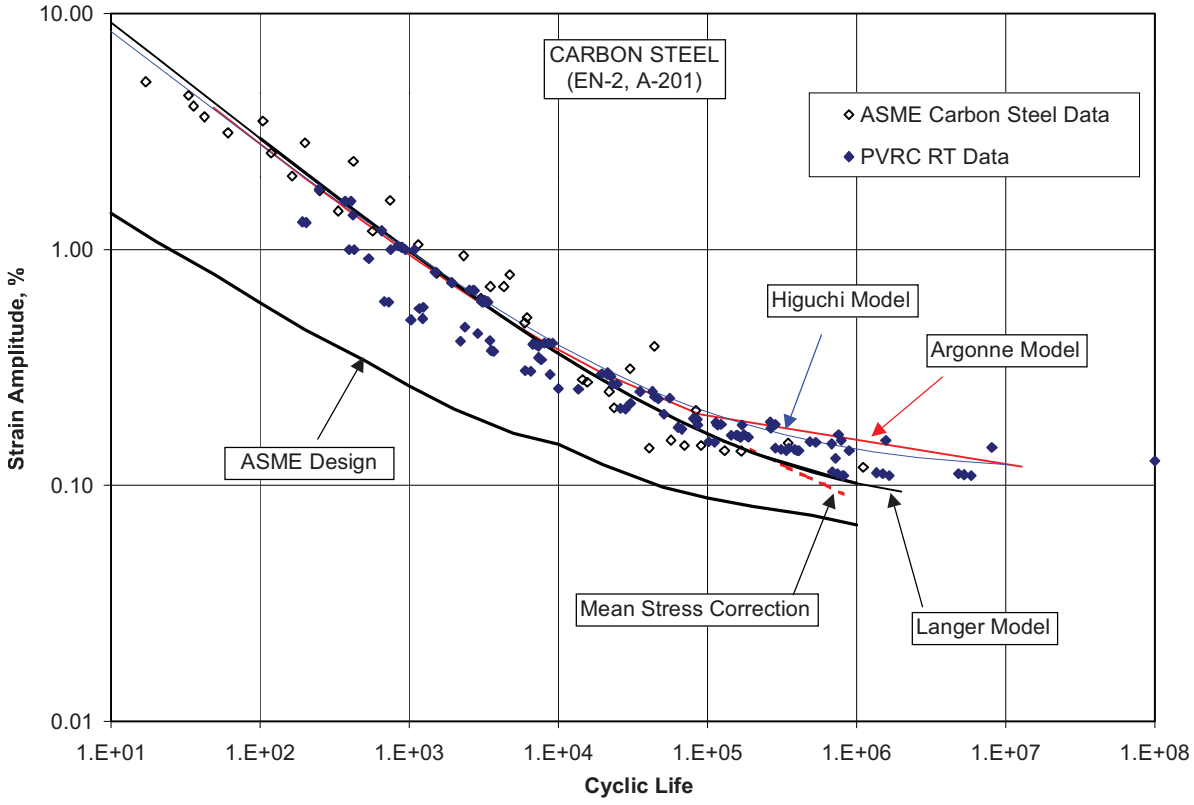

Figure 4-4
Carbon Steel Data and Curves From Figure 4-1 With the Addition of Room Temperature Air Carbon Steel Data From the PVRC Database

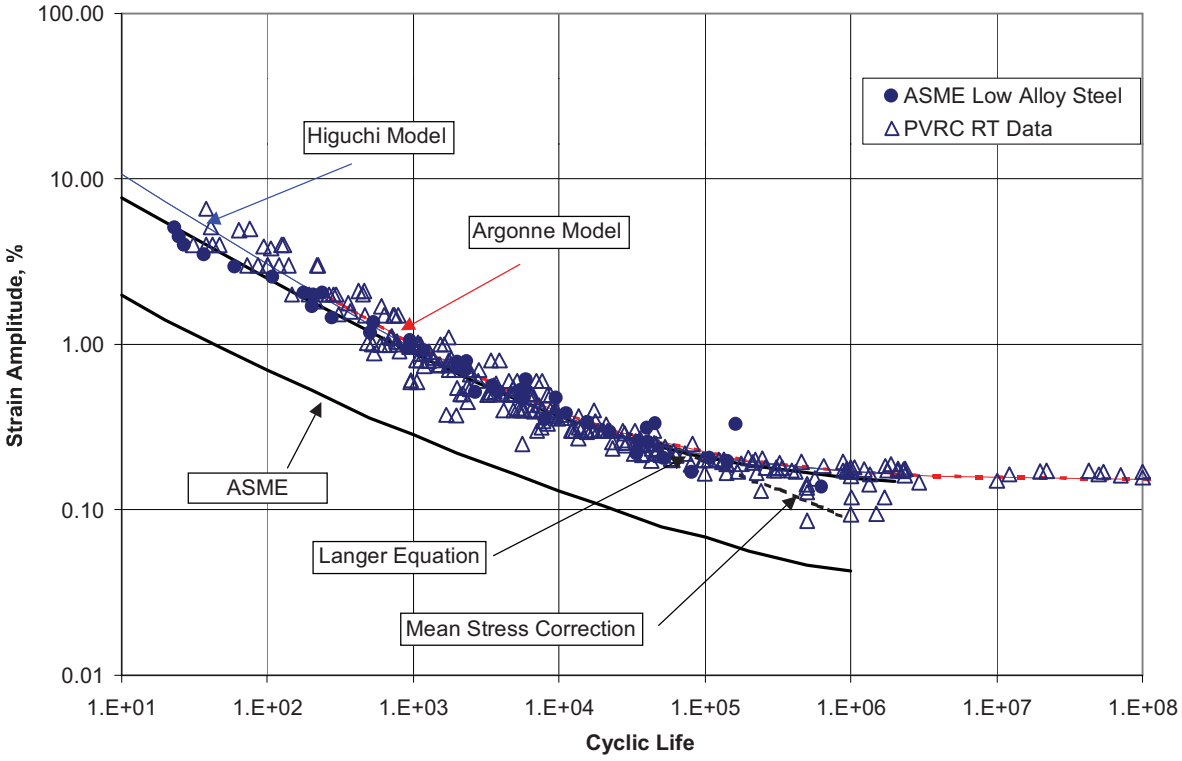

Figure 4-5
Low-Alloy Steel Data and Curves From Figure 4-2 With the Addition of Room Temperature Air Low-Alloy Steel Data From the PVRC Database

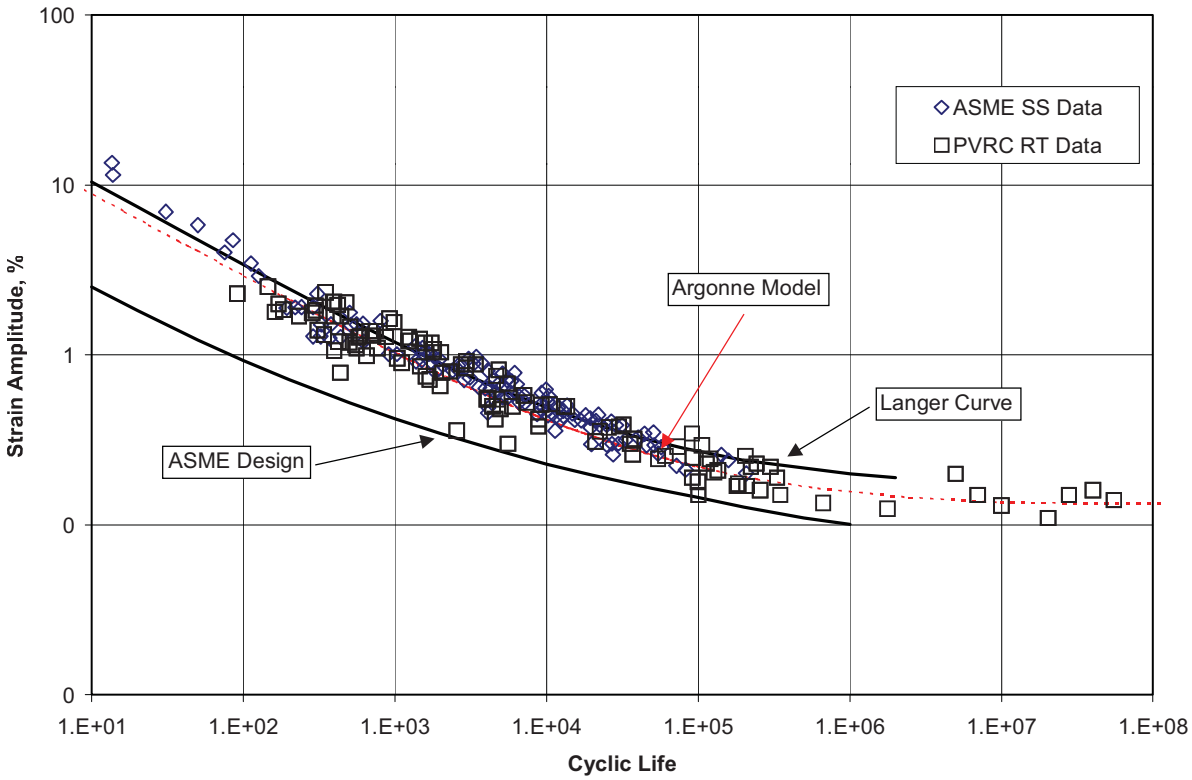

Figure 4-6
Stainless Steel Data and Curves From Figure 4-3 With the Addition of Room Temperature Air Stainless Steel Data From the PVRC Database

Figure 4-7 shows all of the data from the ASME and PVRC data sets, plus the data collected by Jaske and O'Donnell [7]. The Jaske and O'Donnell data show a large amount of scatter through the curve. The mean of the data appears to be below either the Langer Curve or the ANL prediction. Included in these data are results from both load-controlled and strain-controlled experiments. The data files do not identify those data that are obtained from strain-controlled tests and those that are obtained from load-controlled tests.

The apparent discrepancy between the ASME Code mean air curve for austenitic stainless steels and the best-estimate data fit by ANL at the high-cycle end (above 10^4 cycles) for austenitic stainless steel fatigue data obtained in laboratory air environments had been observed previously [7]. Considerable discussion of this difference occurred during the mid-to-late 1970s within the ASME Code bodies concerned with fatigue [8]. At that time, the arguments for adjusting the ASME Code fatigue design curve to eliminate the apparent discrepancy were not deemed to be sufficiently persuasive. The major points made by the discussion participants who favored retaining the existing ASME Code mean air curve data fit were:

- The apparent discrepancy is insufficiently large to justify fine-tuning the high-cycle end of the existing ASME Code mean air curve.

- The apparent discrepancy might have been influenced by load-controlled results within the data set, in contrast with the ASME Code mean air curve that is based on strain-controlled fatigue data.
- The forgiving nature of compositional differences and other metallurgical factors in the low-cycle (plastic strain) region, and the greater influence of these differences and factors in the high-cycle (elastic) region.
- The successful experience with stainless steel components, such as reactor internals, that are subjected to high-cycle, hot functional testing environments prior to service without fatigue failure.

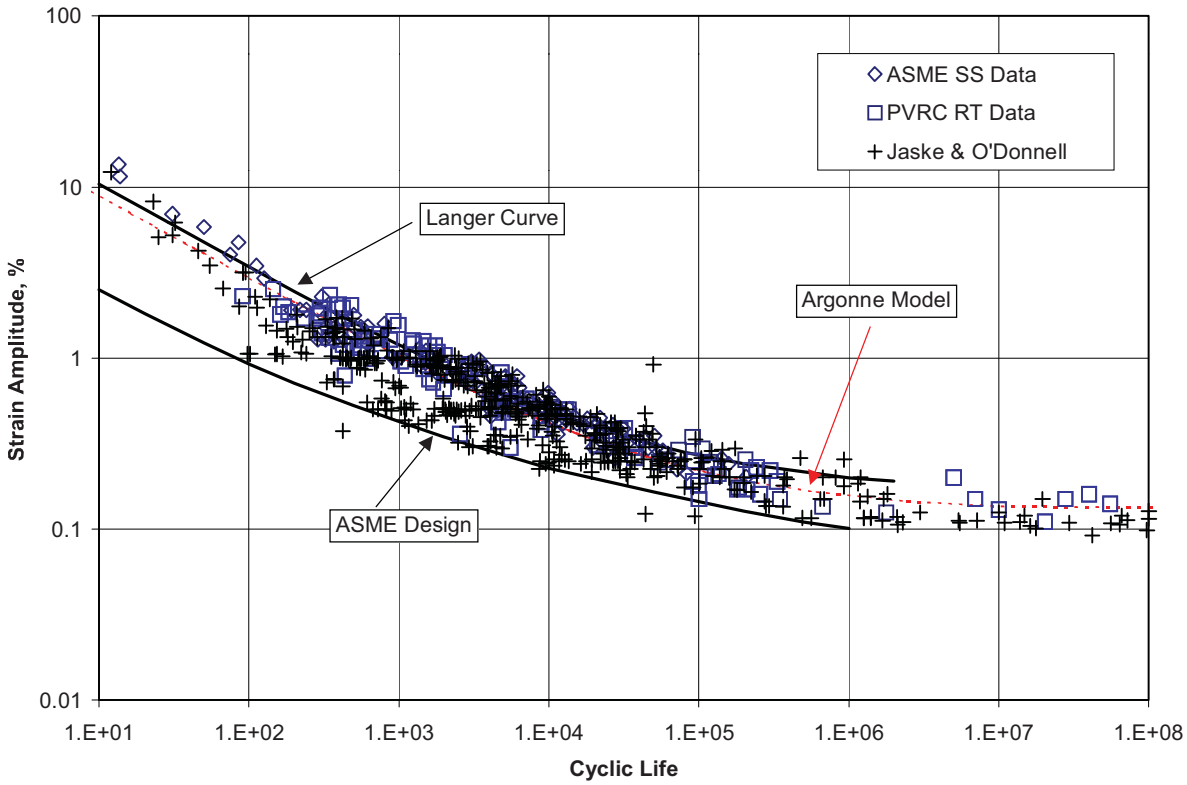

Figure 4-7
Stainless Steel Data and Curves From Figure 4-6 With the Addition of Room Temperature Air Stainless Steel Data From the Jaske and O'Donnell Database

Another way to evaluate the various models is through a comparison of the predicted versus the measured fatigue lives. Figure 4-8 compares the predictions from Equation 4-1 with the actual fatigue lives measured in the ASME carbon steel database. Also shown are lines representing a measured life that is twice the predicted life and 1/2 of the predicted life. The majority of the data fall between these two lines. Figure 4-9 compares the PVRC database for carbon steel data in air compared with the ANL predictions. This figure also has the twice- and 1/2-prediction lines. A significant amount of data falls below the 1/2-prediction data with very little data above the twice prediction line. It appears that the ANL model slightly over-predicts the fatigue life of carbon steel.

The prediction of the low-alloy steel fatigue lives is compared with the measured lives in Figure 4-10. In this case, most of the data fall between the twice- and 1/2-prediction lines. This indicates that the ANL model for low-alloy steel predicts the test results in the PVRC database fairly well.

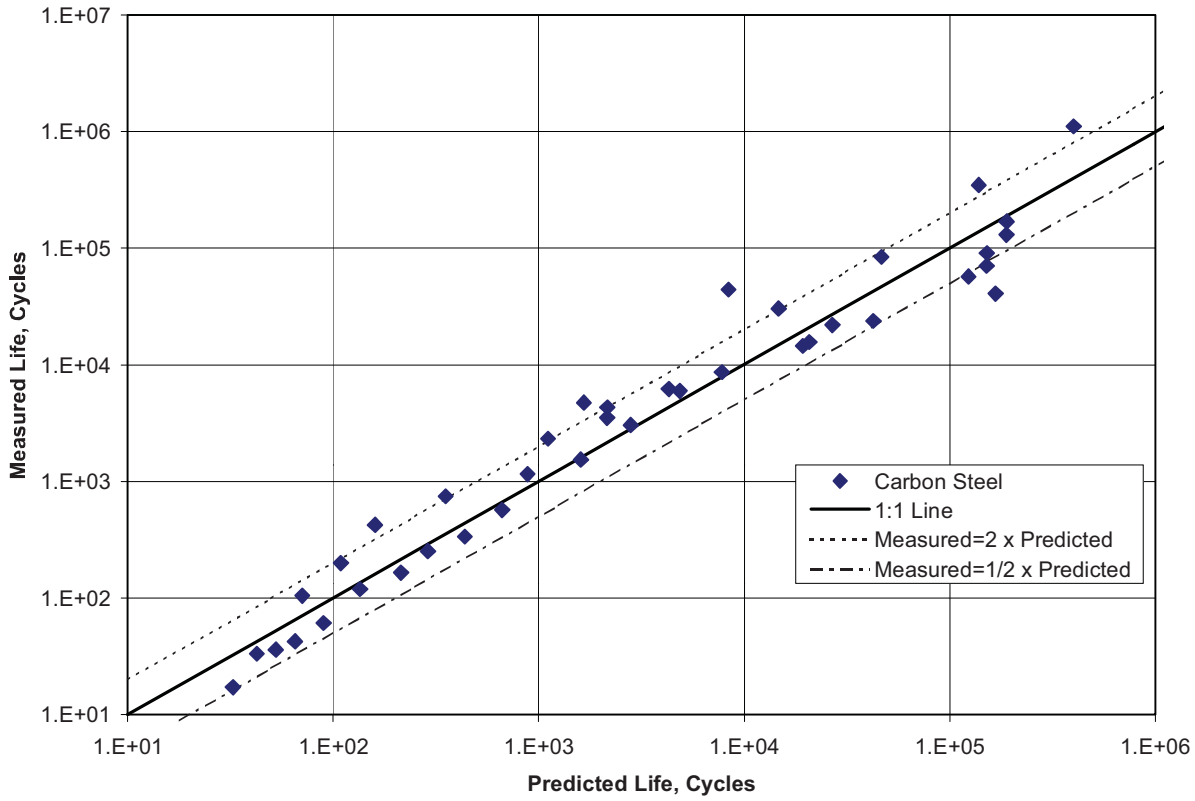

Figure 4-8
Comparison of Predicted Versus Measured Fatigue Lives for Carbon Steel Data Shown in Figure 4-1 Using the Langer Equation for Life Prediction

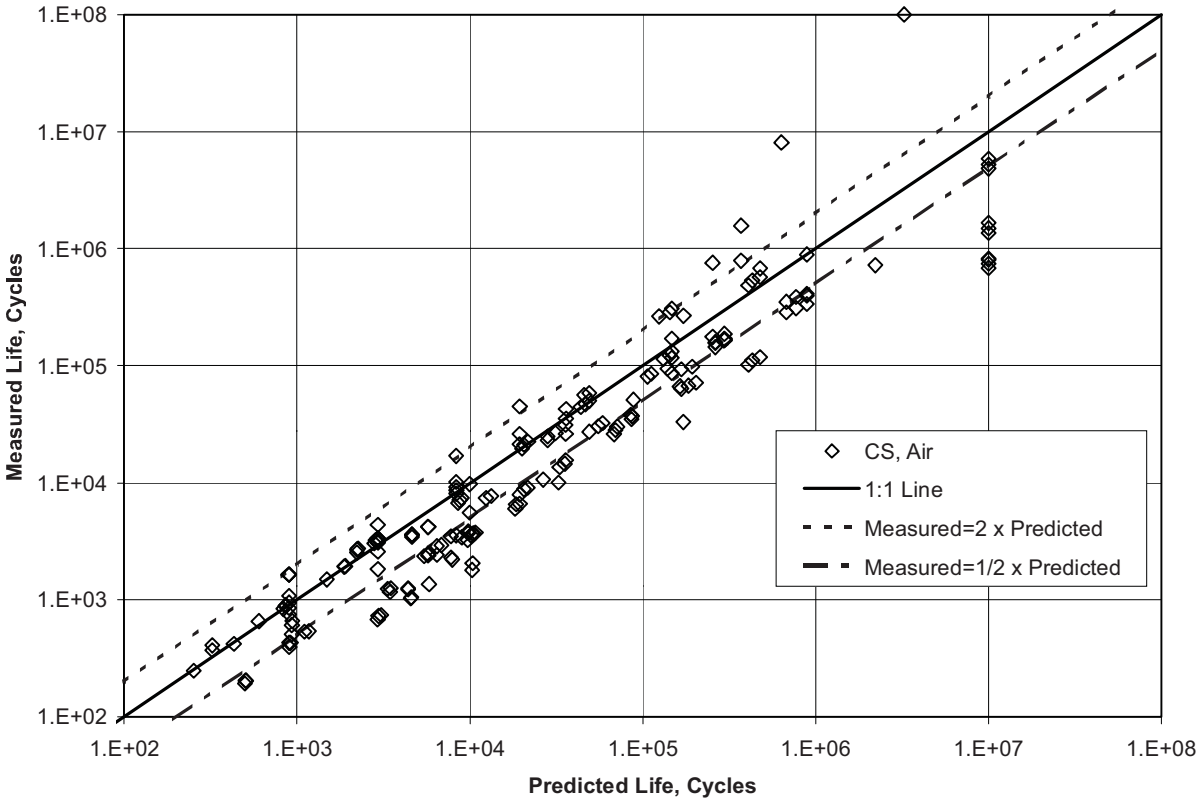

Figure 4-9
Comparison of Predicted Versus Measured Fatigue Lives for Carbon Steel Data From the PVRC Database and Using the Argonne Model for Life Prediction

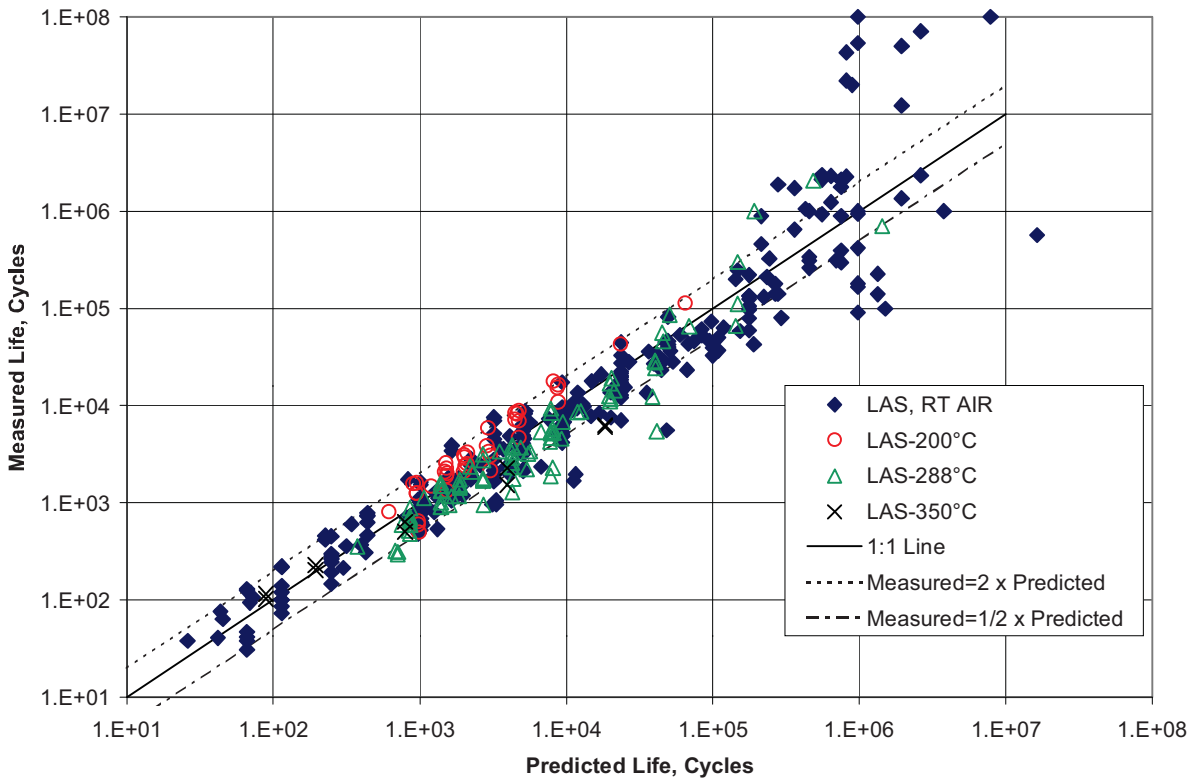

Figure 4-10
Comparison of Predicted Versus Measured Fatigue Lives for Low-Alloy Steel Data From the PVRC Database and Using the Argonne Model for Life Prediction

4.5 Reactor Water Environmental Effects

There are two sets of models that have been developed to predict the fatigue properties of carbon, low-alloy, and austenitic stainless steels in reactor water environments. The two models were developed by ANL [3,4] and the Japanese [5,6]. These models are presented below:

4.5.1 ANL Environmental Model

4.5.1.1 Carbon Steel

$$\ln(N) = 6.010 - 1.975\ln(\varepsilon_a - 0.113) + 0.101 S^* T^* O^* \dot{\varepsilon}^* \qquad \textbf{Eq. 4-9}$$

4.5.1.2 Low-Alloy Steel

$$\ln(N) = 5.729 - 1.808\ln(\varepsilon_a - 0.151) + 0.101 S^* T^* O^* \dot{\varepsilon}^* \qquad \textbf{Eq. 4-10}$$

For Equations 4-9 and 4-10

$$S^* = S \qquad (0 < S \le 0.015 wt\%)$$
$$S^* = 0.015 \qquad (S > 0.015 wt\%)$$

$$T^* = 0 \qquad (T < 150°C)$$
$$T^* = T - 150 \qquad (T = 150 - 350°C)$$

$$O^* = 0 \qquad (DO < 0.05 ppm)$$
$$O^* = \ln(DO / 0.04) \qquad (0.05 ppm \le DO \le 0.5 ppm)$$
$$O^* = \ln(12.5) \qquad (DO > 0.5 ppm)$$

$$\dot{\varepsilon} = 0 \qquad (\dot{\varepsilon} > 1\% / s)$$
$$\dot{\varepsilon} = \ln(\dot{\varepsilon}) \qquad (0.001 \le \dot{\varepsilon} \le 1\% / s)$$
$$\dot{\varepsilon} = \ln(0.001) \qquad (\dot{\varepsilon} < 0.001\% / s)$$

4.5.1.3 Austenitic Stainless Steel (Types 304 and 316)

$$\ln(N) = 5.768 - 2.030 \ln(\varepsilon_a - 0.126) + T^* \dot{\varepsilon}^* O^* \qquad \textbf{Eq. 4-11}$$

4.5.1.4 Austenitic Stainless Steel (Type 316 NG)

$$\ln(N) = 6.9123 - 1.671 \ln(\varepsilon_a - 0.126) + T^* \dot{\varepsilon}^* O^* \qquad \textbf{Eq. 4-12}$$

For Equations 4-11 and 4-12

$$T^* = 0 \qquad (T < 200°C)$$
$$T^* = 1 \qquad (T \ge 200°C)$$

$$\dot{\varepsilon}^* = 0 \qquad (\dot{\varepsilon} > 0.4\% / s)$$
$$\dot{\varepsilon}^* = \ln(\dot{\varepsilon} / 0.4) \qquad (0.0004 \le \dot{\varepsilon} \le 0.4\%.s)$$
$$\dot{\varepsilon}^* = \ln(0.0004 / 0.4) \qquad (\dot{\varepsilon} < 0.0004\% / s)$$

$$O^* = 0.260 \qquad (DO < 0.05 ppm)$$
$$O^* = 0.172 \qquad (DO \ge 0.05 ppm)$$

4.5.2 Japanese (Higuchi) Environmental Model

4.5.2.1 Carbon Steel

$$\varepsilon_a = 25.71 (N_{WP} (\dot{\varepsilon}_T)^{(-0.560 R_P)})^{-0.490} + 0.113 \qquad \textbf{Eq. 4-13}$$

4.5.2.2 Low-Alloy Steel

$$\varepsilon_a = 38.44(N_{WP}(\dot{\varepsilon}_T)^{(-0.496R_P)})^{-0.562} + 0.155 \qquad \textbf{Eq. 4-14}$$

For Equations 4-13 and 4-14

$$R_P = 0.3\ln(DO(ppm)) + 1.13$$
$$0.2 \le R \le 0.198\exp(0.00557T)$$

T=°C

4.5.2.3 Austenitic Stainless Steel

$$\varepsilon_a = 13.1\left[N_f(\varepsilon/0.4)^{-P}\right]^{-0.457} + 0.11 \qquad \textbf{Eq. 4-15}$$

For Equation 4-15

$$P = 0.04 \qquad (T < 100°C)$$
$$P = 9.33x10^{-4}T - 0.053 \qquad (100°C \le T \le 325°C)$$
$$P = 0.25 \qquad (T > 325°C)$$

4.5.3 Environmental Model Comparisons

Figure 4-11 shows the data for the actual life of carbon steel specimens tested in a simulated BWR environment from the PVRC database plotted versus the life predicted for these specimens by the ANL model shown above. As in Figure 4-9, the two dotted lines represent the twice-life and 1/2-life lines. There is a significant amount of scatter in these results. There are no obvious trends in the scatter. What appears to be a line of data above all the rest of the data is not from a single investigator or from a single heat of material. The prediction line appears to fall below what could be considered the mean line. Substantially more data fall above the prediction line than below, and little data is below the 1/2-prediction line, while a substantial amount of data falls above the twice prediction line.

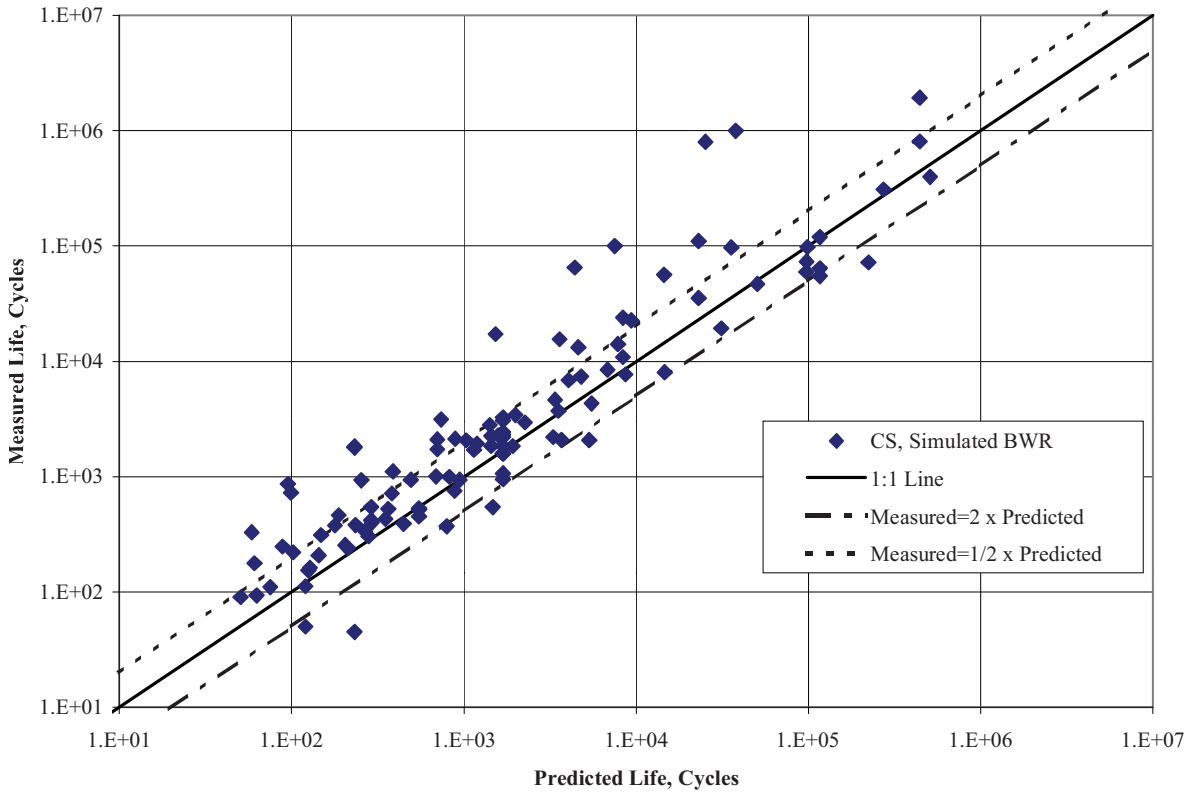

Figure 4-11
Comparison of Predicted Versus Measured Fatigue Lives for Carbon Steel Data in a Simulated BWR Environment From the PVRC Database and Using the Argonne Model for Life Prediction

Figure 4-12 shows the same carbon steel data compared with the predicted lives from the Japanese model shown above. The amount of data scatter is similar to that seen in Figure 4-11. The same data fall above the predicted line, as seen in Figure 4-11. With this model from Japan, the test results appear to be more evenly distributed both above and below the prediction line than with the model from ANL. However, note that Figure 4-12 appears to have a greater number of data points above and below the scatter boundaries. It appears that the model from Japan comes close to predicting the mean fatigue behavior of the carbon steel material in the BWR environment.

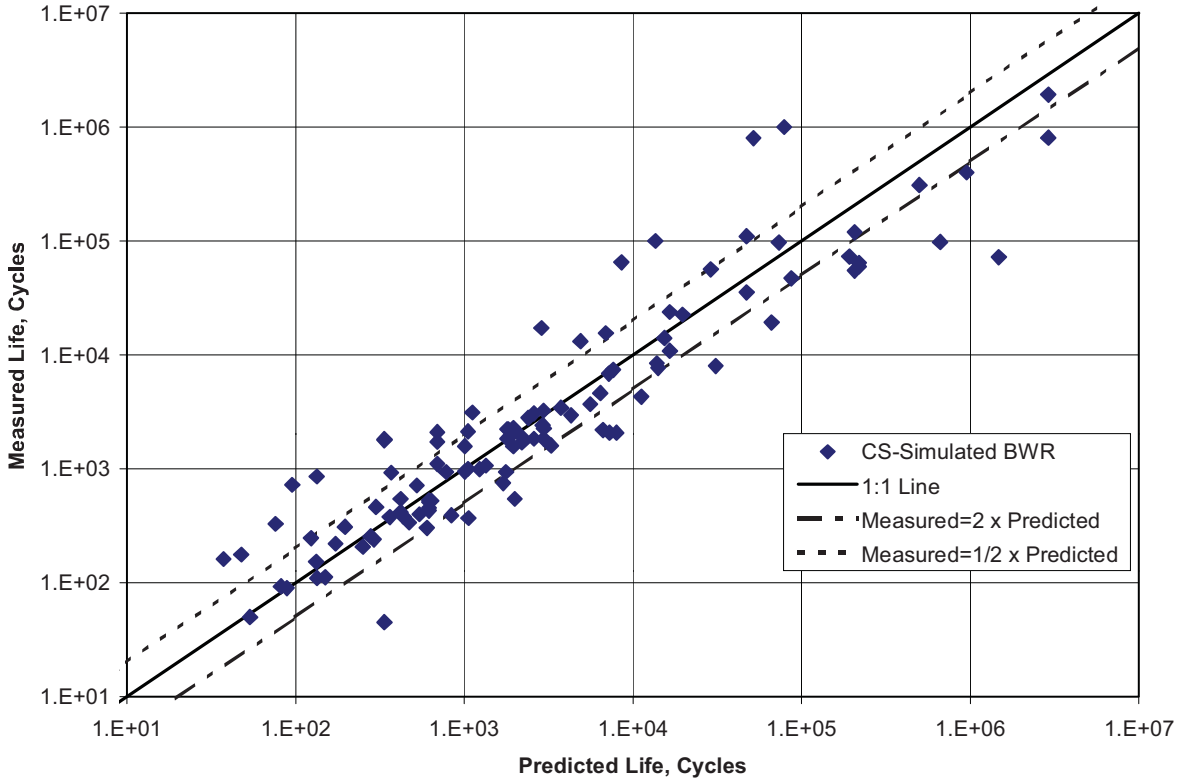

Figure 4-12
Comparison of Predicted Versus Measured Fatigue Lives for Carbon Steel Data in a Simulated BWR Environment From the PVRC Database and Using the Japanese Model for Life Prediction

Figures 4-13 and 4-14 show the same type of comparison using the PVRC fatigue database information for low-alloy steel in a simulated BWR environment. These results are similar to those for the carbon steel data. The Japanese model seems to predict results that are closer to the mean of the data than the ANL model. This seems to be especially true in the higher cyclic life region of the fatigue curve.

Figures 4-15 and 4-16 show comparisons of the predicted versus the measured lives for austenitic stainless steel in a simulated PWR environment using the models developed by ANL and by Japanese investigators. The data in these figures are from the PVRC database. Although the models are different, the results as shown in these figures are similar. Both models appear to predict the mean behavior of the material up to a life of about 10^5 cycles. Above this lifetime both models appear to over-predict fatigue life and the scatter increases about the mean line.

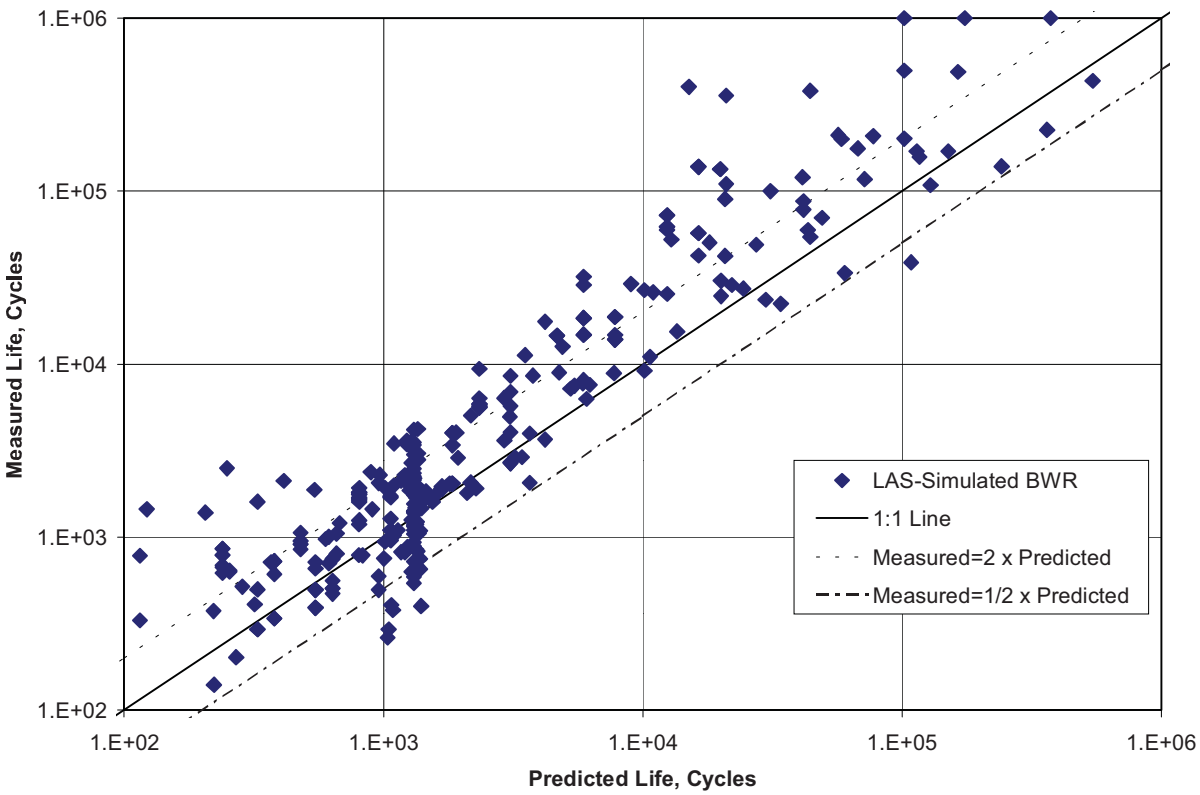

Figure 4-13
Comparison of Predicted Versus Measured Fatigue Lives for Low-Alloy Steel Data in a Simulated BWR Environment From the PVRC Database and Using the Argonne Model for Life Prediction

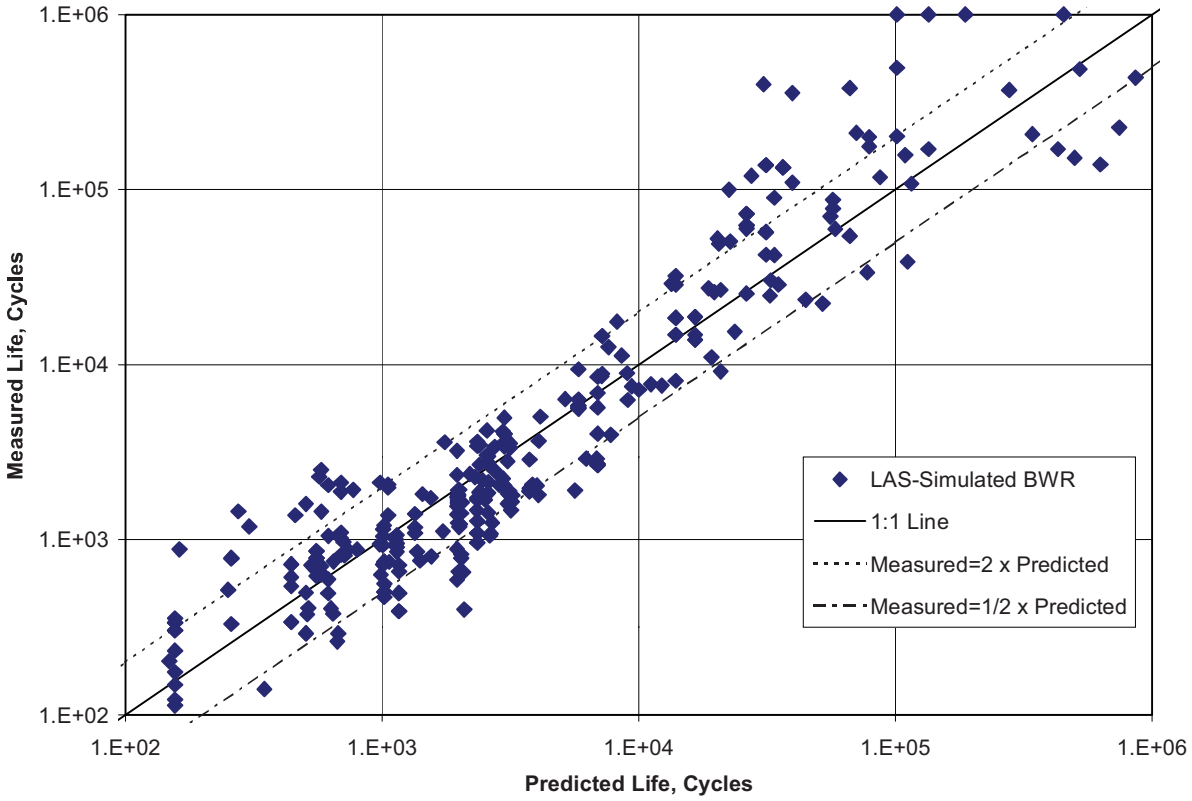

Figure 4-14
Comparison of Predicted Versus Measured Fatigue Lives for Low-Alloy Steel Data in a Simulated BWR Environment From the PVRC Database and Using the Japanese Model for Life Prediction

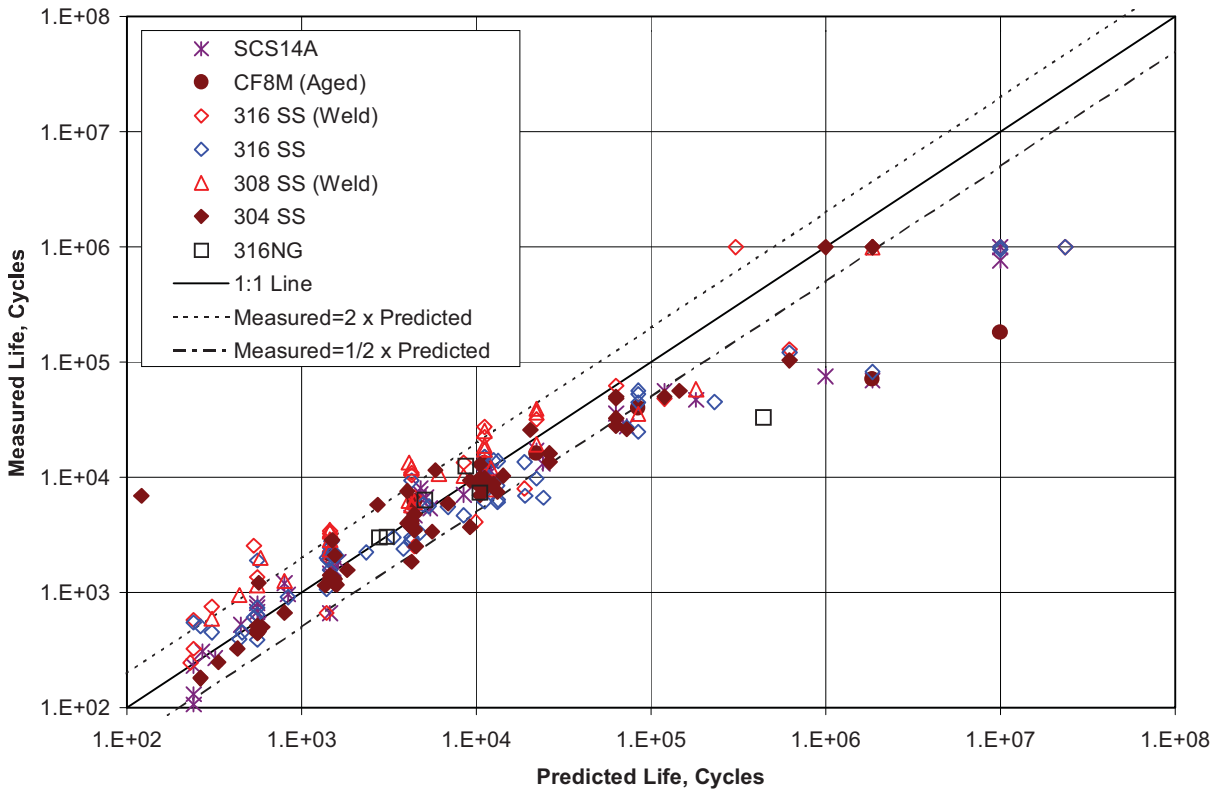

Figure 4-15
Comparison of Predicted Versus Measured Fatigue Lives for Stainless Steel Data in a Simulated PWR Environment From the PVRC Database and Using the Argonne Model for Life Prediction

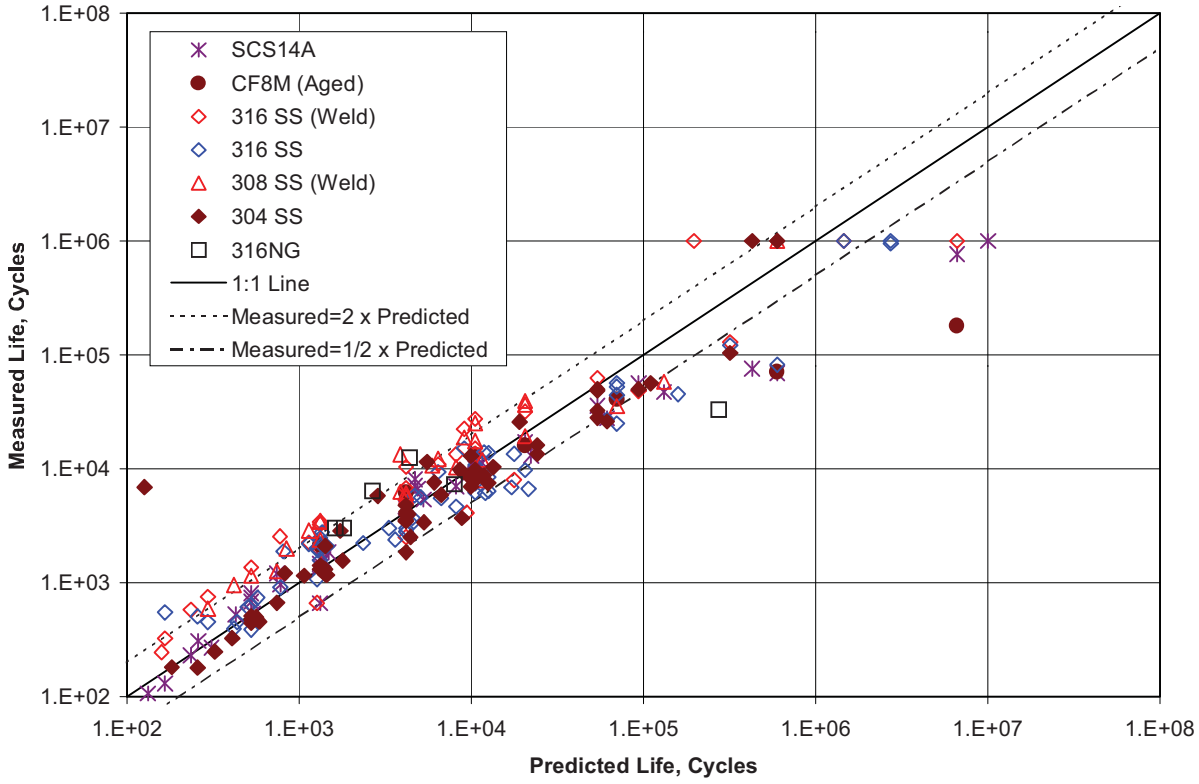

Figure 4-16
Comparison of Predicted Versus Measured Fatigue Lives for Stainless Steel Data in a Simulated PWR Environment From the PVRC Database and Using the Japanese Model for Life Prediction

The comparison of the prediction for the ANL model for 304 stainless steel in a simulated BWR environment and the measured lives of experiments from the PVRC database is shown in Figure 4-17. The scatter is quite large in this figure. The data fall on both sides of the prediction line. At this time there is no Japanese model for stainless steel in a BWR environment.

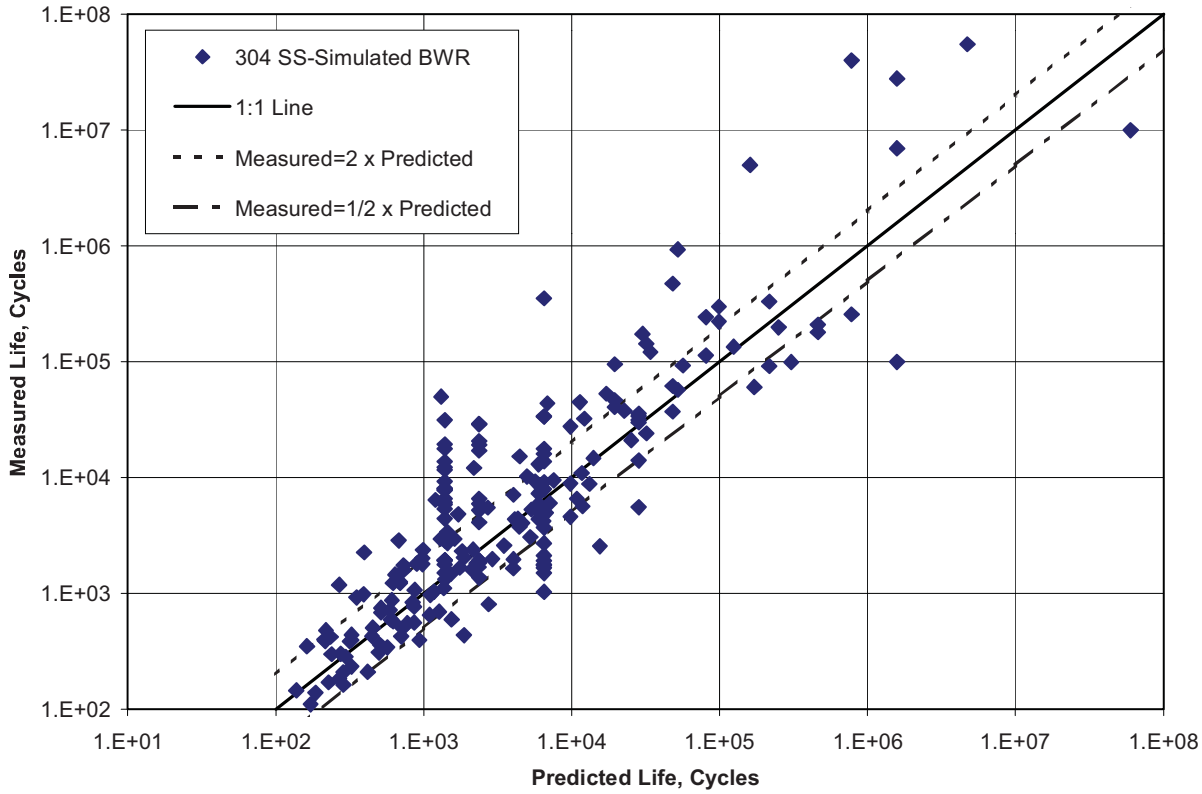

Figure 4-17
Comparison of Predicted Versus Measured Fatigue Lives for 304 Stainless Steel Data in a Simulated BWR Environment From the PVRC Database and Using the Argonne Model for Life Prediction

The various models for describing laboratory air fatigue data and simulated reactor water fatigue data have been examined. In particular, models for describing austenitic stainless steel air fatigue data have been compared with the original ASME Code air fatigue data, the Jaske-O'Donnell air fatigue data, and the PVRC air fatigue database. Models developed by ANL and by Japanese investigators for describing simulated reactor water environmental fatigue data have also been compared. The most significant findings are:

- Uncertainty in the strain-controlled and load-controlled characteristics of the Jaske-O'Donnell austenitic stainless steel air fatigue database limit the ability to resolve issues about the effectiveness of different models.
- Many of the models are sufficiently robust to produce accurate data fits, especially at the higher strain amplitudes (lower numbers of cycles to failure).
- However, scatter in some of the model results, in particular for BWR environments, limits the ability to draw definitive conclusions about the effectiveness of different models for those conditions.
- An explanation for the increased scatter at the lower strain ranges (higher numbers of cycles to failure) could be related to the strain thresholds for rupture of passivation and oxidation layers.

4.6 References

1. Letter from B. F. Langer, plus attachment, to Members, Special Committee to Review Code Stress Basis, "Report of Sub-Task Group on Fatigue," ASME Boiler and Pressure Vessel Code, June 19, 1961.

2. B. F. Langer, "Design of Pressure Vessels for Low-Cycle Fatigue," Transactions ASME, *Journal of Basic Engineering*, pp. 389-402 (1962).

3. H. B. Park and O. Chopra, "A Fracture Mechanics Approach for Estimating Fatigue-Crack Initiation in Carbon and Low-Alloy Steels in LWR Coolant Environments," *PVP.* Vol. 410-2, ASME PVP 2000, Seattle, WA (July 24-28, 2000).

4. O. K. Chopra and W. J. Shack, *Effects of LWR Coolant Environments on Fatigue Design Curves of Austenitic Stainless Steels.* NUREG/CR-5704 (ANL-98/31), Argonne National Laboratory, Argonne, IL, April 1999.

5. M. Higuchi, "Fatigue Curves and Fatigue Design Criteria for Carbon and Low Alloy Steels in High-Temperature Water," *PVP.* Vol. 386, pp. 161-170, ASME PVP (1999).

6. K. Tsutsumi, H. Kanasaki, T. Umakoshi, T. Nakamura and S. Urata, "Fatigue Life Reduction in PWR Water Environment for Stainless Steels," *PVP.* Vol. 410-2, ASME PVP 2000, Seattle, WA (July 24-28, 2000).

7. C.E. Jaske and W. J. O'Donnell, "Fatigue Design Criteria for Pressure Vessel Alloys," ASME Transactions, *Journal of Pressure Vessel Technology*. Vol. 99, No. 4, pp. 584-592 (November 1977).

8. W. F. English, R. L. Greene, D. A Hughes, and R. I. Post; L. F. Coffin, M. J. Manjoine, and D. R. Diercks, Discussion: "Fatigue Design Criteria for Pressure Vessel Alloys," ASME Transactions, *Journal of Pressure Vessel Technology*, Vol. 100, No. 2, pp. 236-243 (May 1978).

5
ASME CODE FATIGUE MARGINS

The margins that exist in an explicit ASME Code fatigue analysis were reviewed and evaluated relative to the information developed in the earlier tasks. The margins that are appropriate for a fatigue analysis, including environmental effects, are covered in the following. The assignment of these margins must account for the fraction that covers moderate environmental effects.

5.1 Initial Consideration of ASME Code Margins

The original consideration of this topic begins with the development of fatigue design by analysis rules in the ASME Code in the 1960s [1]. The *Criteria of the ASME Boiler and Pressure Vessel Code for Design by Analysis in Sections III and VIII, Division 2* [1] states that:

"The design fatigue curves are based on strain-controlled fatigue tests of small polished specimens. A best fit to the experimental data was obtained by applying the method of least squares to the logarithms of the experimental values. The design stress values were obtained from the best-fit curves by applying a factor of two on stress or a factor of twenty on cycles, whichever was more conservative at each point. These factors were intended to cover such effects as environment, size effect, and scatter of data, and thus it is not to be expected that a vessel will actually operate safely for twenty times its specified life."

Cooper [2] has described the partitioning of the factor of twenty for polished specimens tested in air as follows:

- Data scatter is accommodated by a sub-factor of 2.0.
- Size effects are accommodated by a sub-factor of 2.5.
- The combination of surface finish and environment are accommodated by a sub-factor of 4.0.

Surface finish and environment are combined because of the potential for the surface and its finish to be affected by the testing environment. The product of the sub-factors equals the factor of twenty.

5.2 Updating the ASME Code Margins

The term *environment* in both the *Criteria of the ASME Boiler and Pressure Vessel Code for Design by Analysis in Sections III and VIII, Division 2* [1], and the Welding Research Council publication, *Basis and Intent of Section III Fatigue Design Curves* [2], has been interpreted by many, including the Cyclic Life and Environmental Effects (CLEE) Steering Committee of the Pressure Vessel Research Council (PVRC), to mean *moderate environmental effects*. At issue is

the portion of the factor of 20 (at the low-cycle end of the fatigue design curve) inherent in the ASME Code Section III explicit fatigue design curves that can be attributed to moderate effects of environment when materials are tested in a simulated reactor water environment.

In the following, justification is provided for a distribution of uncertainty sub-factors that, taken together, account for an overall factor of 20 margin against cycles to failure for carbon/low-alloy steels. The overall factor of 20 also applies to austenitic stainless steels. However, the NRC has indicated that the overall factor of 20 should be reduced to an overall factor of 10 against cycles to failure for austenitic stainless steels to reflect regulatory concerns about the differences between the ASME mean air curve and the ANL mean air curve. The sub-factors are:

- Size Effect = 1.4 for both carbon/low-alloy and stainless steels
- Surface Finish = 2.0 for both carbon/low-alloy and stainless steels
- Data Scatter = 2.4 for both carbon/low-alloy and stainless steels
- Moderate Environmental Effects = 3.0 for carbon/low-alloy steels and 1.5 for stainless steels

The overall margin at the low-cycle end of the fatigue design curve would be the product of the four sub-factors, in this case equal to a factor of 20 for carbon/low-alloy steels and a factor of either 10 or 20 for stainless steels. The first three of these sub-factors can each be shown to be conservative based upon an evaluation of available test data, leaving the remaining sub-factor to account for moderate environmental effects.

5.3 Sub-Factor for Size Effects

The first sub-factor, for size effects, represents margin needed to account for the difference in fatigue life expected in full-scale components as compared to laboratory test specimens. Chopra and Shack [3] have determined the appropriate value for this factor to be 1.4. There is general industry agreement that this value is conservative.

5.4 Sub-Factor for Surface Finish

The second sub-factor, for surface finish, represents margin needed to account for the difference in fatigue life expected in full-scale components with industrial-grade surface finishes, as opposed to the smooth, polished surfaces of laboratory test specimens. The data assembled by Juvinal [4], as shown in Figure 5-1 (Figure 26 from *Engineering Considerations of Stress, Strain and Strength* [4]), show that, for materials with a tensile strength of 75 ksi (517.1 MPa) or less:

- A fatigue correction factor of 0.5 applies for an as-forged component
- A correction factor of 0.67 applies for a hot-rolled component
- A factor of 0.78 applies for a machined surface

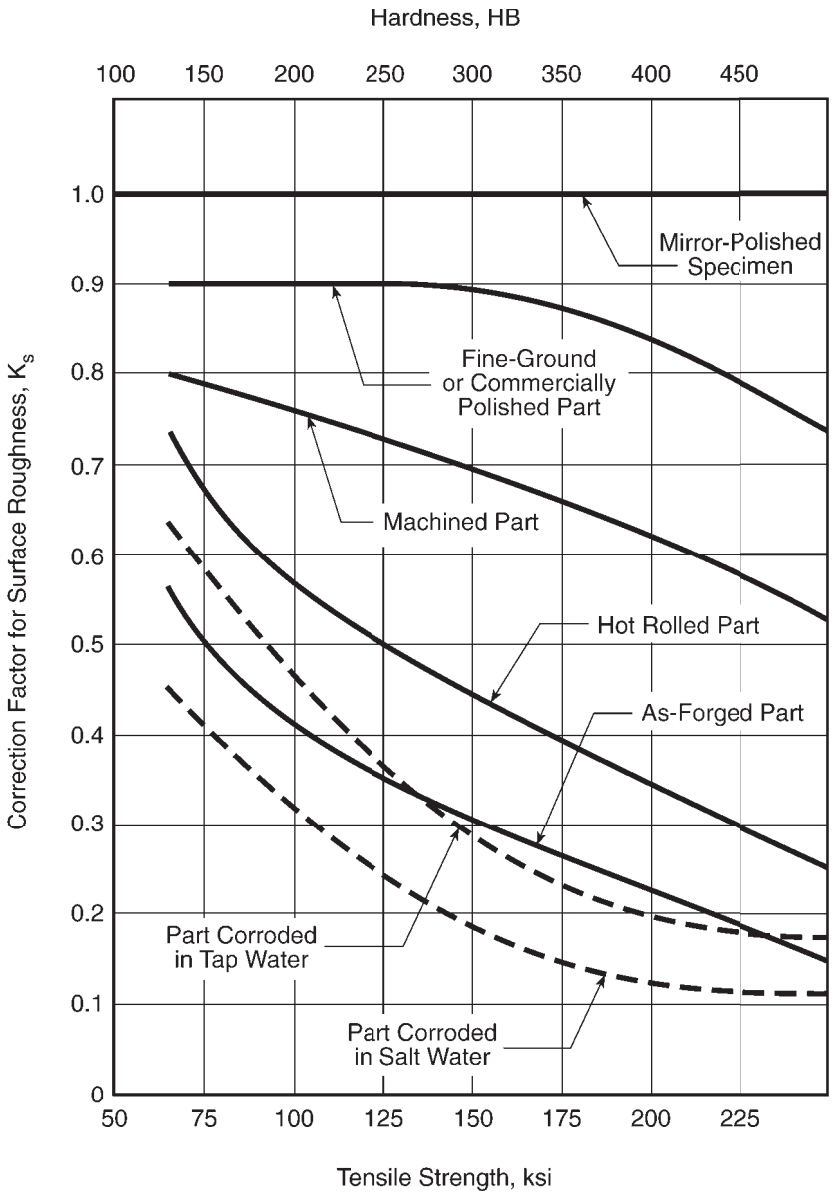

Figure 5-1
Effect of Surface Roughness

To illustrate this point further, fatigue data for components (with commercial-grade finished surfaces) whose internal surfaces were in contact with water have been plotted in Figures 5-2a and 5-2b for KWU tests on tubes [5] and in Figures 5-3a and 5-3b for the GE pipe tests [6]. Also shown in the figures are the mean fit to the ASME mean air curve and the corresponding ASME Code design curve for the material under consideration. The combination of environment, size effect, surface finish effect, etc. is seen to essentially exhaust the factor of 20 on life between the mean air curve and the design curve. When the environmental effect is removed by using the appropriate expression for F_{en}, the fatigue data are shifted back toward the mean air curve and beyond, in some cases. This implies that the size and surface finish effects are essentially negligible. At most, the combination of size and surface finish effects is perhaps a factor of 2. This value compares to 2.8 to 4.2 for the combination as estimated in NUREG/CR-6583 [3].

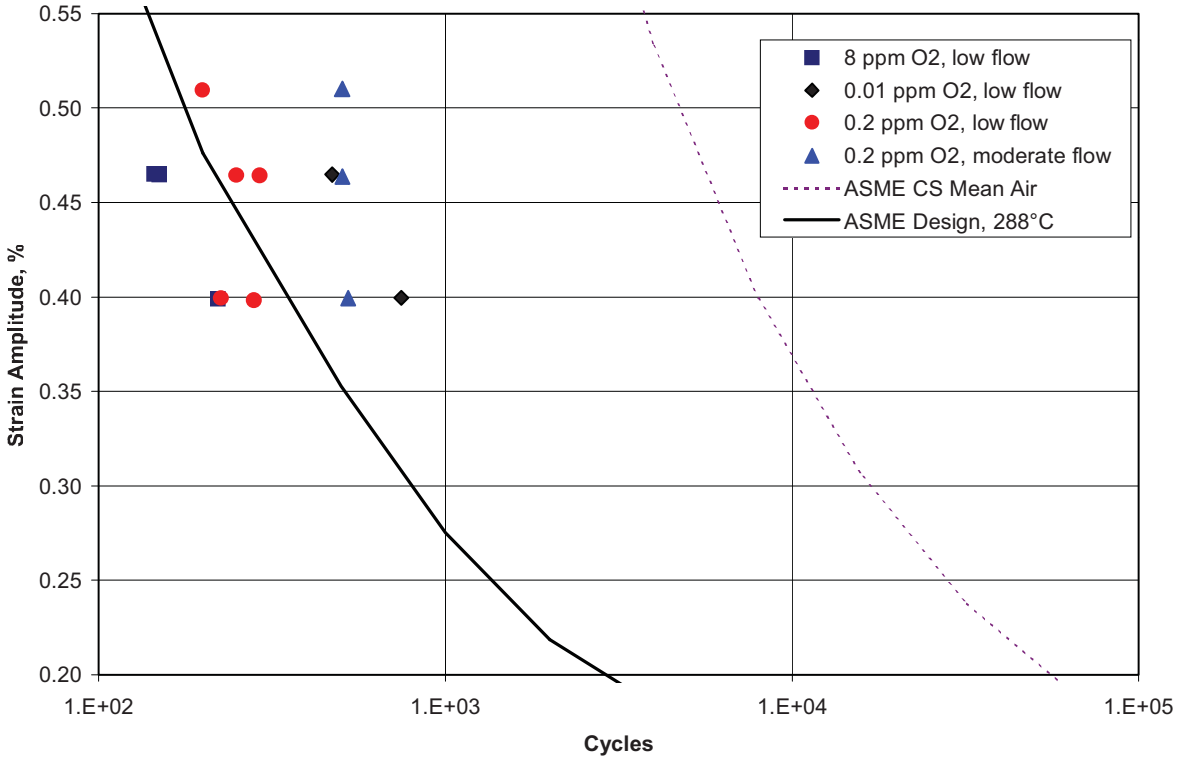

Figure 5-2a
KWU Component Scale Test Results for Carbon Steel

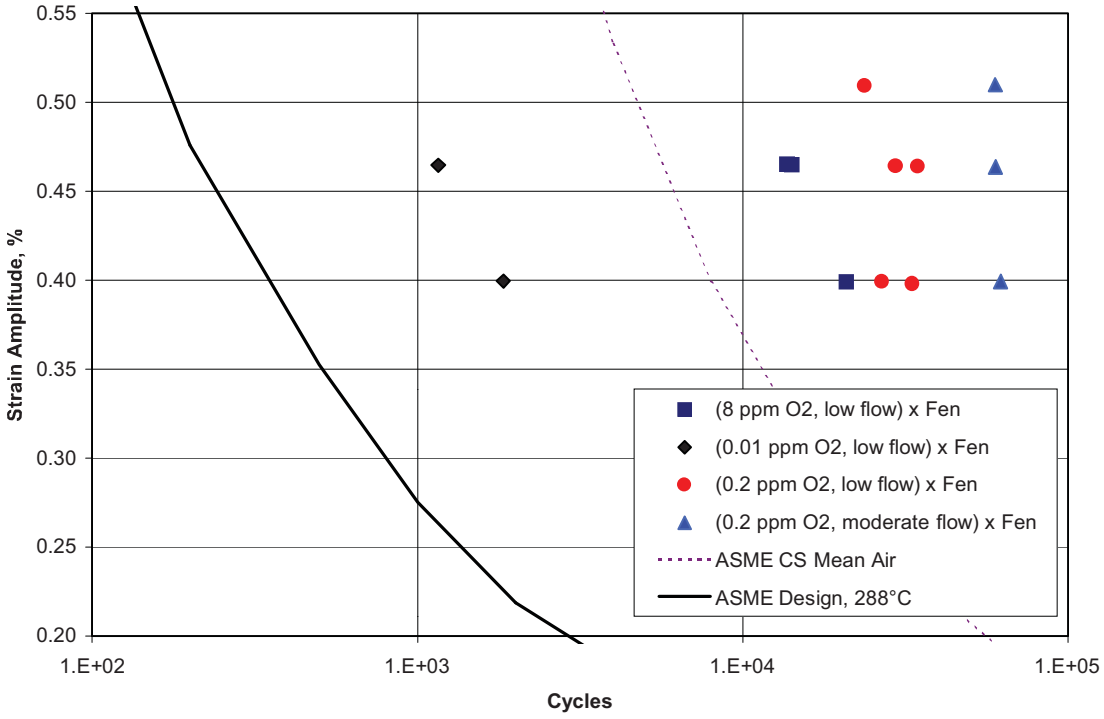

Figure 5-2b
KWU Component Scale Test Results for Carbon Steel Corrected by F_{en}

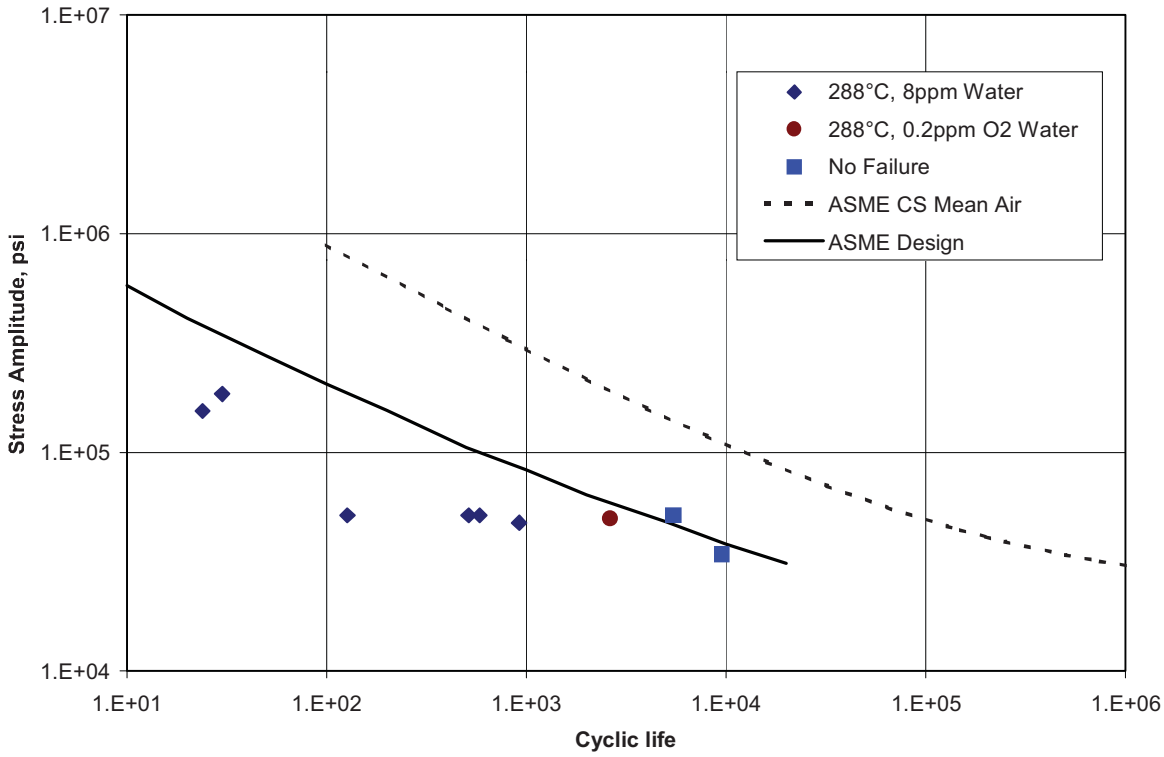

Figure 5-3a
Results From Fatigue Testing of Butt-Welded Pipe Under Simulated BWR Conditions

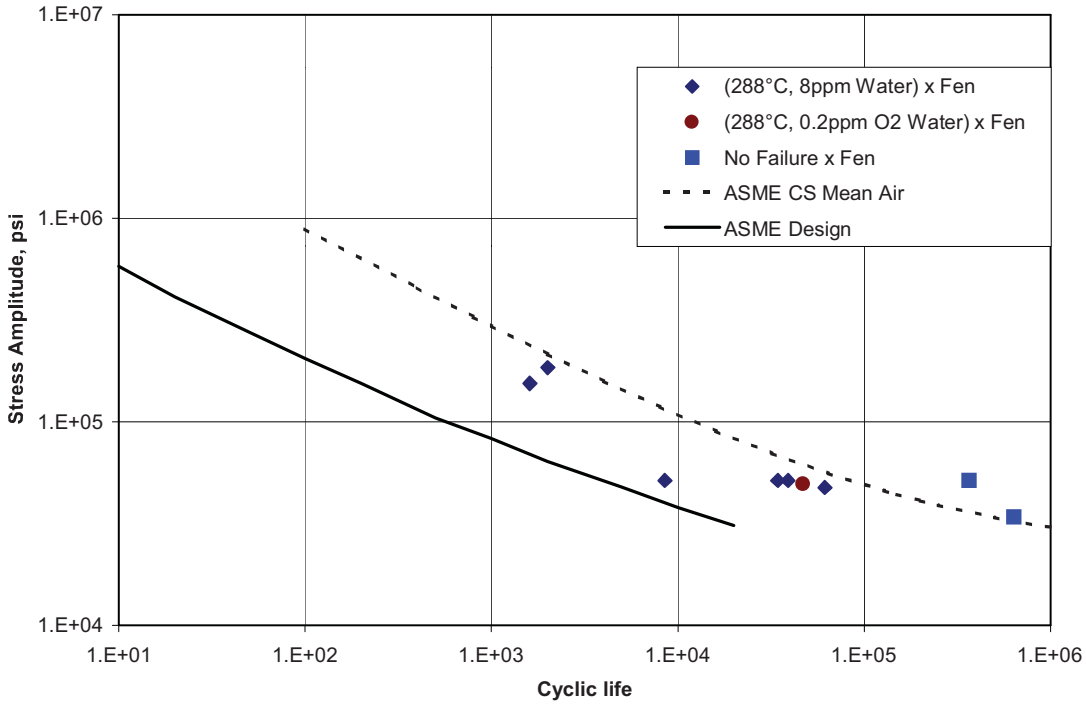

Figure 5-3b
Results From Fatigue Testing of Butt-Welded Pipe Under Simulated BWR Conditions and Corrected by F_{en}

Therefore, a surface finish uncertainty sub-factor of 2.0 can be used very conservatively to account for commercial-grade finishes on actual components in service. This value is also in general agreement with Chopra and Shack [7], who state the following:

> "Because carbon and low-alloy steels and austenitic SSs develop a corrosion scale in LWR environments, the effect of surface finish may not be significant, i.e., the effects of surface finish are included in the environmentally assisted decrease in fatigue life in LWR coolant environments. In water, the sub-factor on life to account for surface finish effects may be as low as 1.5 or may be eliminated completely; a factor of 1.5 on strain and 7 on cycles is adequate to account for the uncertainties that arise from material and loading variability. Therefore, the factor of 20 on life that is used in developing the design fatigue curve includes, as a safety margin, a factor of 3 or 4 on life that may be used to account for the effects of (moderate) environment on the fatigue life of these steels."

5.5 Sub-Factor for Data Scatter

The third sub-factor, for data scatter, represents an uncertainty factor to account for expected variability in fatigue life among the population of actual components if they were exposed to identical conditions of environment and applied loading. That is, this sub-factor accounts for the variation in performance among a group of identical components under identical conditions. In this case, the performance is defined in terms of the number of cycles of loading to which a component can be subjected before experiencing a fatigue crack. In order to determine an appropriate estimate of the variability to be expected in real components, the variability actually found in fatigue test specimens exposed to similar conditions should be evaluated on a statistical basis.

Care must be exercised in performing this evaluation to assure that only one variable is being evaluated at a time. If the test samples representing different test conditions are grouped together, the variation due to these test differences would be added to the true data scatter, thus inflating the apparent statistical variation. Therefore, significant test differences must first be determined and the test data sorted such that each grouping represents similar test conditions. The variability of each grouping should then be determined and the results compared. The highest variability found among any group of similar test samples could be considered a reasonably conservative estimate of variability expected among the population of real components exposed to similar conditions, and can be converted to an uncertainty sub-factor representing data scatter.

The most significant test parameter associated with environmental fatigue testing has been determined to be strain rate. The degree of fatigue life reduction has been found to be greater at relatively low strain rates ($< 0.4\%$/sec) than at relatively high strain rates ($\geq 0.4\%$/sec). Therefore, in determining the data scatter uncertainty factor, the test results must first be sorted into groups tested with similar strain rates. Otherwise, if these samples were mixed together and analyzed for variability, the strain rate effect variability would be added to the sample variability being sought.

5.5.1 Analysis of Data Scatter

Tables 5-1a, 5-1b, and 5-1c illustrate the approach used to analyze austenitic stainless steels fatigue data obtained in simulated reactor water environments. Table 5-1a contains all of the data from the Japanese data set assembled by Tsutsumi et al. [8] for austenitic stainless steels obtained at or near a strain amplitude of 0.6% with a tensile strain rate of 0.4%/sec. Tables 5-1b and 5-1c contain the data from *Fatigue Life Reduction in PWR Water Environment for Stainless Steels* [8], obtained at or near a strain amplitude of 0.6% with a tensile strain rate less than 0.4%/sec. Similarly, Tables 5-2a and 5-2b contain data from *Fatigue Life Reduction in PWR Water Environment for Stainless Steels* [8], obtained at a strain amplitude at or near 0.3%. Table 5-2a contains the data obtained at a tensile strain rate of 0.4%/sec, while Table 5-2b contains the data obtained at a tensile strain rate less than 0.4%/sec. Only test results representing similar conditions are included within each table. This sorting reduces the sample size of each grouping that adds to the uncertainty of statistical analysis, but this will be accounted for later in the process.

In the following sub-sections, the data for both carbon and low-alloy steels, and for austenitic stainless steels, are reanalyzed with a clear separation between data sets at different environmental conditions, with the intent to separate data scatter within an essentially homogeneous environmental data set from the effects of environmental variability. Section 5.5.1 discusses data scatter evaluations for austenitic stainless steels and Section 5.5.2 discusses data scatter evaluation for carbon and low-alloy steel. Finally, Section 5.5.3 draws conclusions about the portion of the factor of 20 at the low-cycle end of the fatigue design curves that can be attributed to moderate environmental effects.

Table 5-1a
Moderate Strain Rate—Austenitic Stainless Steel (0.6% Strain Amplitude)

Material	DO (ppb)	Temperature (°C)	Tensile Strain Rate (%/sec)	Strain Amplitude (%)	Cycles to Failure	Shifted Cycles to Failure
304	5	360	0.4	0.58	1172	1172
316 (Sensitized)	5	325	0.4	0.61	2009	2009
316 (Weld)	5	325	0.4	0.61	666	666
316 (Aged)	5	325	0.4	0.61	1075	1075
316	8000	325	0.4	0.6	2027	2027
316 (Forged)	5	325	0.4	0.6	1572	1572
316	5	325	0.4	0.6	2460	2460
316 (Weld)	5	325	0.4	0.6	1922	1922
304	5	325	0.4	0.6	1411	1411
304 (Sensitized)	5	325	0.4	0.6	1318	1318
308 (Weld)	5	325	0.4	0.6	2381	2381
SCS14A (Aged)	5	325	0.4	0.6	1380	1380
CF8M (Aged)	5	325	0.4	0.6	2136	2136
SCS14A (Aged)	5	325	0.4	0.6	663	663
SCS14A	5	325	0.4	0.6	1461	1461
316	5	325	0.4	0.59	2070	2070
316 (Pre-strained)	5	325	0.4	0.59	2238	2238
304	5	325	0.4	0.59	1344	1344
304	8000	325	0.4	0.59	988	988
SCS14A	5	325	0.4	0.59	1606	1606
316	5	325	0.4	0.58	2089	2089
SCS14A	5	325	0.4	0.575	1856	1856
316	5	300	0.4	0.605	1916	1916
304	5	300	0.4	0.585	1189	1189

Mean value = 1,623 cycles; Standard deviation = 516 cycles; Ratio = 516/1623 = 0.32

Table 5-1b
Reduced Strain Rates—Austenitic Stainless Steel (0.6% Strain Amplitude)

Material	DO (ppb)	Temperature (°C)	Tensile Strain Rate (%/sec)	Strain Amplitude (%)	Cycles to Failure	Shifted Cycles to Failure
304	5	360	0.01	0.585	500	1305
SCS14A (Aged)	5	325	0.001	0.63	308	1462
316 (Sensitized)	5	325	0.01	0.61	608	1586
316 (Weld)	5	325	0.0001	0.61	246	2126
304	5	325	0.004	0.605	326	1079
304	5	325	0.04	0.6	668	1216
308 (Weld)	5	325	0.04	0.6	1264	2300
SCS14A (Aged)	5	325	0.04	0.6	1202	2187
316	5	325	0.01	0.6	644	1680
316 (Forged)	5	325	0.01	0.6	388	1012
316 (Weld)	5	325	0.01	0.6	1365	3560*
316 (Weld)	5	325	0.001	0.6	753	3575*
304	5	325	0.01	0.6	512	1336
304	8000	325	0.01	0.6	470	1226
304	5	325	0.01	0.6	443	1156
304 (Sensitized)	5	325	0.01	0.6	474	1237
308 (Weld)	5	325	0.01	0.6	1156	3016
SCS14A (Aged)	5	325	0.01	0.6	741	1934
SCS14A	5	325	0.01	0.6	808	2108
SCS14A	5	325	0.01	0.6	682	1780
316	5	325	0.004	0.6	396	1311
308 (Weld)	5	325	0.004	0.6	955	3162
316	5	325	0.001	0.6	452	2146

*Potential Over-corrected Shift

Table 5-1c
Reduced Strain Rates—Austenitic Stainless Steel (0.6% Strain Amplitude)

Material	DO (ppb)	Temperature (°C)	Tensile Strain Rate (%/sec)	Strain Amplitude (%)	Cycles to Failure	Shifted Cycles to Failure
308 (Weld)	5	325	0.001	0.6	594	2820
316 (Weld)	5	325	0.0004	0.6	579	3489
SCS14A	5	325	0.0004	0.6	230	1386
316	5	325	0.0001	0.6	550	4752*
316 (Weld)	5	325	0.0001	0.6	325	2808
SCS14A	5	325	0.0001	0.6	131	1132
SCS14A	5	325	0.00004	0.6	107	1173
SCS14A	5	325	0.00001	0.6	80	1258
SCS14A	5	325	0.01	0.595	532	1388
SCS14A	5	325	0.004	0.595	525	1738
316	5	325	0.04	0.59	912	1660
SCS14A	5	325	0.04	0.59	964	1754
316	8000	325	0.01	0.59	803	2095
316	5	325	0.004	0.59	452	1497
SCS14A	5	325	0.001	0.59	269	1277
304	5	325	0.001	0.58	249	1182
316	5	325	0.0004	0.58	507	3055
304	5	325	0.0004	0.58	180	1085
304	5	325	0.0001	0.58	182	1572
316	5	300	0.01	0.6	740	1931
304	5	300	0.01	0.595	457	1192

*Potential Over-corrected Shift
Mean value = 1,903 cycles (Corrected = 1,753 cycles)
Standard deviation = 859 cycles (Corrected = 655 cycles)
Ratio = 0.45 (Corrected = 0.37)

Table 5-2a
Moderate Strain Rate—Austenitic Stainless Steel (0.3% Strain Amplitude)

Material	DO (ppb)	Temperature (°C)	Tensile Strain Rate (%/sec)	Strain Amplitude (%)	Cycles to Failure	Shifted Cycles to Failure
316 (Weld)	5	325	0.4	0.31	4125	4125
316	5	325	0.4	0.3	8799	8799
316 (Pre-strained)	5	325	0.4	0.3	8760	8760
316 (Forged)	5	325	0.4	0.3	10754	10754
316 (Sensitized)	5	325	0.4	0.3	7428	7428
316 (Aged)	5	325	0.4	0.3	6184	6184
316 (Weld)	5	325	0.4	0.3	15142	15142
304	5	325	0.4	0.3	7928	7928
304 (Sensitized)	5	325	0.4	0.3	9879	9879
SCS14A (Aged)	5	325	0.4	0.3	11795	11795
CF8M (Aged)	5	325	0.4	0.3	13327	13327
SCS14A	5	325	0.4	0.3	10154	10154
SCS14A	5	325	0.4	0.3	12000	12000
SCS14A	5	325	0.4	0.295	9242	9242
304	5	325	0.4	0.29	8798	8798
308 (Weld)	5	325	0.4	0.29	7954	7954
304	5	360	0.4	0.28	10326	10326
304	5	300	0.4	0.305	7020	7020
316	5	300	0.4	0.285	6391	6391
316	8000	325	0.4	0.29	8761	8761
304	8000	325	0.4	0.29	10242	10242

Mean value = 9,286 cycles; Standard deviation = 2,524 cycles; Ratio = 0.27

Table 5-2b
Reduced Strain Rates—Austenitic Stainless Steel (0.3% Strain Amplitude)

Material	DO (ppb)	Temperature (°C)	Tensile Strain Rate (%/sec)	Strain Amplitude (%)	Cycles to Failure	Shifted Cycles to Failure
SCS14A (Aged)	5	325	0.04	0.31	5376	9783
316	5	325	0.01	0.3	2807	7324
316 (Forged)	5	325	0.01	0.3	3012	7859
316 (Sensitized)	5	325	0.01	0.3	2800	7306
304	5	325	0.01	0.3	1854	4838
304 (Sensitized)	5	325	0.01	0.3	4186	10923
308 (Weld)	5	325	0.01	0.3	5716	14915
SCS14A (Aged)	5	325	0.01	0.3	4480	11690
316 (Weld)	5	325	0.01	0.3	10403	27141*
308 (Weld)	5	325	0.04	0.3	10684	19445*
SCS14A	5	325	0.01	0.29	7116	18566*
SCS14A	5	325	0.01	0.29	8094	21120*
316	5	325	0.004	0.3	3025	10017
316	5	325	0.001	0.3	2235	10612
304	5	325	0.01	0.295	2522	6581
316	5	325	0.04	0.29	5551	10101
304	5	325	0.04	0.29	5911	10756
304	5	360	0.01	0.3	3970	10359
304	5	300	0.01	0.305	4019	10487
316	5	300	0.01	0.3	3704	9665
316	8000	325	0.01	0.3	4137	7803
304	8000	325	0.01	0.3	2164	4081

*Potential Over-corrected Shift
Mean value = 11,426 cycles (Corrected = 9,172 cycles)
Standard deviation = 5,614 cycles (Corrected = 2,592 cycles)
Ratio = 0.49 (Corrected = 0.28)

5.5.2 Austenitic Stainless Steel Data Scatter Evaluations

In this sub-section, the data *in Fatigue Life Reduction in PWR Water Environment for Stainless Steels* [8] have been reanalyzed with a clear separation between data sets at different environmental test conditions. The data set separation begins by dividing the total population of data points at or near a given strain amplitude into a set for which the testing strain rates were relatively high (0.4%/sec), and a set for which the test strain rates were relatively low (for example, 0.01%/sec, 0.04%/sec, 0.001%/sec, and so on). Essentially, the first data set contains data points for which the effects of simulated reactor water environments are *moderate*, and the second data set contains data points for which the effects of simulated reactor water environments are not moderate. The lack of moderation might vary, but the second data set is analyzed as a single environmental population. Later, the data points in this second data set are shifted using the ln (N) expressions developed by ANL to model the immoderate environmental effects. This permits all of the data to be compared rationally on an equivalent basis.

For example, at a strain amplitude at or near 0.6% (say 0.58% to 0.62%), the complete data set was, as before, divided into two populations. One population consisted of data points obtained at a relatively high strain rate (0.4%/sec) and the other population included all of the data points obtained at other (lower) strain rates. Then, the data obtained at strain rates other than 0.4%/sec were shifted using the ln (N) data fitting formula developed by ANL [9], as shown below.

For an LWR environment, the data fit is given by

$$\ln (N) = 5.768 - 2.030 \ln (\varepsilon_a - 0.126) + T_2^* \eta_1^* O^*, \qquad \textbf{Eq. 5-1}$$

where η_1^*, T_2^*, and O* are the transformed strain rate, temperature, and dissolved oxygen (DO), respectively, defined as follows:

$\eta_1^* = 0$ ($\eta_1 > 0.4$%/sec)
$\eta_1^* = \ln (\eta_1/0.4)$ ($0.0004 \leq \eta_1 \leq 0.4$%/sec)
$\eta_1^* = \ln (0.0004/0.4)$ ($\eta_1 < 0.0004$%/sec)
$T_2^* = 0$ ($T < 200$°C)
$T_2^* = 1.0$ ($T \geq 200$°C)

$O^* = 0.260$ (DO < 0.05 ppm)
$O^* = 0.172$ (DO ≥ 0.05 ppm)

It should be noted that η_1 is the strain rate and that the normalized strain rate, η_1^*, is 0 for a strain rate of 0.4%/sec.

The population of data points at or near 0.6% strain amplitude and a strain rate of 0.4%/sec consisted of 24 data points (see Table 5-1a) with strain amplitudes ranging from 0.575% to 0.61%. This population had an average value of 1,623 cycles to failure, with a standard deviation of 516 cycles. The ratio of the standard deviation to the mean value was 0.32.

The population of data points at or near 0.6% strain amplitude and at lower strain rates consisted of 44 data points (see Tables 5-1b and 5-1c) ranging in strain amplitude from 0.58% to 0.61%. After the ln (N) shift to 0.4%/sec, the average value was found to be 1,903 cycles to failure, with a standard deviation of 859 cycles. However, it was also discovered that the ln (N) formula tended to over-correct for the environment for a few data points, in particular for cast or welded stainless steels that do not exhibit a substantial decrease in fatigue life in environment. When the first of these (over-corrected) data points was eliminated from the set (now 43 data points), the mean value dropped to 1,837 cycles to failure, with a standard deviation of 747 cycles. Removing the next highest (over-corrected) data point gave a mean value of 1,795 cycles to failure and a standard deviation of 705 cycles. Finally, removing the next highest (over-corrected) data point resulted in a mean value of 1,753 cycles to failure and a standard deviation of 655 cycles. The ratio of the standard deviation to the mean is 0.37. This mean value and the associated standard deviation match very well with the mean value and associated standard deviation for the relatively high strain rate data.

In other words, removing three of the 44 data points, representing over-corrected environmental adjustments to fatigue life, allowed the ln (N) shift to produce an environmentally-corrected data set that matched the actual data set in statistical properties almost exactly. Note that, if three times the standard deviation is used as a measure of data scatter, the data scatter factor is approximately ± 1.

The data set at or near 0.6% strain amplitude is by far the largest and the most reliable data set. However, other data sets were also examined. For example, the data set at or near 0.3% strain amplitude was also evaluated. There were a total of 43 data points in this data set, 21 data points in the population obtained at a strain rate of 0.4%/sec (Table 5-2a) and 22 data points obtained at lower strain rates (Table 5-2b). The same procedure was used as before. For the first population, the mean value of the 21 data points was found to be 9,286 cycles to failure, with a standard deviation of 2,524 cycles. The ratio of the standard deviation to the mean value is 0.27. For the 22 data points obtained at lower strain rates, the mean value of the shifted data was 11,426 cycles, with a standard deviation of 5,614 cycles. Again, it was found that the ln (N) formula tended to over-correct for the environment for some of these specimens. In this case, it was found that the tendency to over-correct was more widespread; that is, many more data points did not reflect very much or any of the presumed environmental effect. When the four most over-corrected data points were removed from the population, the mean value for the remaining 18 data points was 9,172 cycles to failure, with a standard deviation of 2,592 cycles. Again, removing the over-corrected data points resulted in a mean value and a standard deviation for the shifted data set that matched the statistical properties of the actual 0.4%/sec data set almost exactly.

The only other data set of any size was that for a strain amplitude at or near 0.4% (Table 5-3). The total population consisted of 13 data points, 12 obtained at a strain rate of 0.4%/sec and only 1 data point obtained at lower strain rates. The mean value for the 12 data points was found to be 4,679 cycles to failure, with a standard deviation of 1,637 cycles. The ratio is 0.35. When the single data point at the lower strain rate was shifted by the ln (N) formula, the fatigue life shifted from 1,561 cycles to 4,073 cycles, reasonably close to the calculated mean value for the actual population.

Table 5-3
All Strain Rates

Material	DO (ppb)	Temperature (°C)	Tensile Strain Rate (%/sec)	Strain Amplitude (%)	Cycles to Failure	Shifted Cycles to Failure
304	5	360	0.01	0.39	1561	4073
316 (Aged)	5	325	0.4	0.42	2392	2392
316 (Weld)	5	325	0.4	0.4	2521	2521
316 (Weld)	5	325	0.4	0.4	6752	6752
308 (Weld)	5	325	0.4	0.4	6102	6102
SCS14A (Aged)	5	325	0.4	0.4	4705	4705
CF8M (Weld)	5	325	0.4	0.4	6155	6155
316	8000	325	0.4	0.39	5308	5308
304	8000	325	0.4	0.39	3050	3050
SCS14A	5	325	0.4	0.38	6691	6691
304	5	325	0.4	0.37	3387	3387
304	5	300	0.4	0.4	3474	3474
316	5	300	0.4	0.375	5612	5612

Mean value = 4,679 cycles for 0.4%/sec data only
Standard deviation = 1,637 cycles for 0.4%/sec data only
Ratio = 0.35 for 0.4%/sec data only

From the examination of these data we conclude that the observations of large data scatter for simulated reactor water environmental testing are not warranted. Only by mixing data sets that represent moderate and immoderate environmental effects can large data scatter effects be observed. This data scatter is amplified when environmental-correction formulas are used to shift the data to a common basis, because of the tendency for the environmental shift formulas to over-correct under some conditions. The over-correction appears to be more widespread at the lower strain amplitudes. One possible explanation for this tendency to over-correct at the lower strain amplitudes is the effect of oxidation or passivation layer rupture, or the lack of rupture, during testing at the lower strain amplitudes. The threshold for oxidation/passivation layer rupture has been estimated to be above 0.3% strain, perhaps with considerable variability. For those specimens that resist oxidation/passivation layer rupture, the over-correction of the environmental effect obscures the statistical analysis of the data.

The actual data variability for similar materials tested under similar environmental conditions is very small. Likewise, when the data obtained under different environmental conditions were shifted using environmental-correction formulas, the data scatter remained very small, provided that the tendency for the environmental-correction formula to over-shift under some conditions was taken into account. In this case, using three times the standard deviation as a measure of

scatter, the analysis showed that, for austenitic stainless steels, the actual data scatter factor was approximately ± 1.

5.5.3 Carbon and Low-Alloy Steel Data Scatter Evaluations

Laboratory data for carbon and low-alloy steel under simulated reactor water environmental conditions have been collected by PVRC as a part of their studies on cyclic life and environmental effects. These data were provided to EPRI for the data scatter assessment. Again, the data populations were separated into two sets—those obtained at relatively high strain rate (for example, 0.4%/sec), referred to as the moderate environmental effects population, and those obtained at relatively low strain rates, referred to as the immoderate environmental effects population. Again, this type of separation of data populations permits variability due to data scatter within a population to be isolated from variability caused by stronger reactor water environmental influence.

As with the austenitic stainless steel data, the two populations were further subdivided into subsets with relatively homogeneous testing parameters. For example, data points at reactor operating temperatures (288°C (550 °F), 300°C (572 °F), etc.) and at approximately the same strain amplitude (for example, 0.6% strain), were grouped together. Much more data were available for low-alloy steels than for carbon steels so that, in some cases, the findings are limited to those applicable to low-alloy steels. The influence of dissolved oxygen (DO) was not found to distort the statistical evaluation, with the exception of the very highest DO levels (8 ppm). The term high DO is used to describe the 8 ppm data, while data at all other DO levels is described as low DO data. Weld data largely fit into the general populations, with the single exception of data from a single Japanese investigator.

As an example, 25 data points were found in the PVRC database for low-alloy (for example, SA-533B) steel obtained at a relatively high strain rate (0.4%/sec), at reactor operating temperature (for example, 288°C (550°F)), and at 0.6% strain amplitude. Weld data and both high DO and low DO data are included. Of the 25 data points, 11 were included in the high DO subset and 14 were included in the low DO subset. These data are listed in Table 5-4. The low DO mean value was found to be 2,378 cycles with an estimated standard deviation of 1,055 cycles. The high DO subset had a mean value of 1,693 cycles with a standard deviation of 419 cycles. The ratio of the standard deviation to the mean value was 0.44 for the low DO population and only 0.25 for the high DO population. The mean value for the combined populations was 2,076 cycles with a standard deviation of 892 cycles. The ratio is 0.43.

Table 5-4
Low-Alloy Steel (0.6% Strain Amplitude)

Material	DO	Temperature (°C)	Strain Amplitude (%)	Cycles to Failure	Investigator
533B LAS	High	290	0.6	1600	Higuchi
533B LAS	High	290	0.6	1690	Higuchi
533B LAS	High	290	0.6	1640	Higuchi
508-3 LAS	Low	250	0.58	3040	Kasai
508-3 LAS	Low	290	0.605	2284	Kasai
508-3 LAS	Low	250	0.58	4210	Kasai
508-3 LAS	Low	290	0.59	2810	Kasai
508-3 LAS	High	290	0.585	2120	Kasai
508-3 LAS	High	290	0.575	2372	Kasai
533B LAS	Low	288	0.6	1728	Nakao
533B LAS	Low	288	0.6	1692	Nakao
533B LAS	Low	288	0.6	1276	Nakao
508-3 LAS	High	290	0.593	783	Endou
508-3 LAS	Low	250	0.584	1695	Endou
508-3 LAS	Low	290	0.587	1899	Endou
508-3 LAS	High	288	0.6	1660	Higuchi
508-3 LAS	High	288	0.6	1920	Higuchi
508-3 LAS	High	288	0.6	1250	Higuchi
508-3 LAS	Low	288	0.6	3540	Higuchi
508-3 LAS	Low	288	0.6	3625	Higuchi
508-3 LAS	Low	288	0.6	3435	Higuchi
533B LAS Weld	High	290	0.6	1810	Higuchi
533B LAS Weld	High	290	0.6	1774	Higuchi
533B LAS Weld	Low	288	0.6	960	Nakao
533B LAS Weld	Low	288	0.6	1091	Nakao

Mean value = 2,076 cycles; Standard deviation = 892 cycles; Ratio = 0.43

The PVRC database contained 8 data points at a strain amplitude of 0.5%, all from various Japanese investigators on carbon/low-alloy steels. The Japanese data included two high DO data points that fit into the general population. These data points are listed in Table 5-5. The mean of the Japanese data was 2,872 cycles with a standard deviation of 850 cycles. The ratio is only 0.30.

Table 5-5
Carbon Steel/Low-Alloy Steel (0.5% Strain Amplitude)

Material	DO	Temperature (°C)	Strain Amplitude (%)	Cycles to Failure	Investigator
533B LAS	High	290	0.5	3348	Higuchi
533B LAS	High	290	0.5	3550	Higuchi
533B LAS	Low	288	0.5	1965	Nakao
508-3 LAS	Low	288	0.498	4022	Nagata
508-2 LAS	Low	288	0.5	2875	Nakao
533B LAS Weld	Low	288	0.5	1888	Nakao
533B LAS Weld	Low	288	0.5	1898	Nakao
333B-3 CS	Low	288	0.5	3426	Higuchi

Mean value = 2,872 cycles; Standard deviation = 850 cycles; Ratio = 0.30

The PVRC database contained 16 data points at 0.4% strain amplitude and moderately high strain rates. All of the data points except one were for low-alloy steel and all came from Japanese investigators. Weld data and high DO data fit into the general population, with the exception of three outliers. These data points were included in the data evaluation. High DO data fit into the general population with no exceptions. These data points are listed in Table 5-6. The data mean for the 16 data points was 6,089 cycles, with a standard deviation of 3,454 cycles. The ratio is 0.58, reflecting the inclusion of three potential outliers and the combined low DO and high DO populations. Excluding the three outliers gives a revised mean of 6,028 cycles with a standard deviation of 2,077 cycles, thereby reducing the ratio to 0.35.

Table 5-6
Carbon Steel/Low-Alloy Steel (0.4% Strain Amplitude)

Material	DO	Temperature (°C)	Strain Amplitude (%)	Cycles to Failure	Investigator
533B LAS	High	290	0.4	9400	Higuchi
533B LAS	High	290	0.4	6340	Higuchi
508-3 LAS	Low	250	0.395	8573	Kasai
533B LAS	Low	288	0.408	6353	Nagata
533B LAS	Low	288	0.4	8528	Nakao
533B LAS	Low	288	0.4	5700	Nakao
533B LAS	Low	288	0.4	6900	Nakao
533B LAS	Low	288	0.4	4030	Nakao
333B-3 CS	Low	288	0.4	15550*	Higuchi
508-3 LAS	High	290	0.404	1911*	Endou
508-3 LAS	High	288	0.4	5702	Higuchi
533B LAS Weld	High	290	0.4	5610	Higuchi
533B LAS Weld	High	290	0.4	5855	Higuchi
533B LAS Weld	Low	288	0.4	2670	Nakao
533B LAS Weld	Low	288	0.4	2708	Nakao
508-1 LAS	High	300	0.4	1600*	Kitigawa

*Potential Outliers
Mean value = 6,089 cycles (Corrected = 6,028 cycles)
Standard deviation = 3,454 cycles (Corrected = 2,077 cycles)
Ratio = 0.57 (Corrected = 0.35)

The PVRC database contained 15 data points at 0.3% strain amplitude and relatively high strain rates. All of the data points came from Japanese investigators. Three data points were for carbon steel, with 12 data points for low-alloy steel. High DO data, including those for carbon steel piping material, fit into the general population, as did all of the weld data. One data point for low-alloy steel at high DO appeared to be an outlier but was included in the analysis set. These data points are listed in Table 5-7. The data mean was found to be 18,440 cycles with a standard deviation of 9,001 cycles. The ratio for this more inclusive population is 0.49. If the outlier is removed, the mean value is 19,600 cycles and the standard deviation is 8,094, so that the ratio is only 0.41.

Table 5-7
Carbon Steel/Low-Alloy Steel (0.3% Strain Amplitude)

Material	DO	Temperature (°C)	Strain Amplitude (%)	Cycles to Failure	Investigator
533B LAS	High	290	0.3	32080	Higuchi
533B LAS	High	290	0.3	28700	Higuchi
533B LAS	Low	288	0.3	14760	Nakao
508-3 LAS	High	288	0.3	8080	Higuchi
533B LAS Weld	High	290	0.3	18500	Higuchi
533B LAS Weld	High	290	0.3	14800	Higuchi
508-3 LAS	Low	288	0.285	26020	Nakao
533B LAS	Low	288	0.28	26730	Nakao
508-3 LAS	Low	288	0.298	29000	Nagata
533B LAS Weld	Low	288	0.3	13840	Nakao
533B LAS Weld	Low	288	0.3	18730	Nakao
333B-2 CS	High	290	0.3	8460	Higuchi
333B-2 CS	Low	288	0.3	10860	Higuchi
333B-2 CS	Low	288	0.3	23840	Higuchi
508-1 LAS	High	300	0.3	2200*	Kitigawa

*Potential Outlier
Mean value = 18,440 cycles (Corrected = 19,600 cycles)
Standard deviation = 9,001 cycles (Corrected = 8,094 cycles)
Ratio = 0.49 (Corrected = 0.41)

Note that the data scatter in all of these calculations is less than or equal to the data scatter attributed to air environments. For carbon and low-alloy steels, the highest data scatter factor (3 times the standard deviation) for any grouping was found to be 1.47.

5.5.4 Summary

From the examination of these data, it is concluded that the observations of large data scatter for simulated reactor water environmental testing are not warranted. Only by mixing data sets that represent moderate and immoderate environmental effects can large data scatter effects be observed. This relatively low data variability was observed by separating laboratory test data into two populations—a population containing test data obtained at relatively high strain rate (for example, 0.4%/sec) and a population containing test data obtained at relatively slow strain rates (for example, 0.004%/sec). The implication of this statistical separation is that the relatively high strain rate population exhibits moderate environmental effects, while the relatively slow strain rate population, in general, exhibits a reduction in fatigue life that is greater than moderate.

The statistical analysis of the separated populations shows that:

- Data variability for the relatively high strain rate population is much less than has been reported in the literature when the statistical analyses are based on combined populations. The ratio of the standard deviations to the mean values for both austenitic stainless steels and carbon/low-alloy steels tested at relatively high strain rates is in the range of 0.2 to 0.5, even when data populations are enlarged to include weld data.
- Very high dissolved oxygen levels do not compromise the relatively high strain rate data variance for austenitic stainless steels and for low-alloy steels. This is true for carbon steels, in general, with an occasional data point that could be an outlier.
- The addition of weld metal fatigue data increased the ratio of standard deviation to mean value in the relatively high strain rate population by about a factor of 2, from a ratio of about 0.25 to about 0.50. In many cases, the most extreme measured values within a strain amplitude population, on both the low side and on the high side, were weld metal data points.
- When the population of data points obtained at relatively low strain rates was shifted, using the ln (N) formulas developed by ANL, virtually identical statistical parameters (for example, mean value, standard deviation) to those for the relatively high strain rate population were calculated. This was particularly true when a few over-corrected data points were eliminated from the low strain rate population. In other words, one of the items giving rise to estimates of large data scatter is the tendency for a few low strain rate data points, that are relatively unaffected by reactor water environments, to be over-corrected by the environmental shift formulas, thus skewing the statistical analysis.

The sub-factors for carbon and low-alloy steels are 1.4 (size effect), 2.0 (surface roughness), and 2.4 (data scatter). Therefore, the remaining sub-factor for moderate environmental effects is obtained by dividing the factor of 20 by the product of 1.4 x 2.0 x 2.4, which gives a sub-factor of 3.0 for carbon and low-alloy steels.

For stainless steels, the same uncertainty sub-factors apply, that is, a factor of 1.4 (size effect), 2.0 (surface finish), and 2.4 for data scatter. Therefore, the remaining sub-factor for moderate environmental effects is obtained by dividing the overall factor of 20 by the product of 1.4 x 2.0 x 2.4, giving a sub-factor of 3.0. If the overall factor is reduced to 10, the sub-factor would be 1.5.

Therefore, the findings from this data scatter analysis support the recommendations of the PVRC that moderate environmental effects factors of 3 for carbon and low-alloy steel, and 1.5 for austenitic stainless steels, are very conservative. Greater moderate environmental effects factors can be justified.

5.6 References

1. *Criteria of the ASME Boiler and Pressure Vessel Code for Design by Analysis in Sections III and VIII, Division 2.* The American Society of Mechanical Engineers, New York, 1969.

2. Cooper, W. E., "Basis and Intent of Section III Fatigue Design Curves." Welding Research Council publication *Technical Information from Workshop on Cyclic Life and Environmental Effects in Nuclear Applications*, workshop in Clearwater Beach, Florida (January 20-21, 1992).

3. O. K. Chopra and W. J. Shack, *Effects of LWR Coolant Environments on Fatigue Design Curves of Carbon and Low-Alloy Steels.* NUREG/CR-6583 (ANL-97/18), Argonne National Laboratory, Argonne, IL, March 1998.

4. R. C. Juvinal. "Engineering Considerations of Stress, Strain and Strength", *Metals Handbook, Volume II, Failure Analysis and Prevention*. McGraw-Hill Book Company, New York 1967.

5. J. Hickling, *Low-Cycle Corrosion Fatigue of Unalloyed and Low-Alloy Steels in LWR Systems: Review of German Experience.* Report prepared for EPRI, Palo Alto, CA: January 1997.

6. E. Kiss, J. D. Heald, and D. A. Hale, "Low-Cycle Fatigue of Prototypic Piping," General Electric Company, San Jose, CA. GEAP-10135 (January 1970).

7. O. K. Chopra and W. J. Shack, "Methods for Incorporating the Effects of LWR Coolant Environment into ASME Code Fatigue Evaluations," *Probabilistic and Environmental Aspects of Fracture and Fatigue. PVP.* Vol. 386, ASME PVP 1999, New York, NY (August 1999).

8. K. Tsutsumi, H. Kanasaki, T. Umakoshi, T. Nakamura, S. Urata, H. Mizuta, and S. Nomoto, "Fatigue Life Reduction in PWR Water Environment for Stainless Steels." *PVP.* Vol. 410-2, pp. 23-34, ASME PVP 2000, Seattle, WA (July 24-27, 2000).

9. O. K. Chopra and W. J. Shack, *Effects of LWR Coolant Environments on Fatigue Design Curves of Austenitic Stainless Steels.* NUREG/CR-5704 (ANL-98/31), Argonne National Laboratory, Argonne, IL, April 1999.

6
PROPOSED REACTOR WATER ENVIRONMENT TEST PROGRAM

Based on the carbon, low-alloy, and austenitic stainless steel fatigue data evaluated in this report, a program of critical fatigue testing is recommended. The recommended test program is intended to rectify data deficiencies and to confirm observations that are based on limited data.

For example, the vast majority of the existing data has been obtained at high strain amplitudes and low strain rates on cylindrical (uniform gauge) test specimens under simulated reactor water coolant chemistries and extremely low or stagnant simulated coolant flow velocities. For these simulated reactor water environment test conditions, the environmental fatigue crack initiation mechanism appears to be rupture of the protective oxidation or passivation layer, with reoxidation or repassivation prevented by sustained straining at very low strain rates and associated low oxidation potential of the simulated coolant.

Information presented in Section 3 of this report describes the compensating effects of simulated reactor water flow rate on environmental fatigue crack initiation behavior of carbon steel specimens and components. Experimental results for both carbon steel laboratory specimens and full-scale components suggest that representative flow rates suppress observed strain rate effects by flushing deleterious material (for example, MnS) from the surface and improving the coolant oxidation potential. Therefore, the need for similar data for low-alloy and austenitic stainless steels, in order to determine whether the same phenomena are observed for these materials under more realistic conditions, is critical.

It is proposed that a full series of laboratory tests on austenitic stainless steel and a more limited number of tests on low-alloy steel be conducted with realistic fatigue specimen geometry and realistic reactor water coolant environmental conditions, in particular, coolant flow rate. The realistic fatigue test specimens would be based on the geometry recommended in Figure 1 and Figure 7 of ASTM E 606 (“Standard Practice for Strain-Controlled Fatigue Testing”), as modified to account for either internal or external simulated reactor coolant flow conditions. Paragraph 7.1 and Notes 14 and 15 of ASTM E 606 recommend caution in the use of tubular, uniform gauge or hourglass specimens. Therefore, some control specimens tested in air will be needed to ensure that the autoclave test bed and specimen geometry produce accurate results.

The alternative to laboratory test specimens would be full-scale component tests with appropriate internal simulated reactor water flow rates. Two possibilities might be available. The KWU autoclave (see Section 3) that was used for the 180° tube bend tests is still operational and could be used for testing low-alloy and stainless steel tubes. The other possibility is the apparatus used by General Electric Company for the butt-welded piping with internal simulated reactor water flow (see Section 2). That apparatus has been dismantled, but could be reassembled at moderate cost. Full-scale testing has a number of advantages including more realistic localized strain

distributions and a limited area of oxidation or passivation layer rupture. If full-scale testing is not feasible or is not cost-effective, then laboratory autoclave testing should be pursued.

The autoclave for the simulated reactor water coolant tests must be capable of addressing the range of simulated coolant flow rates of interest, from about 0.3 m/s (10 in/s) to about 5 m/s (200 in/s). In addition, the autoclave must be able to address the test temperature range (room temperature to 300°C (572°F)), and the dissolved oxygen range of interest (0.01 ppm to 0.2 ppm). Both the KWU autoclave and the General Electric internal flow systems are somewhat limited in this regard.

Phase 1(a) of the proposed test program would involve a rapid assessment of coolant flow rate effects on Type 304 austenitic stainless steel. The intent is to generate early test results that provide order-of-magnitude information. Hollow, uniform-gauge specimens or 180° tube bend test articles would be used for these Phase 1 tests. Three flow rates would be examined – 0.3 m/s, 3 m/s, and 5 m/s. Two strain amplitudes would be examined – 0.3% and 0.6%. Only two strain rates would be investigated – 0.4%/s and 0.004 5/s. Two dissolved oxygen levels would be tested – 0.01 and 0.2 ppm. Finally, two different test temperatures would be used – 60°C (140°F) and 288°C (550°F). A more limited set of tests would be pursued for a full-scale test series, two flow rates (low and high) and one temperature (288°C (550°F)). A single (low) strain rate would be investigated.

Phase 1(b) of the proposed test program would involve a rapid assessment of coolant flow rate effects on SA-533B1 and SA-508-2 low-alloy steel. Only two flow rates would be tested – 0.5 m/s and 5 m/s. Only one strain amplitude would be tested – 0.6%. The same two strain rates would be tested, as well as the same two dissolved oxygen concentrations and temperatures. Again, the full-scale test program would be more limited.

At the end of the Phase 1 program, enough information would be available to determine the order-of-magnitude of influence of simulated reactor coolant flow rate on environmental fatigue crack initiation for both austenitic stainless steel and low-alloy ferritic steel. It is expected that the test results for low-alloy steel would be essentially identical to the information generated for carbon steel. If this result is confirmed, no Phase 2 test program for low-alloy steel is planned. It is hoped that the effect of coolant flow on the passivation layer of austenitic stainless steel will be similar to the effect of coolant flow on the oxidation layer of both carbon and low-alloy steel.

However, if full-scale testing is not available, additional Phase 2 testing of austenitic stainless steel might be required. This Phase 2 testing might require some form of localized straining, such as that provided by an hourglass specimen or a notched specimen. In such a case, the autoclave would be required to provide external flow rates of sufficient velocity. For the solid hourglass specimen, the diametral strain at the minimum hourglass cross-section would be measured, with strain control feedback to the applied axial strain. For a notched specimen, the best approach would be an inelastic finite element calculation to determine the localized strain at the root of the notch that corresponds to the axial strain applied to the specimen.

The alternative to a solid hourglass specimen with external diametral strain measurement would be a tubular specimen with converging-diverging flow past an internal hourglass shape. Rather than measure the diametral strain directly during the test, it would be planned to analyze the

tubular specimen to develop the programmed axial strain profile that corresponds to the localized axial strain amplitude that is being controlled.

The Phase 2 test program is also planned to consider a wider range of flow rates, strain rates, strain amplitudes, temperatures, and dissolved oxygen levels.

The Phase 1 schedule involves selection of an autoclave testing facility in late 2001, with a detailed Phase 1 test completed at the same time. Phase 1(a) tests would be completed by the second quarter of 2002, with Phase 1(b) tests completed by the end of 2002. A final report on the Phase 1 testing would be completed by December 2002. Phase 2 would be scheduled, as required, during 2003, and perhaps extending out to 2004.

Meetings with the NRC staff would be scheduled for January 2002, prior to the start of the Phase 1 testing, late in 2002 after the Phase 1 testing is complete, and at other times when necessary for information exchange and coordination.

7
CONCLUSIONS

The results of the laboratory S-N data review show that laboratory fatigue crack initiation data for carbon steels in an air environment at various temperatures are in good agreement with the ASME Code carbon steel mean air curve, with a data scatter factor of about 3. In addition, laboratory fatigue crack initiation data for carbon steels in simulated PWR reactor water environments satisfy the PVRC environmental parameter thresholds for moderate environmental effects, with no data points corrected by F_{en}/Z approaching the ASME Code carbon steel design fatigue curve.

In contrast, most laboratory fatigue crack initiation data for carbon steels in simulated BWR reactor water environments satisfy the PVRC environmental parameter thresholds for moderate environmental effects. These data points, after correction by F_{en}, approach the ASME Code carbon steel mean air curve. A few data points actually fall below the ASME Code carbon steel fatigue design curve and, even after correction by F_{en}/Z, approach the ASME Code carbon steel fatigue design curve. However, all data points are above the ASME Code fatigue design curve after environmental correction and moderate environmental effects adjustment.

Laboratory fatigue crack initiation data for low-alloy steels in an air environment at various temperatures are in excellent agreement with the ASME Code low-alloy steel mean air curve, with a data scatter factor of about 2. Laboratory fatigue crack initiation data for low-alloy steels in simulated PWR reactor water environments satisfy the PVRC environmental parameter thresholds for moderate environmental effects, with no data points corrected by F_{en}/Z approaching the ASME Code low-alloy steel design fatigue curve.

With the exception of a very few data points obtained at very high strain range (very low cycle fatigue), laboratory fatigue crack initiation data for low-alloy steels in simulated BWR reactor water environments satisfy the PVRC environmental parameter thresholds for moderate environmental effects. Data points shifted by F_{en} are generally over-corrected relative to the ASME Code low-alloy steel mean air curve, especially above a cyclic life of 10,000 cycles. However, a few data points fall below the ASME Code low-alloy steel fatigue design curve and, even after correction by F_{en}/Z, approach the ASME Code carbon steel fatigue design curve. With respect to component, or structural, fatigue tests, PVRC fatigue test data were reviewed. Both carbon and low-alloy steel components had one component surface exposed to stagnant, oxygen-saturated water that approximated worst-case BWR reactor water environments. The test conditions were such that the PVRC environmental parameter thresholds for moderate environmental effects were not met. Laboratory fatigue data results would have predicted crack initiation at or below the ASME Code fatigue design curve. However, instead, crack initiation was above and, in some cases, well above the ASME Code fatigue design curve. In these cases, correcting the fatigue life prediction by F_{en} would provide an overly conservative estimate.

Also, the General Electric Company tested circumferential butt welds in carbon steel piping exposed on one surface to stagnant BWR water environments. The test results showed several data points that were well below the ASME Code carbon steel fatigue design curve. When the data points were shifted to account for the environment by F_{en}, the shifted data points were appropriately close to the ASME Code carbon steel mean air curve. When the data points were shifted by F_{en}/Z, the data points moved appropriately toward the ASME Code carbon steel fatigue design curve.

Flow rate effects for both carbon and low-alloy steels have been shown in both laboratory fatigue tests and full-scale component fatigue tests to be critical for reducing reactor water environmental effects. While the data are somewhat sparse, the trend is clear. The effect of flow rate essentially eliminates the influence of low strain rates and brings the data within the moderate environmental effect boundaries. Similar data for austenitic stainless steel is urgently needed.

Laboratory fatigue crack initiation data for austenitic stainless steels in an air environment at various temperatures do not agree very well with the ASME Code mean air curve, with more than half of the data lying below the air curve data fit. The Argonne National Laboratory (ANL) mean air curve data fit is in much better agreement, confirming criticism of the ASME Code mean air curve from the late 1970s. However, the strain control versus load control characteristics of much of the data set cannot be determined.

The F_{en} environmental correction to simulated PWR reactor water environmental fatigue data provides an accurate shift to the ANL mean air curve for the austenitic stainless steels.

The data scatter for austenitic stainless steels in simulated BWR reactor water environments is substantial, and the F_{en} environmental correction does not improve the data scatter to any great extent, nor does the moderate environmental effects adjustment. The issue appears to be the adequacy of the F_{en} expressions to characterize the reactor water environmental effects. For the purposes of this evaluation, a Z factor of 1.5 was used. No PVRC moderate environmental effects thresholds were applied in the F_{en} process.

A significant amount of component/structural fatigue test data is available for austenitic stainless steel components tested under conditions where one surface is exposed to stagnant, high-oxygen water. These component tests show little or no environmental reduction in fatigue life. However, the most penalizing laboratory conditions for austenitic stainless steel occur for low dissolved oxygen and low temperature at high strain amplitude. This appears to be due to the fact that repassivation of the ruptured surface passivation layer is inhibited because of low oxidation potential and chemical activation. The effect of reactor water flow rate is critical in this regard.

Finally, data scatter for austenitic stainless steels at fixed strain amplitude has been determined to be relatively small, supporting a moderate environmental correction Z factor of 2.5 to 3.0, rather than the Z factor of 1.5 that has been used in this data evaluation.

Target:
Nuclear Power

About EPRI

EPRI creates science and technology solutions for the global energy and energy services industry. U.S. electric utilities established the Electric Power Research Institute in 1973 as a nonprofit research consortium for the benefit of utility members, their customers, and society. Now known simply as EPRI, the company provides a wide range of innovative products and services to more than 1000 energy-related organizations in 40 countries. EPRI's multidisciplinary team of scientists and engineers draws on a worldwide network of technical and business expertise to help solve today's toughest energy and environmental problems.

EPRI. Electrify the World

Printed on recycled paper in the United States of America

1003079

EPRI • 3412 Hillview Avenue, Palo Alto, California 94304 • PO Box 10412, Palo Alto, California 94303 • USA
800.313.3774 • 650.855.2121 • askepri@epri.com • www.epri.com